Potential of Driving Style Adaptation for a Maneuver Prediction System at Urban Intersections

Am Fachbereich Maschinenbau an der
Technischen Universität Darmstadt
zur Erlangung des Grades eines
Doktor-Ingenieurs (Dr.-Ing.)
genehmigte

Dissertation

vorgelegt von

Claas Rodemerk, M.Sc.
aus Rosbach v. d. Höhe

Berichterstatter:	Prof. Dr. rer. nat. Hermann Winner
Mitberichterstatter:	Prof. Dr.-Ing. Klaus Dietmayer

Tag der Einreichung:	24.10.2016
Tag der mündlichen Prüfung:	10.01.2017

Darmstadt 2017
D 17

Vorwort

Die vorliegende Arbeit entstand während meiner Tätigkeit als wissenschaftlicher Mitarbeiter am Fachgebiet Fahrzeugtechnik (FZD) der Technischen Universität Darmstadt.

Mein besonderer Dank gilt Herrn Prof. Dr. rer. nat. Hermann Winner für die Unterstützung in der Promotionsphase, sein Vertrauen sowie die zahlreichen fachlichen Diskussionen und Anregungen, die maßgeblich zum Gelingen der vorliegenden Arbeit beigetragen haben.

Herrn Prof. Dr.-Ing. Klaus Dietmayer danke ich für die freundliche Übernahme des Korreferats und den fachlichen Austausch im Entstehungsprozess der Dissertation.

Die vorgestellten Forschungsfragen basieren auf den Ergebnissen eines Kooperationsprojekts mit Honda R&D Europe (Deutschland) GmbH. Mein Dank gilt insbesondere Herrn Dr. Robert Kastner für den regen fachlichen Austausch in den vergangenen Jahren.

Weiterhin bedanke ich mich bei allen ehemaligen und aktuellen Mitarbeitern von FZD einschließlich der Werkstätten und des Sekretariats für die hervorragende Zusammenarbeit, die stets für ein sehr angenehmes und produktives Arbeitsklima gesorgt hat. Insbesondere meinen Bürokollegen, die mich während der letzten 4 Jahren als Doktorand begleitet haben, danke ich für die vielen fachlichen und privaten Diskussionen und die angenehme Zeit.

Darüber hinaus bedanke ich mich bei allen Studenten, die mich in meiner Zeit als wissenschaftlicher Mitarbeiter in Form von zahlreichen Projektarbeiten, Abschlussarbeiten oder als wissenschaftliche Hilfskräfte begleitet und unterstützt haben und durch ihren Einsatz einen wertvollen Teil zu der vorliegenden Arbeit beigetragen haben.

Meiner Familie bin ich für ihre stete Unterstützung und Förderung während meiner gesamten Ausbildung und insbesondere während der Promotionszeit sehr dankbar. Mein ganz besonderer Dank gilt meiner Frau Annemarie für ihre fortwährende Unterstützung in allen Lebenslagen.

Claas Rodemerk Darmstadt, Oktober 2016

Table of Contents

Abbreviations

Abbreviation	Description
ACC	adaptive cruise control
ADAS	advanced driver assistance system
CAN	controller area network
CAM	camera
DOP	dilution of precision
FOT	field operation test
(E)CDF	(empirical) cumulative distribution function
EEG	electroencephalogram
GNSS	global navigation satellite system
GPS	global positioning system
IAS	intersection assistance system
IDM	intelligent driver model
INS	Inertial Navigation System
IMU	Inertial Measurement Unit
LIDAR	Light detection and ranging
OC	oncoming
OSM	openstreetmap
POS	position
RFID	radio-frequency identification
RMSE	root mean square error
RADAR	radio detection and ranging
STVO	Straßenverkehrsordnung
SQDIFF	normalized squared Euclidean distance
TTI	time to intersection
TTC	time to collision
V2X	vehicle-to-X-communication

Symbols and Indices

Symbol	Unit	Description
a	m/s²	acceleration
acp	%	accelerator pedal
age	years	age of test subjects
d	m	distance, width
dd	-	sum of object likelihoods
di	-	distance interval
c	N/°	cornering stiffness
E	-	ego
f	-	transfer function
fr	Hz	frequency
g	m/s²	gravity
h	m	prediction horizon
I	pixel	content of search window
L	-	left
LH	-	maneuver probability
m	-	maneuver
ma	kg	mass
M	-	number of potential maneuvers
MG	-	group of maneuver sequences
O	-	object
p	%	probability / likelihood
PV	-	preceding vehicle
pres	bar	pressure
q	m	width of road
Q	m²	quality of variation
QM, QMT	%	quality measure
r	miscellaneous	range
ra	-	transmission ratio
R	-	right
Res	miscellaneous	resolution of signal
S	-	straight
SM	%	sensitivity measure
t	s	time
$tr/\bar{t}r$	%	trust / mistrust in quality measure
ttc	s	time to collision
ttmi	s	time to maneuver initialization
v	km/h, m/s	vehicle's speed
u	-	number of indicators

Symbol	Unit	Description
x	-	x-axis
y	-	y-axis
w	-	factor/weight
WB	m	wheelbase
α	°	angle between edges of digital map
$\dot{\beta}$	°/s, rad/s	side slip angle change rate
γ	miscellaneous	limit
δ	°, rad	steering wheel angle
Δ	miscellaneous	difference
ε	miscellaneous	error, limit
θ	°, rad	angle of object detected by radar
κ	1/m	curvature
ρ	°, rad	head / gaze rotation angle
τ	s	time gap
φ	°, rad	angle between center of circle and intersection center
ϕ	°, rad	heading deviation of leading vehicle
ψ	°, rad	heading angle
$\dot{\psi}$	°/s, rad/s	yaw rate

Index	Description
act	active, actual
ai	aerial image
b	discretized bin
brake	braking
char	characteristic
city	urban areas
comb	combined
comf	comfortable
cp	compound
del	delay
di	distance intervals
DR	dead reckoning
ego	ego-vehicle
ex	exist
exc	exclusion
fr	front
HG	head- and gaze tracking
in	interval size
ind	indicator
int	intersection
im	image processing
L, l, left	left / left turn
lim	limit

loc	localization
lon	longitudinal
me	mean
map	digital map
mat	matched
mea	measured
mod	modified
NaN	not a number
non-act	non-active
obs	observation
obj	object
org	original
pp	predicted path
pre	predicted
Q5	5 % quantile
Q95	95 % quantile
rad	radial
re	relevant
real	real
ref	reference point
rel	relative
R, r, right	right / right turn
S, s, straight	straight driving
sm	small
sc	shoulder check
stop	stopping line
su	start up
st	stop
stat	static
str	steering rack
tr	training
tra	travelled
trans	transition
QMT	trusted quality measure
v	speed
var	variation
veh	vehicle
y	lateral
δ	steering wheel angle
$\dot{\psi}$	yaw rate
κ	curvature

Summary

Navigating through urban intersections is a challenging task for human drivers in general. More than 50 % of accidents with personal injuries caused by passenger car drivers in urban conditions happen at intersections. Currently, no driver assistance system in production is able to issue early warnings for pending collisions at urban intersections. One of the reasons is the warning dilemma at intersections arising from the variety of potential maneuvers a driver can perform.

To overcome this dilemma, an approach is presented in this work to detect drivers' intentions on guidance level at urban intersections. The term guidance level is used here according to three-level hierarchy of the vehicle driving task described by Donges. The driver's core task on guidance level is to select a target track and target speed for safe driving. An intention here is understood as a driver's plan to execute a maneuver and is formulated before a maneuver is initialized. The goal of the intention detection system introduced here is to detect a maneuver intention based on data measured during intersection approach and to predict a pending maneuver before commencement. The prediction quality achieved by the intention detection system solely based on automotive series sensors is analyzed. The turn indicator state is not used in the intention detection process at all. The approach introduced in this work is applicable for maneuver intention detection at arbitrary urban intersections. The intention detection is based on so-called “indicators”. Indicators have at least one input signal and one output signal for each potential intention. Indicators use transfer functions to calculate the maneuver likelihoods from any kind of input signal for all potential maneuvers. The indicators' transfer functions are calculated following the basics of Maximum-Likelihood principle. A quality measure to assess the quality of indicators and select indicators being beneficial for intention detection is introduced. The following data are used for intention detection: driver's control inputs during intersection approach, driver's head and gaze motion and mirror positions, environment perception information and intersection-specific information extracted from a digital map. Using independent indicators allows for the easy combination of different types of input signals in the prediction process. Different inference methods for the combination of indicators are discussed. Aside from inference methods with low computational complexity, a Bayesian network is applied as well.

To analyze the feasibility of the approach introduced here, an experimental vehicle is equipped with a prototypic implementation of the intention detection system introduced in this work, using a close-to-production GNSS receiver and navigation map data for localization only. Test drives with 30 test subjects are carried out in the city of Darmstadt. Data recorded in the test drives is used to train indicators' transfer functions and to

evaluate the system's detection performance. A classification scheme for urban intersections is introduced and the performance evaluation is presented separately for different types of intersections. Due to inaccuracies arising from the localization, ego-motion based reference points are defined in this work for the system' s evaluation. These localization-inaccuracy-free reference points are calculated a posteriori to turn maneuvers based on the vehicle's motion. Using these reference points, average true-prediction rates of the implemented system on priority roads are 87.5 % for straight driving maneuvers, 81.5 % for right turns and 84.1 % for left turns, at 1 s second before maneuvers are initialized.

All intention detection systems identified in related works focus on the detection of at least one intention connected with an action that the driver is about to perform. Here, a complimentary approach is introduced: The intention detection system is modified in order to exclude an intention related to a maneuver that the driver is not going to perform. A number of exclusions are calculated for multiple horizons in front of the ego-vehicle. The advantage of this approach is that it overcomes the limitations of a classic "positive detection" approach: If a "positive detection" system cannot discriminate amongst at least two potential and concurring intentions, no decision is made. In this case the exclusion approach is able to exclude a third potential intention.

Several studies can be found in literature addressing varying driving styles among different drivers. Thus, this work analyses the potential of increasing true prediction rates by adapting the indicators' transfer functions to individual driving styles. All test subjects are classified into sporty, medium or relaxed drivers based on longitudinal accelerations tolerated by drivers in the study. The driving-style adaption process is able to increase prediction performance by more than 30 % for single maneuvers of drivers of the medium group at stop-sign- or give way-sign-regulated intersections. No appreciable effect to the detection performance could be found for other priority regulations.

1 Introduction and Motivation

1.1 Motivation

A review of German accident statistics shows that among 2.4 millions accidents on German roads reported to the police in 2014, more than 392,000 people were harmed in traffic accidents in that year, including 3,377 fatalities. While the majority of fatalities occur in situations outside of towns, most accidents with injuries happen within city limits: 53 % of all people seriously injured in traffic accidents and 68 % of all people with minor injuries are harmed in accidents in urban conditions.[1]

Enormous progress has been made within the last years in terms of automated driving and it is assumed that automated driving will come into series production for highway driving within the next decade.[2] As a result of using automated vehicles, traffic accidents with injured or killed are supposed to decrease.[3] It is expected that expanding the field of operation of automated vehicles to situations outside of towns and driving on rural roads is likely to follow subsequently. However, serial application of automated vehicles driving in urban conditions is supposed to be a long way off due to the more challenging surroundings in urban areas.[4] Especially difficult urban driving situations include large intersections without traffic lights, the presence of cyclists near the vehicle, or missing lane markings.[5] Thus, medium-term, human drivers will still be necessary for driving in urban conditions.

Focusing on the reasons for traffic accidents with personal injuries shows that the majority of accidents (> 91 %) happen due to improper human behavior.[6,7] Out of more than 300,000 accidents with personal injuries reported to the German police in 2014, human error was noted as accident reason approximately 362,000 times. This means,

---

[1] Statistisches Bundesamt: Zeitreihen 2014 (2015), p.44.

[2] Pudenz, K.: Schrittweise Automatisierung bis 2025 (2012).

[3] Unselt, T.; Schöneburg, R. Bakker J.: Einführung autonomer Fahrzeugsysteme (2013), p.239.

[4] Grundhoff, S.: Autos ohne Fahrer (2013).

[5] Knecht, J.: Probleme des Autonomen Fahrens (2016).

[6] Only 8.6 % of all accidents reported in Germany in 2014 are caused by general causes (road conditions, influence of weather or obstacles on the road and technical failures).

[7] Statistisches Bundesamt: Zeitreihen 2014 (2015), pp. 49–50.

that on average, 1.2 human errors are recorded as reasons for each accident. Drivers of passenger cars cause 68 % of accidents with personal injuries.[7] Focusing on accidents with passenger cars shows that 17.6 % are caused by human error concerning priority or precedence regulations and 18.6 % are caused due to errors in turning.[8] Urban intersections are especially dangerous in regards to accidents with fatalities and personal injuries. In 2014, 54 % of all personal injuries caused by passenger car drivers in urban conditions happened at intersections.[9] Furthermore, existing advanced driver assistance systems (ADAS) in mass production are expected to affect the total spread of accidents in such a way that the proportion of accidents at intersections will increase in the future.[10] Thus, in order to reduce the number of people harmed in traffic accidents, there is a need for intersection assistance systems (IAS) to assist the driver at intersections. An IAS warns the driver of impending collisions with other road users at intersections. Road users are defined as other vehicles, cyclists, motorcyclists, or pedestrians.

1.2 Challenges of Intersection Assistance

The basic goal of IAS is to help the driver avoid accidents at intersections by providing information or warnings of potential collisions as early and reliably as possible. The goal is to issue warnings of potential collisions several seconds before a collision happens in order to expand the reaction time available to the driver for collision avoidance. Enke[11] gives an estimate of the benefit of an extended driver reaction time. According to this estimation, 90 % of all accidents at intersections might have been avoided if the drivers' reactions had been one second earlier. Thus, this work puts a special emphasis on predicting maneuvers at least one second before they are initiated by the driver.

While predicting impending collisions on straight roads is handled by extrapolating the actual motion of the ego-vehicle and objects detected in the surroundings, predicting collisions at intersections presents a much greater challenge. This is due to the potential maneuvers each traffic participant can perform at intersections. Therefore, an IAS has to face two main challenges: object detection and the warning dilemma. Object detection at intersections is very challenging. Objects that belong to crossing traffic demand a field of view that needs to be covered by environment perception sensors.[12] Further-

[8] Statistisches Bundesamt: Zeitreihen 2014 (2015), p.151.

[9] Statistisches Bundesamt: Zeitreihen 2014 (2015), p.303.

[10] Kessler, C.: Aktive Sicherheit (2006). as cited in: Mages, M.: Diss., Einbiege- und Kreuzenassistenten (2009), p.2.

[11] Enke, M.: Collision probability (1979), pp. 789–802.

[12] Darms, M. et al.: Classification and tracking of dynamic objects (2008), pp. 1197–1198.

more, visual field obstructions, like other traffic participants or static objects like trees, hedges, or buildings, prevent object detections during an intersection approach phase.[13] Nevertheless, the challenge of reliable object detection can be solved using vehicular communication systems based on vehicle-to-X-communication (V2X) including cooperative environment perception systems.[14]

However, the warning dilemma still remains even if information from other traffic objects is available. The warning dilemma in general describes the tradeoff between early warnings with a potentially higher false warning rate and later but less actionable warnings.[15] In the case of intersection assistance, the warning dilemma becomes even worse when considering all drivers' maneuver options. Depending on the maneuver planned by the drivers, different objects are relevant for means of collision avoidance. Figure 1-1 shows an abstracted urban intersection, connecting two roads with a total of three potential maneuvers considered for each vehicle: turning right (R), driving straight (S) and turning left (L).

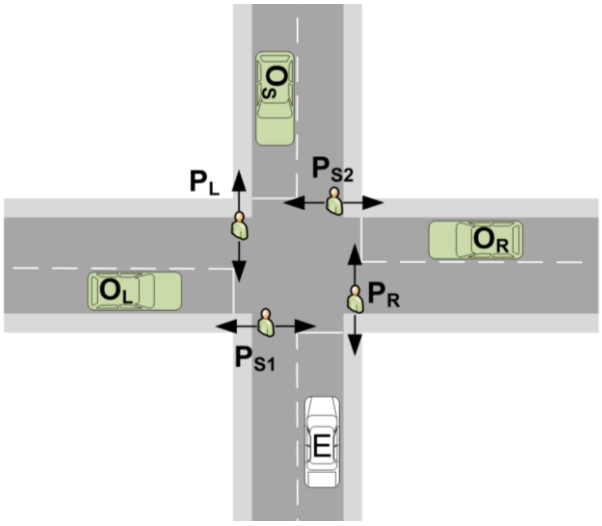

Figure 1-1: Urban four-way intersection

Depending on the ego-vehicle's maneuver (E) and the maneuver of other traffic objects (O_L,O_R,O_S) and pedestrians (P_R,P_L,P_{S1},P_{S2}),[16] the objects relevant for an IAS in the ego-vehicle are marked with an x in Table 1-1. All object maneuvers are labeled from the view of each object.

[13] Mages, M.: Diss., Einbiege- und Kreuzenassistenten (2009), p.57.

[14] Fuchs, H. et al.: Vehicle-2-X (2016), p.664.

[15] Fecher, N.; Hoffmann, J.: Driver Warning Elements (2016), pp. 867–869.

[16] Note that the consideration done here for pedestrians is also valid for cyclist crossing roads.

Table 1-1: Relevance of objects for the ego-vehicle

object (O/P)	O_L			O_R			O_S			P_R	P_{S2}	P_L	P_{S1}
object (O) maneuver	R	S	L	R	S	L	R	S	L	S	S	S	S
ego (E) maneuver													
R	-	x	-	-	-	-	-	-	x	x	-	-	(x)
S	-	x	x	x	x	x	-	-	x	-	(x)	-	(x)
L	-	x	x	-	x	x	x	x	-	-	-	x	(x)

Potential collisions of the ego-vehicle with pedestrians P_{S1} and P_{S2} are addressed by forward collision avoidance systems[17] and pedestrian emergency braking systems.[18] These systems have come onto market in the last years.[19] Here, no ADAS especially designed for intersections is required and the corresponding situations marked with (x) in Table 1-1 are grayed out.

Without knowing what the driver of the ego-vehicle and drivers of the object vehicles are about to do, IAS have to warn of all potential collision objects in the situation. This leads to warnings being issued for all 11 cases not grayed out in Table 1-1 (three potential maneuvers of each O_L, O_R, O_S and two pedestrians P_R, P_L crossing the roads). Aside from considering collisions with pedestrians P_{S1} and P_{S2}, an ego-vehicle turning right has three potential collisions, while driving straight offers up to six collision possibilities and turning left results in up to seven potential collisions. False positive alarms of an assistance system are annoying to the driver and lower the acceptance of a system.[20] Furthermore, studies show that frequent false positive alarms lead to ignoring all alarms completely.[21] Apart from the true positive detection rate (sensitivity) of a system, reaching a low false positive rate is highly prioritized in ADAS development.[22] In addition to the risk of annoying the driver with frequent false positive warnings, studies show that a cognitive overload of the driver caused by too much information leads to distraction.[23] For all such classifying systems, the resulting performance is a tradeoff between false

[17] Hulshof, W. et al.: Autonomous Emergency Braking Test Results (2013).

[18] Coelingh, E. et al.: Collision Warning with Full Auto Brake and Pedestrian Detection (2010).

[19] Rieken, J. et al.: Development Process of Forward Collision Prevention Systems (2016), p.1178.

[20] Berndt, H. et al.: Driver Braking Behavior (2007), pp. 387–398.

[21] Dingus, T. A. et al.: Automotive Headway Maintenance (1997).

[22] Mücke, S.; Breuer, J.: Bewertung von Sicherheitssystemen in Fahrversuchen (2007), p.124.

[23] Endsley, M. R.: Toward a theory of situation awareness in dynamic systems (1995), pp. 32–64.

negatives and false positives.[24] Therefore, inferring the driver's intention is a crucial factor for intersection assistance systems. By inferring the maneuver intended by the driver, the warning dilemma at intersections is moderated. However, the "classic" warning dilemma (concerning the warning time) remains. The benefit of knowing the driver's maneuver intention is that the set of potential collision objects is reduced to relevant objects for the predicted maneuver.

1.3 Using Detected Intentions

The intention detection system introduced here offers the information of a pending maneuver to ADAS for collision avoidance at intersections: In general, turning left with crossing lanes of oncoming traffic is a challenging task for the driver due to the complexity of the maneuver.[25] A survey of various studies analyzing left turn accidents and the effect of priority regulations is presented by Scholz and Ortlepp.[26] If a left turn intention of the ego-vehicle's driver is detected by a maneuver intention detection system, this information can be used to initiate collision warnings, even if the turn indicator has not been activated by the driver. Detecting turn intentions is especially beneficial for purposes of collision avoidance with vulnerable road users, such as pedestrians and cyclists travelling parallel to the ego-vehicle. If vulnerable road users are detected and a turn intention leading to conflicting trajectories, a warning to the driver can be issued. Thus, a turn intention detection system extends the functionality of state-of-the-art blind spot monitoring systems:[27] Here, the vehicle's turn indicator has to be activated to trigger alerts. In addition, most of the systems available on the market are deactivated at low speeds.[28] Furthermore, oncoming vulnerable road users can be considered for collision avoidance as well, if they are detected by the ego-vehicle's sensor systems. Turn assistance systems are especially in the focus of research for heavy commercial vehicles. An analysis of German accident statistics shows that turning and intelligent backup assistance systems can address a total of 5 % of accidents with commercial vehicles. Note that these 5 % cover about 70 % of all accidents with commercial vehicles and vulnerable road users.[29]

---

[24] Shashua, A. et al.: Pedestrian detection for driving assistance systems (2004), p.4.

[25] Mages, M. et al.: Intersection Assistance (2016), p.1269.

[26] Scholz, T.; Ortlepp, J.: Auswirkungen der Sonderphase für Linksabbieger (2010), pp. 19–35.

[27] Bartels, A. et al.: Lane Change Assistance (2016), pp. 1235–1257.

[28] Bartels, A. et al.: Lane Change Assistance (2016), p.1241.

[29] Kühn, M. et al.: Fahrerassistenzsysteme für schwere Lkw (2012).

1.4 Definitions and Scope of Work

First of all, the use of the terms prediction and intention within this work is defined as:

- Prediction: In accordance with a common definition, a prediction is a statement that is made about an event in the future that has not yet happened.[30] Here, the term prediction is used because this work deals with predicting driver's intentions to perform a maneuver before the execution of a maneuver is started.
- Intention: An intention is defined as "an act or instance of determining mentally upon some action or result".[31] Here, intention is used in the context of a short-term goal that a human plans to achieve. This definition coincides with the Rubicon model of action phases given by Gollwitzer and Heckhausen to describe the mental development of human actions[32] as shown in Figure 1-2. Rubicon describes a limit of irreversible mental commitment.

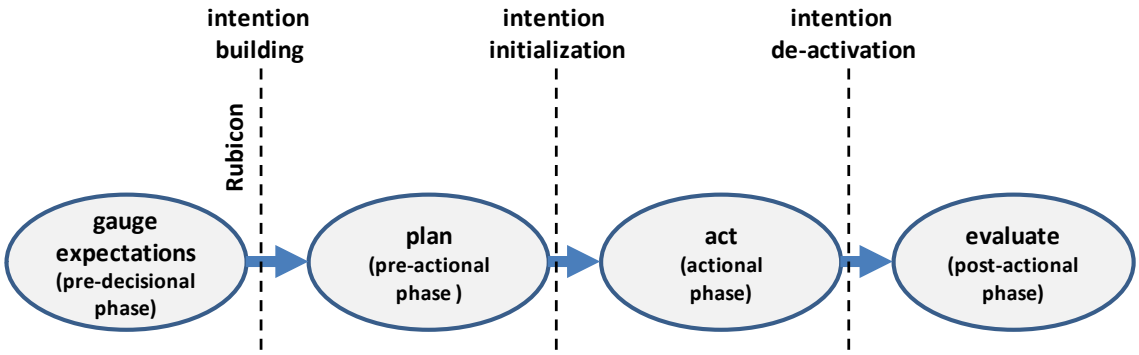

Figure 1-2: Rubicon model of action phases

- Maneuver initialization: The initialization of a maneuver describes the beginning of the execution of a maneuver. In this work, maneuvers are initialized after the reference point of a maneuver has been reached.[33]

This work focuses on the detection of driver intentions on guidance level at urban intersections according to the three-level hierarchy of the vehicle driving task formulated by Donges.[34] The driver's intention to execute a maneuver is always formulated before a maneuver is initialized. The prediction quality achieved by a system solely based on

[30] Merriam-Webster, I.: Dictionary (2015). Access: 29.07.2016.

[31] N.N.: Dictionary (2016). Access: 29.07.2016.

[32] Heckhausen, J.: Motivation und Handeln (2010), p.8.

[33] See section 6.3 for definition of reference points.

[34] Donges, E.: Driver Behavior Models (2016), pp. 21–22.

automotive series sensors is analyzed. By detecting intentions on guidance level (right turns, left turns or straight driving) at arbitrary urban intersections, the system predicts these driving maneuvers. In cases where the ego-vehicle and the object vehicles are equipped with systems able to detect maneuver intentions, only relevant objects are selected for collision warnings.

Many prototypic intersection assistance systems have been developed in research projects within the last years, but hardly any ADAS for early collision warning at intersections have gone into series application until now. This is due to the limitations of environment perception in real driving situations. Furthermore, most prototype systems use high precision localization systems or require communication systems to provide their functionality, which are not available in series production even now. A survey of prototype systems and approaches is given by Stoff[35] and Mages et al.[36]

1.5 Structure of the Thesis

The work presented here consists of 9 sections in total.

Section 2 introduces methods of intention detection and maneuver prediction at urban intersections in general followed by a survey of related works and state-of-the-art systems. This survey is used to identify open points in state-of-the-art intention detection at urban intersections. Based on the open points, research questions are derived in section 3 and a methodology to analyze the research questions is presented. According to the methodology, a test vehicle for training data generation is needed. The methods applied to gather data with the test vehicle, including a description of the measurement data, are given in section 4.

The basic working principle of the indicator-based maneuver prediction developed in this work is introduced in section 5. The indicators used for maneuver prediction are introduced in this section, which includes a method to assess and optimize indicator quality. An inference method is needed to condense the indicators' outputs into maneuver predictions. Several inference methods are discussed in section 6. For an evaluation of the maneuver prediction performance, reference points are defined here, as well. An alternative approach focusing on the exclusion of maneuvers that will not be executed by the driver is proposed. Subsequently, section 7 presents the prediction quality reached by the prototypic maneuver prediction system implemented in this work.

---

[35] Stoff, A.: Diss., Automatisierter Kreuzungsassistent, pp. 3–8.

[36] Mages, M. et al.: Intersection Assistance (2016), pp. 1259–1285.

An open point identified in state-of-the-art systems is that the individual driver's behavior is hardly addressed as a means of maneuver prediction, so far. Thus, section 8 focuses on differences in individual driving styles and presents methods for adapting the prediction system to different driving styles. Effects to the prediction performance are also addressed here. Furthermore, additional functionalities needed for an adaptation and challenges arising because of biasing in the adaptation process are discussed.

Section 9 summarizes the scientific goals with respect to the results obtained in sections 7 and 8. The outcome of this work is discussed critically in Section 9 and further research perspectives are presented.

2 Driver Intention Detection

Direct detection of human intentions is not possible because intentions are mental goals the driver aims to achieve. Inferring human intentions is only indirectly possible by evaluating actions carried out by the human or analyzing parameters of the driving situation and the environment of the ego-vehicle. Figure 2-1 summarizes information potentially useful for driver intention detection using the classification scheme of driver, vehicle and environment.[37] Information not suitable for intention detection at intersections for series or close-to-production sensor systems are identified based on data from the test subject study done within this work.[38]

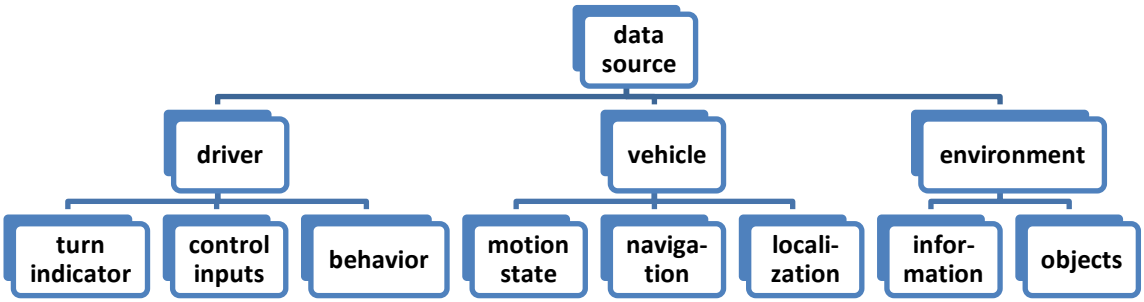

Figure 2-1: Principal methods for maneuver detection

2.1 Driver

The most obvious way to infer drivers' maneuver intentions while approaching an intersection is using the vehicle's turn indicator state. When drivers use the turn indicator habitually and in a timely manner before executing turns, no further detection system is necessary. Indeed, driving studies show an average turn indicator usage rate of approx. 75 % for turn maneuvers.[39] Thus, maneuver intention detection relying solely on the turn indicator state is supposed to fail in at least 25 % of all turn maneuvers. Even worse, in instances where drivers approach an intersection that has multiple lanes heading towards the intersection and activate their turn indicator for a lane change maneuver,

[37] Bubb, H.: Haptik im Kraftfahrzeug (2001), p.155.

[38] Details of the test subject study are given in section 4.4.

[39] Ponziani, R.: Turn Signal Usage Rate Results (2012), p.6.

a false positive turn maneuver is predicted. Thus, this work focuses on maneuver prediction without using the turn indicator state at all.

Another way to detect drivers' maneuver intentions is evaluating the driver control inputs to the vehicle. An analysis of minimum and maximum steering wheel angles δ in 1300 intersection approaches with straight driving maneuvers in the test subject study done in this project shows that $|\delta| > 50°$ is needed to detect turn maneuvers.[40] In order to check the temporal link between $|\delta| > 50°$ and maneuver initialization,[41] intersection approach sequences of either right and left turn maneuvers gathered in the same test subject study are used. Here, 78 % of all left turns and 54 % of all right turns show a time delay of $t \geq 1$ s after maneuver initialization before $|\delta| > 50°$ is reached.[40] Thus, detecting turn maneuvers by the steering wheel angle is not a prediction of a pending maneuver, but a detection of a maneuver already physically carried out. Hence, the steering wheel angle is not beneficial for a maneuver intention detection system. Further driver control inputs are the operation of the accelerator and brake pedal as well as the gear selection in manual gearbox automobiles. These inputs influence the speed profile during intersection approach. Exploiting the speed profile and driver control inputs during the intersection approach phase provides information on how (un)likely the execution of a maneuver is.

In addition, the driver himself and his behavior during intersection approach can be used to derive maneuver intentions. Inferring a driver's intended steering actions before they are started is possible by using an electroencephalography (EEG) as brain-computer interface.[42] Due to feasibility concerns, wiring the driver to an EEG is not a realistic possibility in series application, so this approach is discarded here. However, analyzing drivers' viewing behavior by evaluating head and gaze motions during intersection approach can be done with series or close-to-production sensor systems.[43] If maneuver-specific patterns can be detected in the viewing behavior that takes place before maneuver initialization, this information could be used for maneuver prediction.

---

[40] See Annex A.

[41] Initialization of a turn maneuver is determined using the calculated reference point as described in section 6.3.2.

[42] Ikenishi, T. et al.: Steering Intention Based on Brain-Computer Interface (2007).

[43] Müller, C.: Fahrerbeobachtung als wichtiger Baustein für autonomes Fahren (2016).

2.2 Vehicle

Aside from driver input, data from the vehicle's motion state can be used for maneuver detection at intersections. Using lateral acceleration a_{lat} instead of steering wheel angle δ is a potential method for detecting turn maneuvers. However, this would result in even higher time delays between maneuver initialization and maneuver detection as opposed to using the steering wheel angle due to the time lag between δ and a_{lat}.[44] This assumption is confirmed by results of the test subject study. The amount of turn maneuvers detected with a time delay of $t \geq 1$ s between maneuver initialization and exceeding the turn detection limit is higher than using δ for maneuver detection. The same applies to using the vehicle's yaw rate $\dot{\psi}$ instead of δ.[45] These results are in line with expectations because $\dot{\psi}$ and a_{lat} are results of a change in the vehicle's heading initiated by the driver via the steering wheel. In conclusion, both values are not useful for maneuver prediction because of their late availability. In situations where the driver is using the vehicle's navigation system for guidance, it is assumed that the driver will follow the driving instructions given by the system in most cases. Whereas access to either a built-in navigation device, a mobile device or smartphone-based device is available in most vehicles currently, the usage of those systems is not guaranteed. A study completed in 2011 shows that 46 % of 359 people questioned use their navigation system less than once a month. Only 6 % stated a daily usage of their navigation device.[46] Specifically, drives in well-known areas or on frequently driven routes were not entered into navigation systems.[47] Some approaches can be found in the literature for trying to automatically detect the drivers destination from prior drives to overcome this issue.[48,49] However, a navigation-based approach fails when the driver alters the route due to traffic conditions or visits an interim destination. Lindkvist et al. state that two thirds of drivers with local knowledge tend to change their normal route during a trip on a familiar journey due to congestion reasons.[50] Thus, although routing guidance information is available with high lead times before maneuver initialization, it is discarded in this work.

---

[44] Mitschke, M.: Dynamik von Kraftfahrzeugen (2003), pp. 497–598.

[45] See Annex A.

[46] Plötz, M.; Vockenroth, N.: Navigationssysteme (2011), p.5.

[47] Svahn, F.: In-Car Navigation Usage: An End-User Survey on Existing Systems (2004), pp. 14–15.

[48] Hofmann, M. et al.: Prädiktion potentieller Zielorte (2001).

[49] Mitrovic, D.: Driving Events Recognition (2005), pp. 198–205.

[50] Lindkvist, A. e.: DRIVE II project V2054 (1995). as cited in Svahn, F.: In-Car Navigation Usage: An End-User Survey on Existing Systems (2004), p.7.

In the case of an intersection that has dedicated lanes that allow just one maneuver, drivers' maneuver intentions can be derived from the localization in a dedicated lane. Therefore, a high precision digital map of the intersection is needed in combination with a high precision localization. Based on a lane width of $d_l = 2.5$ m,[51] the maximum localization error ε_{loc} (containing errors of the digital map and positioning) has to be smaller than $\frac{d_l}{2}$. The availability of localization systems offering an accuracy of $\varepsilon_{loc} < 1.25$ m even in urban conditions is uncertain. As a matter of principle, the approach cannot be applied to intersections without dedicated lanes. Thus, it is not applicable for maneuver prediction in general.

2.3 Environment

Information from objects detected in the environment of the ego-vehicle and intersection-specific information is useful to predict maneuvers at intersections, as well. Intersection information is any kind of information describing the intersection itself (geometry, number and direction of lanes, priority regulation) as well as information of potential driving maneuvers. In intersections where maneuvers are not possible or permitted due to restrictions or lack of roads, these maneuver intentions are excluded. Furthermore, information from the ego-vehicle's environment is used as well: Positions and motions of other traffic participants relative to the ego-vehicle can be used in some situations to derive the ego-vehicle's maneuver. The existence of adjacent lanes to the ego-vehicle and their driving directions can be used to derive limitations of potential maneuvers. Static elements of the intersection like road markings and direction arrows detected on the road surface are useful for maneuver prediction as well. In general, evaluating the environment around the ego-vehicle is possible before a maneuver is initialized by the driver. Thus, using environmental information supports the intention detection process at intersections.

2.4 Related Work

Many works have been published in recent years concerning the detection of driver intentions in several situations and for various purposes. A short survey of the most common fields of research dealing with driver intention detection is given here.

[51] Baier, R.: Richtlinien für die Anlage von Stadtstraßen (2007).

Numerous research papers have been published on the detection of lane changes and overtaking intentions. Exemplary work for this field of intention detection can be found by Morris et al.,[52] Henning [53], Tsogas,[54] and Berndt.[55] Closely linked to the research topic lane change intention is the topic of Adaptive Cruise Control (ACC)-related intentions. Schroven et al.[56] present an approach to enhance the usability of ACC systems by adding information from drivers' lane change intentions. Dagli et al.[57] introduce an approach based on driver's motivations inferred from the situation and apply it to ACC-controlled driving on highways. As well as research to detect drivers' intentions to perform evasion maneuvers presented by Welke,[58] and intention-based optimization of shift strategy of automatic gearboxes given by Takahashi and Kuroda[59] or Bai,[60] several works have been published dealing with the detection of drivers' intentions related to navigation and route guidance.[49]

Many approaches can be found in literature focusing on intention detection and maneuver prediction at intersections. Nevertheless, even now, hardly any systems for assisting the driver at intersections is available in mass production. Aside from a system offered by Volvo preventing drivers from pulling out after stopping at an intersection in the case of a detected collision risk with oncoming traffic,[61] Mercedes-Benz offers "BAS PLUS with Cross-Traffic Assist". In the latter, emergency braking is applied in case a collision risk with cross traffic to the ego lane is detected.[62] For crash prediction, these systems rely on the relative positions and speeds of detected vehicles. No prediction of the ego-vehicle's maneuver during intersection approach is considered here, so far.

Lots of research to detect drivers stopping/braking intentions at intersections can be found in the literature. Exemplary systems are presented by Koter[63] and Hayashi et al.[64]

---

[52] Morris, B. et al.: Lane change intent prediction (2011), pp. 895–901.

[53] Henning, M.: Diss., Preparation for lane change (2010).

[54] Tsogas, M. et al.: Detection of maneuvers using evidence theory (2008), pp. 126–131.

[55] Berndt, H.: Diss., Fahrerabsichtserkennung und Gefährlichkeitsabschätzung (2016), pp. 76–81.

[56] Schroven, F.; Giebel, T.: Fahrerintentionserkennung für Fahrerassistenzsysteme (2008), pp. 61–71.

[57] Dagli, I.; Reichardt, D.: Motivation-based approach to behavior prediction (2002), pp. 227–233.

[58] Welke, S.: Diss., Lenkmanöverprädiktion.

[59] Takahashi, H.; Kuroda, K.: Mental model for inferring driver's intention (1996), pp. 1789–1794.

[60] Bai, J.; Zhang, L.: Identification of Driver's Intentions (2010), pp. 1–4.

[61] ADAC e.V.: Autotest Volvo XC90, p.9.

[62] N.N.: BAS Plus (2016).

[63] Koter, R.: Advanced Indication of Braking (1998).

[64] Hayashi, K. et al.: Prediction of stopping maneuver considering driver's state (2006), pp. 1191–1196.

Detecting braking and stopping intentions at intersections helps recognize if a driver is aware of the priority regulation. In the situation where no stopping intention is detected and the entering of a priority road with cross traffic is predicted, either a warning and/or automatic brake is applied.[65,66] A similar approach is presented by Kosch et al. for detecting stopping intentions at red traffic lights.[67]

For means of maneuver detection on guidance level at intersections (turning or straight driving), several approaches based on high precision digital maps and high precision localization have been identified in the literature review. Systems introduced by Lefèvre et al.[68] or Schendzielorz et al.[69] rely on the determination in which lane each vehicle is located and derive the probability of potential driving directions from the lane assignment. Furthermore, there are several types of intersection assistance systems in existence based on an activated turn indicator for determination of left turn intention as introduced by Meitinger.[70] Numerous works can be found in the literature for maneuver detection of either the ego-vehicle's or other vehicle's turn maneuvers by trajectory analysis. Examples for these kinds of approaches are given by Berndt and Dietmayer[71] or Kurt et al.[72] Approaches evaluating the vehicle's speed for maneuver detection as introduced by Liebner et al.[73] perform well for discriminating between straight driving and turn maneuvers on priority roads, even in the presence of a preceding vehicle.[74] By design, these approaches are not applicable for maneuver prediction in situations with priority regulations demanding the driver to slow down or stop for every potential maneuver.

Just within the last few years, the driver and his behavior have started being considered an additional source of information for maneuver prediction. In general, approaches based on driver's brain activity measured by electro-encephalography are expected to result in the earliest maneuver prediction.[75] However, utilizing a brain-computer inter-

[65] Mages, M.: Diss., Einbiege- und Kreuzenassistenten (2009), p.27.

[66] Meitinger, K.-H.: Diss., Aktive Sicherheitssysteme für Kreuzungen (2009), p.37.

[67] Kosch, T.; Ehmanns, D.: Entwicklung von Kreuzungsassistenzsystemen (2006), pp. 1–7.

[68] Lefevre, S. et al.: Context-based estimation of driver intent at road intersections (2011), pp. 67–72.

[69] Schendzielorz, T. et al.: Vehicle maneuver estimation at urban intersections (2013), pp. 1442–1447.

[70] Meitinger, K.-H.: Diss., Aktive Sicherheitssysteme für Kreuzungen (2009), p.70.

[71] Berndt, H.; Dietmayer, K.: Driver intention inference (2009), pp. 102–107.

[72] Kurt, A. et al.: Hybrid-state driver/vehicle modelling (2010), pp. 806–811.

[73] Liebner, M. et al.: Driver intent inference at urban intersections (2012), pp. 1162–1167.

[74] Liebner, M. et al.: Velocity-Based Driver Intent Inference (2013), pp. 10–21.

[75] Ikenishi, T. et al.: Steering Intentions Using EEG (2008), pp. 1274–1283.

face by wiring the driver to the vehicle is not acceptable for series application. In order to use the driver and his behavior for the prediction process, newer approaches by Liebner et al.[76] and Doshi et al.[77] consider the driver's head pose and gaze direction as an alternative. An approach taking even the driver's body motions into account is presented by Cheng and Trivedi.[78] Doshi and Trivedi[79] present an overview of approaches for several fields of driver intention detection. Existing works are classified according to the intention or maneuver to be detected and the information used for the detection process.

A different approach is presented by Liebner and Klanner.[80] The authors give a recent survey of research published in the field of driver intention detection, as well. The authors use a classification tree to systematically present existing works by classifying the driver intention detection system by discriminative or generative methods. Discriminative methods use observed features to select a class that best fits out of a pre-defined set of classes. In contrast, generative methods output the most likely class identified and the probabilities for all classes.[81] Additionally, they are able to handle partially missing data, which is the reason why generative methods are preferred to discriminative most of the time when there are more than two classes to be distinguished.[79] In the classification tree of Liebner and Klanner[80], a sub-level is defined by describing the level of interaction for each method. The lowest level in the tree lists the methods applied for intention inference itself. The following discriminative methods are introduced in short by the authors: Artificial neural networks, support / relevance vector machines, decision trees/random forests, conditional random fields, prototype-based methods and utility-based methods. Concerning generative methods, the authors address Bayesian networks, parametric models, (layered) hidden Markov models, Gaussian processes, and dynamic Bayesian networks. In addition to outlining the basic idea of these methods, examples of existing research is given, as well. A recent survey of works focusing especially on the driver's behavior is presented by Berndt.[82]

---

[76] Liebner, M. et al.: Der Fahrer im Mittelpunkt (2012), pp. 87–96.

[77] Doshi, A.; Trivedi, M.: exploration of eye gaze and head motion (2008), pp. 49–54.

[78] Cheng, S. Y.; Trivedi, M. M.: Turn-Intent Analysis Using Body Pose (2006), pp. 28–37.

[79] Doshi, A.; Trivedi, M. M.: Tactical driver behavior prediction and intent inference: A review (2011), pp. 1892–1897.

[80] Liebner, M.; Klanner, F.: Driver Intent Inference and Risk Assessment (2016), pp. 900–906.

[81] Liebner, M.; Klanner, F.: Driver Intent Inference and Risk Assessment (2016), p.896.

[82] Berndt, H.: Diss., Fahrerabsichtserkennung und Gefährlichkeitsabschätzung (2016), pp. 17–25.

2.5 Conclusion of Related Work

Although lots of approaches for the detection of driver's intentions at intersections have been identified in related work, no approach was found to be designed to detect maneuver intentions on guidance level with respect to all of these conditions:

- Driver's maneuver intentions on guidance level are detected at arbitrary urban intersections.
- Maneuver intentions are detected before maneuvers are initialized by the driver.
- Intention detection is done without using high-precision localization and a-priori information of the intersection not included in normal navigation maps.
- The prediction system only relies on series or close-to-production sensor systems.

This is identified as the first open point to be addressed in this work.

While, for example, in the area of gearbox control, automatic adaptation of the gearbox's behavior to individual driving styles[83] has come into series application several years ago,[84] hardly any approach could be identified in the literature addressing the adaptation of an intention detection system to different driving styles. Thus, the question of whether or not driving-style-adapted intention prediction at urban intersections is beneficial is identified as the second open point in this work. Furthermore, all approaches identified focus on the prediction of maneuvers planned by the driver. No approach could be found excluding maneuvers at intersections that are not planned by the driver. Consequently, the third open point is identified, in which the potential of excluding alternative maneuver intentions will be analyzed.

[83] N.N.: Adaptive Transmission Management (2011).

[84] Auto.de: Als die Automatik schalten lernte (2015).

3 Methodology

3.1 Research Questions

The research questions (RQ) derived from open points in state-of-the-art systems are introduced in this section.

This work focuses on the prediction of driver intentions at arbitrary X-or T-shaped urban intersections with varying geometry and for arbitrary drivers. The RQs analyzed within this work are listed below:

1. What is the highest prediction performance that can be reached by an intention detection system for urban intersections?
    a. How can intention detection be accomplished at arbitrary urban intersections?
    b. What type of information acquired during intersection approach is beneficial for intention detection?
    c. What detection performance can be reached by a prototypic implementation based on series or close-to-production sensor systems?

Addressing the second open point, a literature review confirms experiences from daily driving: Driving styles vary among different drivers. Klanner[85] shows that drivers classified as ”sporty drivers” drive at higher speeds longer and use higher decelerations at intersections. Various approaches for the classification of driving styles can be found in the literature.[86,87] This raises the second research question:

2. Is it possible to increase the prediction performance identified in research question one by adapting the detection system to different driving styles?
    a. In what way do intersection approach behaviors differ among different driver types?
    b. How can the adaptation be accomplished?
    c. What challenges arise with the implementation of an automatic driving-style adaptation method?

[85] Klanner, F.: Diss., Entwicklung eines Querverkehrsassistenten.

[86] Johnson, D. A.; Trivedi, M. M.: Driving style recognition (2011).

[87] Hebenstreit, B.: Fahrstiltypen (1999).

Concerning the third open point identified above, all approaches found in literature try to detect the maneuver the driver intends to do. In the case where more than one concurrent maneuver option has nearly the same probability of execution, a maneuver prediction can only be carried out with a high degree of difficulty, to the point of non-feasibility. No approach could be found that tries to detect alternative intentions not planned by the driver (exclusions). This leads to research question three:

3. Is an alternative approach that excludes intentions not planned by the driver beneficial instead of detecting the actual intention?
    a. How can alternative intentions be excluded?
    b. Which benefits and disadvantages exist for an exclusion-based system?
    c. Using the same information as in research question one, what performance can be reached by a prototypic intention exclusion system?

3.2 Methodology

To analyze the first bundle of research questions, a system is developed for detecting drivers' intentions based on series or close-to-production sensor systems. In order to assess if the system is suitable for use at arbitrary urban X- or T-shaped intersections, a classification scheme for discriminating urban intersections is designed.[88] Based on this scheme, different settings are identified for the driver intention detection system. Furthermore, the intention detection performance reached at different intersection types is analyzed. Different types of information acquired with series or close-to-production sensor systems during intersection approach are analyzed depending on the maneuver executed at the intersection. Considering the limitations and inaccuracies arising from state-of-the-art automotive series sensor systems, the detection performance of the prototypic intention detection system is analyzed.

Effects of measurement inaccuracies and especially inaccuracies arising from the vehicle's localization are discussed. To predict drivers' maneuver intentions before maneuvers are initialized, information is used that is available prior to the start of maneuvers. Based on section 2.1-2.3, this information is:

- drivers' control inputs during intersection approach (approach behavior / driver-vehicle interaction)
- drivers' head and gaze motion and mirror fixations (driver behavior) acquired via a vision-based head tracking device

[88] See section 4.4.1.

- intersection-specific information extracted from a digital map and a localization system (environment)
- environment perception information (surrounding objects of any type)

The system developed here focuses on the most common urban intersections connecting two roads by T-shaped or X-shaped intersections. Depending on the shape of the intersection, the ego-vehicle's driver has either 2 or 3 potential maneuver options.[89] The methodology used to assess all research questions mentioned above is summarized in Figure 3-1.

Addressing research question one, a range of information potentially useful for maneuver prediction is identified along with its availability during intersection approach. From this, information is identified that can be measured with automotive series sensors. With respect to future developments in sensor technologies, information potentially useful for maneuver prediction acquired from close-to-production sensors is considered as well. All input signals of the prediction system are analyzed for feasibility of maneuver prediction in pre-tests. Training data is generated in test drives with test subjects in urban conditions for all information suitable for maneuver prediction. The training data is used to set up the indicators' transfer functions. An inference method is applied to generate maneuver predictions from the indicators' outputs. To assess the system's prediction quality, maneuver-specific reference points are defined and an evaluation measure is applied to the system's prediction.

Research question number two is addressed based on the assumption that drivers show an individual and "typical" driving style with limited variation in their behavior. [90] Here, an analysis seeks to prove whether there is an improvement or not in detection performance by adapting parameters of the intention detection system to the typical behavior of the driver. Therefore, the intersection approach behavior of different drivers is analyzed to find typical behavior. For the prototypic system implemented here, only intersection approach data from within one driving style is used in the training process to adapt the system to a specific driving style. The system's prediction performance is compared to the performance reached with training data gathered from all test subjects The challenges that arise in series application from an adaptive system for automatic driver adaptation are analyzed and a prototypic implementation is outlined.

---

[89] Note that this is the maximum number of potential maneuvers and does not include information of whether the maneuvers are legal to execute.

[90] Limited variation here means that the driver sticks to his "typical" behavior most of the times.

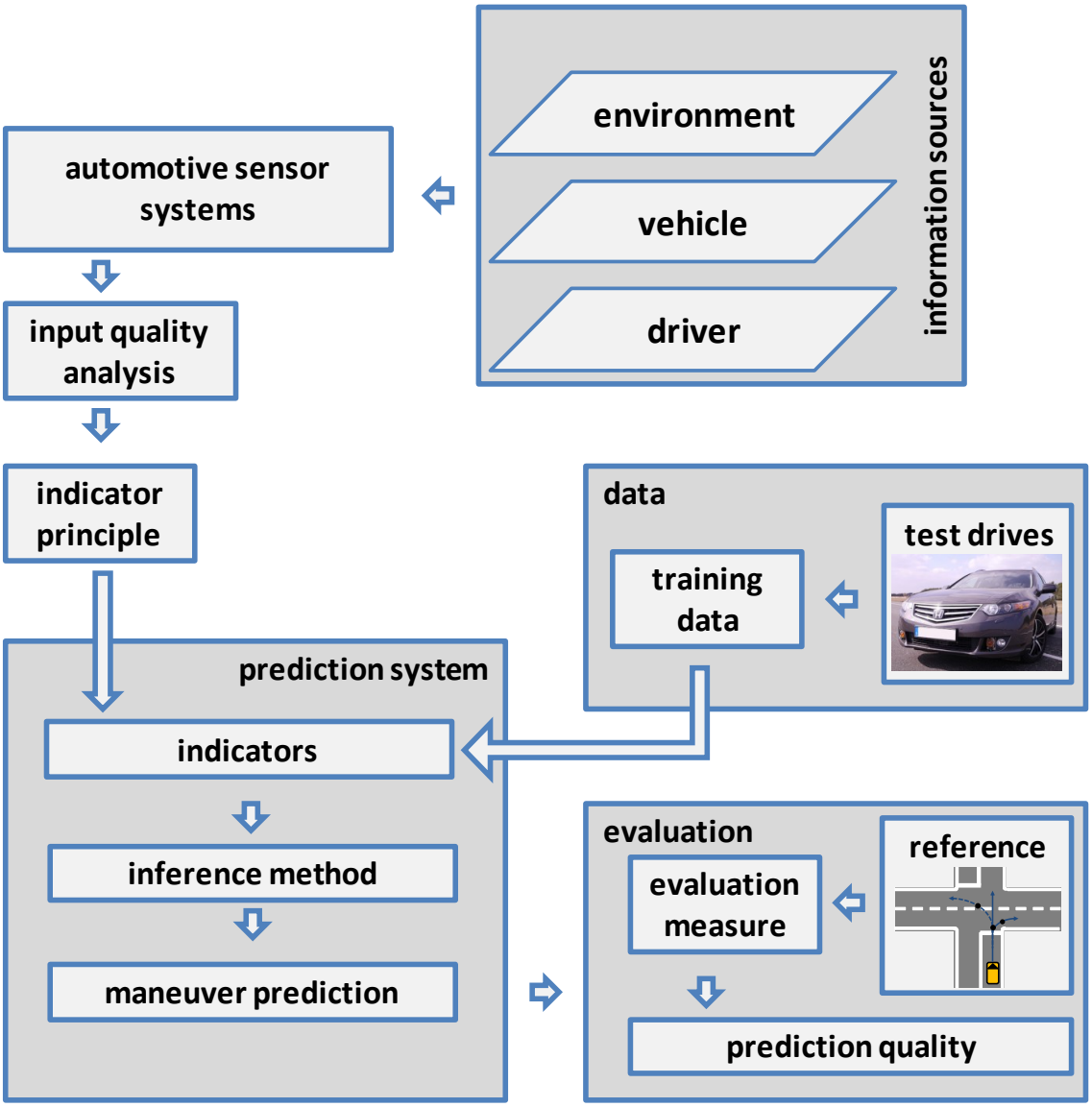

Figure 3-1: Basic methodology

Research question number three is assessed by using the process described above. The basic principle of the intention detection system designed for research question one is modified to be applicable for analyzing research question three. Though, here, no detection of a maneuver intention is carried out, instead alternative intentions (and maneuvers) that the driver will not perform within a specific horizon are excluded. Thus, the underlying calculations are altered as well as the evaluation measure. While for research question one training data corresponding to the maneuver executed is used, for research question three training data from everything but the maneuver executed by the driver is used to determine the excluded intention.[91] The remainder of the method is the same as in research question one.

[91] See section 6.6.3.

4 Data Generation

In general, generating training data can either be done virtually or in real driving tests. With virtual data generation, intersection approaches are simulated using pre-defined approach models in vehicle dynamics software such as IPG CarMaker.[92] While this method has the benefit that the data generated is free of noise and inaccuracies, the results are of limited use and vary with the parameters used in the simulation. Transferability of test results to real driving is not guaranteed.

Another method of generating virtual data is using driving simulators. Here, it is possible to use test subjects and to record their driving behavior. However, the degree of conformity of behavior in simulators to real driving is subject to ongoing research.[93] Whether test subjects show similar behavior in a driving simulator to behaviour in real driving conditions varies with the task that is simulated and the degree of immersion created by the simulator.[94]

Test drives for data generation can either be carried out on closed test tracks or in real traffic. Using closed test tracks improves the reproducibility of tests in comparison to public roads because test conditions (e.g. other traffic objects) are controlled. However, it is not guaranteed that conducting a study with test subjects on closed test tracks results in the same results as driving on public roads: Depending on the tests, test subjects are aware that situations on a test track are artificial and might adapt their normal behavior. Furthermore, test tracks offer limited road. Using a real urban road network therefore offers a greater variety of intersection situations and enhances the validity of results. In all tests with test subjects, safe test conditions have the highest priority.[95] In cases assessing functionalities with active intervention in vehicle guidance, tests have to be done on closed test tracks where critical situations are only simulated.[96]

Test drives within this work are only used for collecting training data and no intervention in vehicle guidance is done. Thus, using a closed test track is not necessary and data is generated by test subjects driving a vehicle in real urban traffic.

---

[92] IPG Automotive GmbH: CarMaker (2016).

[93] Zöller, I. et al.: Wissenssammlung für valide Fahrsimulation (2015), pp. 70–73.

[94] Jentsch, M.: Diss., Eignung von Daten im Fahrsimulator (2014), pp. 181–182.

[95] Jentsch, M.: Diss., Eignung von Daten im Fahrsimulator (2014), p.11.

[96] Hoffmann, J.: Diss., Das Darmstädter Verfahren (EVITA), p.21.

To evaluate the prediction performance of the approach implemented here, a prototype system is realized and integrated into a test vehicle. The vehicle is used for road tests in urban conditions in the city of Darmstadt, Germany. The data acquired in test drives is used for generating the indicator's transfer functions. The prototype system is implemented using series or close-to-production prototype sensor systems only and normal precision navigation maps extracted from openstreetmap (OSM).[97] All measurement equipment is integrated inside of the test vehicle to keep it looking inconspicuous in order to avoid influencing the behavior of other traffic participants. The test vehicle used by the test subjects is shown in Figure 4-1.

Figure 4-1: Test vehicle

All information acquired from the sensor systems is stored using a real-time prototype control unit. Data is captured with a frequency of $fr = 10$ Hz. Calculations for intention maneuver detection are carried out at this frequency as well. Apart from data of the vehicle's physical motion state directly acquired from CAN bus, the vehicle is equipped with additional sensor systems described in sections 4.1 - 4.3. A schematic description of the vehicle's setup is given in Figure 4-2.

[97] N.N.: OpenStreetMap (2016).

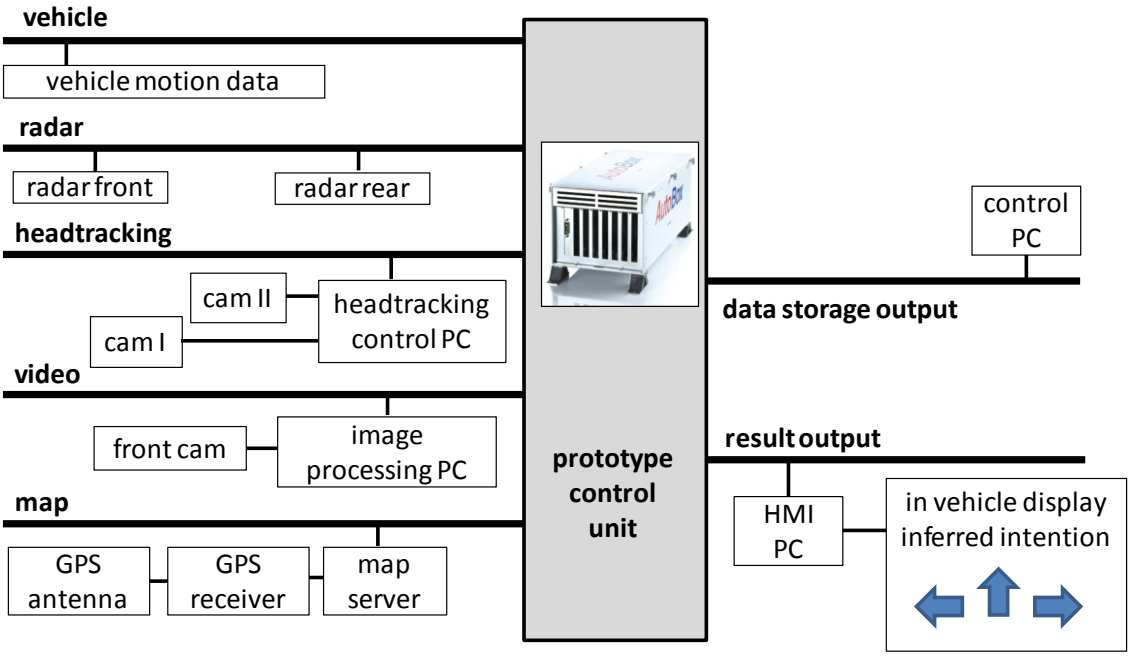

Figure 4-2: Schematic description of hardware setup

4.1 Radar Sensors and Head tracking

Four 77 GHz prototype radar sensors with extended lateral field of view (as compared to series sensors) are mounted at the front and rear edges of the bumpers and orientated in the vehicle's longitudinal direction. The sensor setup enables the detection of objects in front of and behind the ego-vehicle and in adjacent lanes. Furthermore, an infrared stereo camera-based head tracking device for contactless head and gaze tracking is mounted on the test vehicle’s dashboard. The driver does not need to wear any kind of markers, helmet or glasses and the system is able to operate under varying lighting conditions in real driving situations. The prototype integration on the vehicle's dashboard is shown in Figure 4-3. In between the two infrared cameras an infrared light source is mounted to illuminate the driver's face. Without the active illumination, the system's tracking capability is reduced to a limited functionality.

Figure 4-3: Head tracker on the vehicle's dashboard

The infrared cameras are connected to a dedicated PC running the head tracker software. Besides the internal image processing to calculate the driver's head pose, a "world model" is defined here. This model of the vehicle's cockpit contains the positions of selected objects in relation to the cameras. Here, the elements windscreen, speedometer, navigation system, radio and three rear-view mirrors (right, left and center) are modeled. If the driver's gaze direction is intersecting with one of these predefined elements, a fixation on the object is detected.

4.2 Positioning and Digital Map

4.2.1 Working Principle

The operating principle of the positioning system used in the test vehicle is shown in Figure 4-4. A conventional single frequency global positioning system (GPS) receiver with dead-reckoning functionality[98] in combination with a MATLAB-based map server is used for localization in the test vehicle.

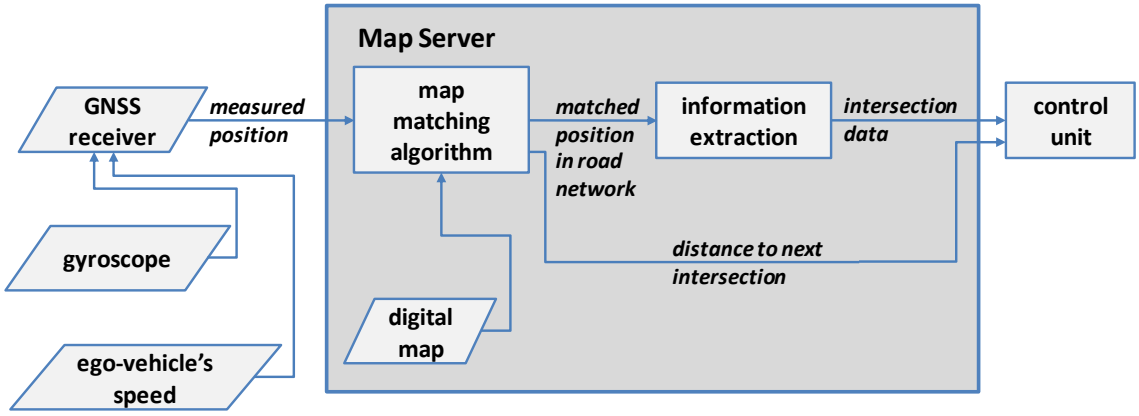

Figure 4-4: Operating principle

The map server acquires the measured GPS position of the receiver and determines the most probable position within the digital road network by means of map matching. The vehicle's matched position is used to extract further information from the digital map data. The map matching is done using a state-of-the-art map matching procedure described by Lou et al.[99] and Haunert.[100]

[98] Kleine-Besten, T. et al.: Navigation and Transport Telematics (2016), pp. 1356–1358.

[99] Lou, Y. et al.: Map-matching for low-sampling-rate GPS trajectories (2009), pp. 352–361.

[100] Haunert, J.-H.; Budig, B.: Map Matching Given Incomplete Road Data (2012), pp. 510–513.

4.2.2 Information Extracted from Digital Map

First of all, the information is needed to determine if an intersection is within a relevant area in front of the ego-vehicle. The ego-vehicle's driving direction on a digital road is determined by comparing the last matched positions as shown in Figure 4-5. With the known driving direction, the upcoming nodes of the road network in front of the vehicle are analyzed to find an intersection and to determine the distance remaining and information of potential maneuver options.[101] Based on an analysis of the road network used for test drives in this work,[102] the allocation of angles and maneuvers shown in Table 4-1 is applied. The allocation goes in line with studies done by Schnabel et al.[103] and Mangel[104] who found 77 % of all 4-way intersections analyzed in the city of Munich to be within $70° \leq |\alpha| \leq 90°$.

Table 4-1: Allocation of directions

angle	$\propto < -30°$	$-30° \leq \alpha \leq 30°$	$30° < \alpha$
driving direction	left	straight	right

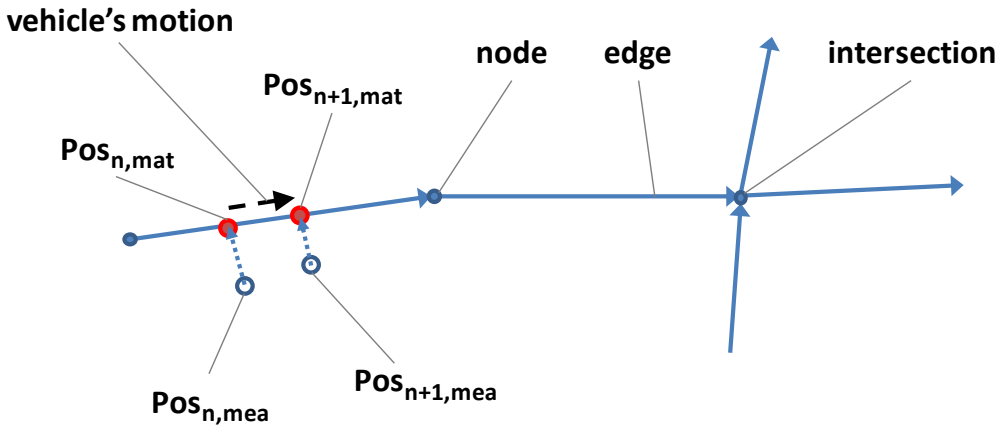

Figure 4-5: Intersection detection

Consecutively, the priority regulation of the intersection is extracted from the digital map. Because the priority regulation may depend on the road used for approaching the intersection as shown in Figure 4-6, the priority regulation has to be annotated to the map for each edge connected to the node.

[101] Further details of the localization system are provided in Annex C.

[102] See section 4.4.3.

[103] Schnabel, W. et al.: Straßenverkehrstechnik (2011), p.380. as cited in: Stoff, A.: Diss., Automatisierter Kreuzungsassistent, p.20.

[104] Mangel, T.: Diss., Inter-Vehicle Communication at Intersections (2012).

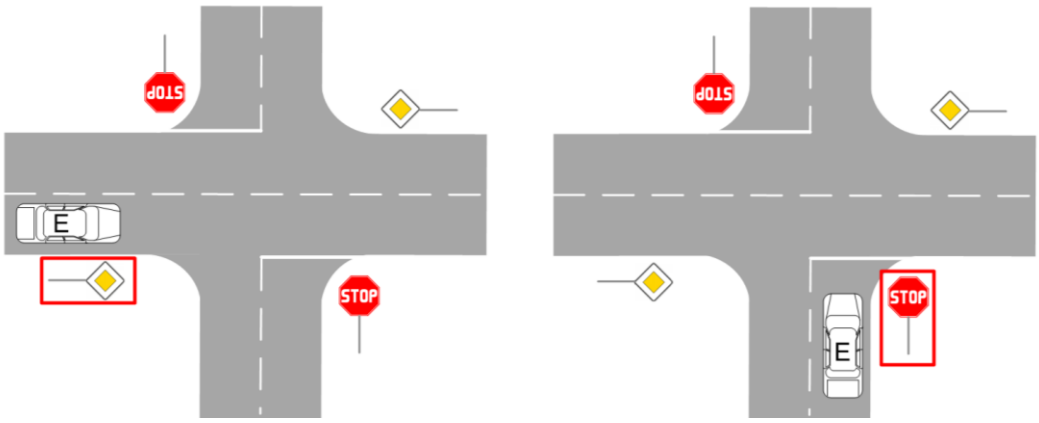

Figure 4-6: Priority regulations

4.3 Image Processing

This section summarizes the procedure of extracting environmental information by means of image processing.[105] A front camera mounted on the test vehicle is used for detection of direction arrows on the road surface and types of lane markings. The image processing system is provided with the ego-vehicle's speed v_{ego}, the steering wheel angle δ and, when applicable, the distance to a leading vehicle for limiting the detection area. The following section gives a short survey of the detection process.

Road marking detection is carried out by matching search windows containing parts of the captured image with pre-defined templates. The amount of data captured by the camera is reduced by cutting areas without relevant information (ego-vehicle's bonnet and everything above the horizon). The remaining part of the image is converted to grayscale and transformed to bird's eye view. An area of interest is defined by a path estimation based on a linear single-track model.[106] According to the curvature of the estimated path, the search windows for template matching are orientated and distorted as shown in Figure 4-7. The right part of the figure shows the search windows when driving straight. The left part shows the search windows adapted to the predicted driving corridor. There are separate search windows used for either the ego lane, the adjacent left and the adjacent right lane. To improve the system's robustness and to reduce influences of pitching motion, three different templates with different pitch angles are matched in parallel.

[105] A detailed survey of the working principle is provided in Annex D.

[106] Schramm, D. et al.: Vehicle dynamics (2014), pp. 223–226.

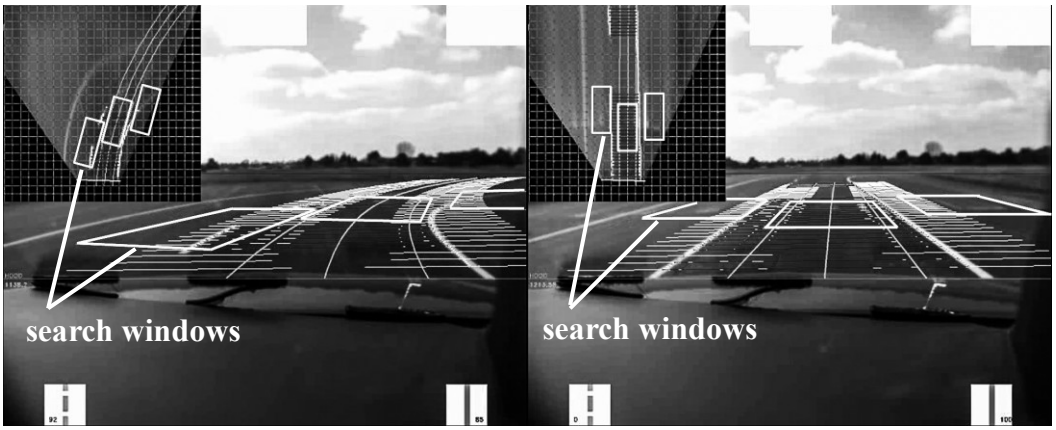

Figure 4-7: Path prediction and search windows

The templates used for the matching process are created following the official rules for road markings in Germany and are shown in Table 4-2.[107] Due to partly shadowed or worn-out road markings in real driving conditions, neither an edge-based nor a region-based matching method results in sufficient detection performance if applied independently. Thus, a hybrid approach is selected here based on a region-based template matching and an edge-based corner detector.

Table 4-2: Register of road markings

description	straight	left	right	ahead-right	ahead-left	lane reduction from right	lane reduction from left	left-right
region-based matching template								
edge-based matching template								

Up to two different direction arrows are detected for either the ego-vehicle's lane, the adjacent lane to the left and to the right of the ego-vehicle as shown in Figure 4-8. The left picture shows the driver's view of the scene with two direction arrows visible on the road in the ego-lane. The detected arrows are superimposed with the driver's view in the

[107] BASt: Richtlinien für die Markierung von Straßen (1980).

upper part of the right picture. If a direction arrow is detected, the information is saved until either another arrow is detected or the vehicle's travelled distance exceeds a defined limit γ_{tra}.

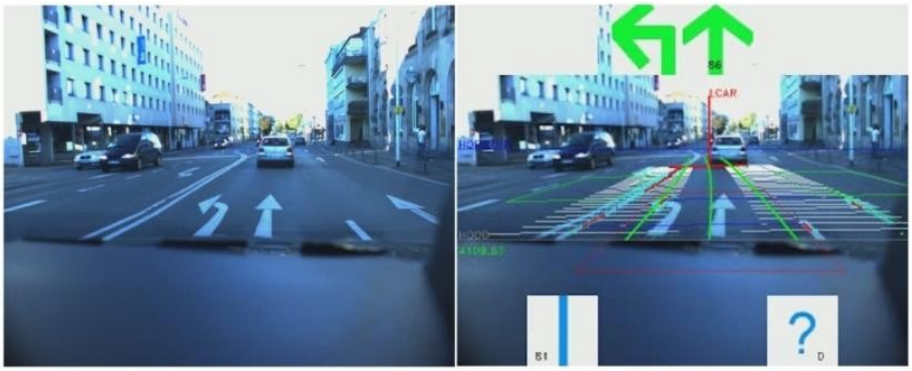

Figure 4-8: Direction arrows

4.4 Test Drives

4.4.1 Classification of Intersection Types

In order to design a route for test drives, a preselection of intersections to be contained in the test route has to be done. Because the driver's approach behavior is expected to vary with the right-of-way regulations, intersections are classified according to their priority regulations. The classification scheme used here is based on German road traffic regulations (StVO) and is limited to intersections without overpasses. The basic regulation of priority to right is given in § 8 StVO. Exceptions from this regulation apply to intersections equipped with traffic sign no. 205 (give way), 206 (stop), 301 (priority at next intersection), 306 (priority road) and roundabouts.[108] A list of the traffic signs referred to is given in StVO annex 2 (Vorschriftzeichen)[109] and StVO annex 3 (Richtzeichen).[110] Furthermore, § 37 StVO describes superior regulations that overrule the regulations mentioned above: Traffic lights, permanent lights and green right turn arrows permitting vehicles to turn right into right-hand traffic even when red traffic lights are lit.[111] Roundabouts are not addressed for maneuver prediction due there being only one potential maneuver on guidance level (entering the roundabout). A short sur-

[108] Bundesministeriums der Justiz und für Verbraucherschutz: StVO (2015), p.5.

[109] Bundesministeriums der Justiz und für Verbraucherschutz: StVO (2015), Annex 2, pp. 35-53.

[110] Bundesministeriums der Justiz und für Verbraucherschutz: StVO (2015), Annex 3, pp. 53-67.

[111] Bundesministeriums der Justiz und für Verbraucherschutz: StVO (2015), pp. 19–20.

vey of the classification system is given subsequently.[112] Intersections operated by traffic lights are divided into two classes: intersections with separate direction-specific traffic lights (class 1) and intersections with combined traffic lights regulating all lanes and their driving directions (class 2) including intersections with green right turn arrows. In class 1, no priority traffic has to be considered for any maneuver of the ego-vehicle. While class 2 is the same as class 1 for straight driving and right turns,[113] oncoming traffic has to be considered by the driver for left turns. Intersections operated by stop or give way signs form class 3 and class 4. Here, crossing traffic has priority to the ego-vehicle in any case. Oncoming vehicles only have priority to the ego-vehicle when the ego-vehicle is turning left and oncoming vehicles are continuing straight ahead or turning right. The difference between these two classes is that stopping for all maneuvers is mandatory in class 3, while it is not required by definition in class 4. Class 5 includes intersections with priority signs "priority road" and " priority at next intersection ". Priority regulations are the same as in class 2. Classes 6 and 7 contain turning priority roads in both directions. On right turning priority roads (class 6), the ego-vehicle has to consider oncoming traffic from the right on the priority road for straight driving and left turns. For left turning priority roads (class 7), the ego-vehicle has priority for each maneuver.[114] Intersections operated by priority to right regulation are represented in class 8. Here, oncoming traffic has priority to ego-vehicle left turns and crossing traffic from the right is relevant for all maneuvers. Intersections with bypass lanes on the right (allowing right turns without having to line up at traffic lights) are represented by class 9. For a straight driving or left turning ego-vehicle, the situation is the same as class 2. In case of right turns, only crossing priority traffic from the left is relevant for the ego-vehicle's driver.

4.4.2 Execution of Test Drives

Different methods for conducting test drives with test subjects are introduced and discussed in the following.

1. Free driving in urban conditions

   The simplest way of executing test drives is leaving the choice of routes to the test subjects. While this method results in natural driving behavior of test subjects, it will also result in driving on main streets most of the time and will lead to completely different routes amongst the drivers.

[112] See Annex E for more details of the classification system.

[113] Note this does not include vulnerable road users travelling in parallel to the ego-vehicle.

[114] Based on the assumption of three potential maneuvers at the intersection.

2. Navigation to prominent spots

   Test subjects are instructed to navigate to prominent spots in the city and choose their own route. While this method is supposed to have minimal influence on the test subject's driving behavior, local knowledge is mandatory. Drivers without local knowledge cannot participate or have to use provided maps. Additionally, the effects of test subjects looking for the correct routing is expected to influence their driving style. Also, the other disadvantages of the first method apply in the same way.

3. Memorize parts of a predefined route

   The third method relies on using a predefined route provided in parts to the test subjects. Test subjects are asked to remember a section of the route and upon reaching a predefined spot, they stop to memorize the next part. The benefit of this method is that a preplanned route is driven. However, aside from the increased time requirement, this approach is more demanding of test subjects and error prone.

4. Navigation using road signs

   Applying the fourth method, test subjects are asked to follow road signs, e.g. indicating directions to other cities or city districts. While this method will keep the test subjects only on main roads, test subjects won't show natural driving behavior if they focus on looking for road signs.

5. Navigation device

   The fifth method uses a navigation device providing a predefined route. The advantage of this method is that routing instructions are directly given to the driver. The disadvantage is that usage of a navigation device has been shown to influence driving style. Pre-tests have shown that drivers tend to directly react to routing instructions given by the navigation device: As soon as the navigation device announced an upcoming turn, drivers adapted their speed and some drivers even activated the turn indicator at an unusually long distance from the intersection.

6. Test conductor giving routing instructions

   This method relies on a test conductor being present in the vehicle and guiding test subjects through the route. To avoid immediate reactions to the conductor's instructions (as in method five) the conductor always provides the next but one driving instructions.[115] Thus, instructions are always given at least one intersec-

[115] As a matter of principle, the procedure is only applied starting with the 2nd intersection.

tion before a maneuver has to be executed by the driver. This method enables using a pre-defined route containing the desired share of intersection classes and maneuvers for the tests drives without influencing the driver's behavior. Furthermore, drivers can be directly compared to each other when driving on the same route. Moreover, an operator is needed in the vehicle anyway to operate the measurement and data recording systems.

Comparing the methods discussed above shows that method 6 relying on routing instructions given by the operator is the most promising method for test drives with test subjects in real traffic conditions. Consequently, this method is selected here.

4.4.3 Test Route

Based on the intersection classification, an urban test route is generated. The route is used for test drives and contains intersections from all 9 classes. The design goals considered for the test route are:

- Share of intersection classes

  The potential for accident avoidance by maneuver prediction varies among the intersection classes. On minor roads with priority to right regulations, average speeds during intersection approach are lower than on priority roads. Here, emergency braking has the potential to avoid accidents even at low time to collision values (*ttc)*.[116] Thus, the focus on this work is laid on priority roads (class 1, 2 and 5) which form the majority of intersections in the test route. Nevertheless, intersections of all other classes are included in the test route as well.

- Equal share of maneuvers at intersections

  The route is designed to have the same number of intersection approaches for every maneuver (right turns, left turns and straight driving) within one class. This ensures the availability of sufficient training data for each maneuver. Without specific attention to this design goal, test data on priority roads would mainly consist of straight driving maneuvers.[117]

---

[116] Exemplarily assuming a max. deceleration of $a = 6\ \frac{\mathrm{m}}{\mathrm{s}^2}$ and a ego-vehicle speed of $v = 20\ \frac{\mathrm{km}}{\mathrm{h}}$ results in a full braking time of $t = 0.9\ \mathrm{s}$ for collision avoidance.

[117] Analyzing urban road networks shows that priority roads usually run straight through urban areas. Thus, following a priority road mainly generates straight driving sequences.

- Covering different districts within the city

  Influences on driving behavior arising from local knowledge cannot be excluded a priori. Thus, a design goal is to use a variety of different districts of the city to minimize the influence of local knowledge.

- Varying size and geometry of intersections

  To enable the prediction system to handle different intersections without prior knowledge of the intersection's geometry, different intersection designs have to be included in the test route. An analysis of existing roads shows that intersection designs mostly vary on priority roads due to different road widths, while intersections in residential roads are more similar to each other. This means that the test route has to include intersections with different numbers of lanes as well as intersections with and without dedicated turning lanes.

- Safety of tests

  Safe execution of test drives is an essential demand on the route design. Especially when tests are done with test subjects on public roads, keeping the risk for the test subjects as low as possible has the highest priority. The definition of the test route contributes to this goal by avoiding risky situations on the route. Here, risky situations are identified as intersections with obstructed and blocked driver's view at the stop line. The test route only consists of driving in urban conditions with a much higher frequency of turn maneuvers than in normal driving conditions. Thus, driving on the test route is more challenging and fatiguing than normal driving[118] To maintain safe driving conditions, the maximum duration of the test drives is limited and the efficiency of the tests is kept high. Efficiency here means that there are as few transit sections as possible. Transit sections are parts of the route outside of the intersection approach areas that have to be travelled to get to the next intersection.

Taking all points listed above into account, a test route consisting of 149 different intersection approaches at an overall length of 22 kilometers of urban driving is defined in an iterative process. The test route developed for the city of Darmstadt, Germany is shown in Figure 4-9. Details of the route used for the test drives are given annex F. The route starts on the upper right side of the figure in the direction indicated by the arrow and ends in the lower part of the figure marked with a circle.

[118] Köhlker, L. et al.: Beanspruchung des Fahrers bei einer Kreuzungsüberquerung (2013), pp. 237–250.

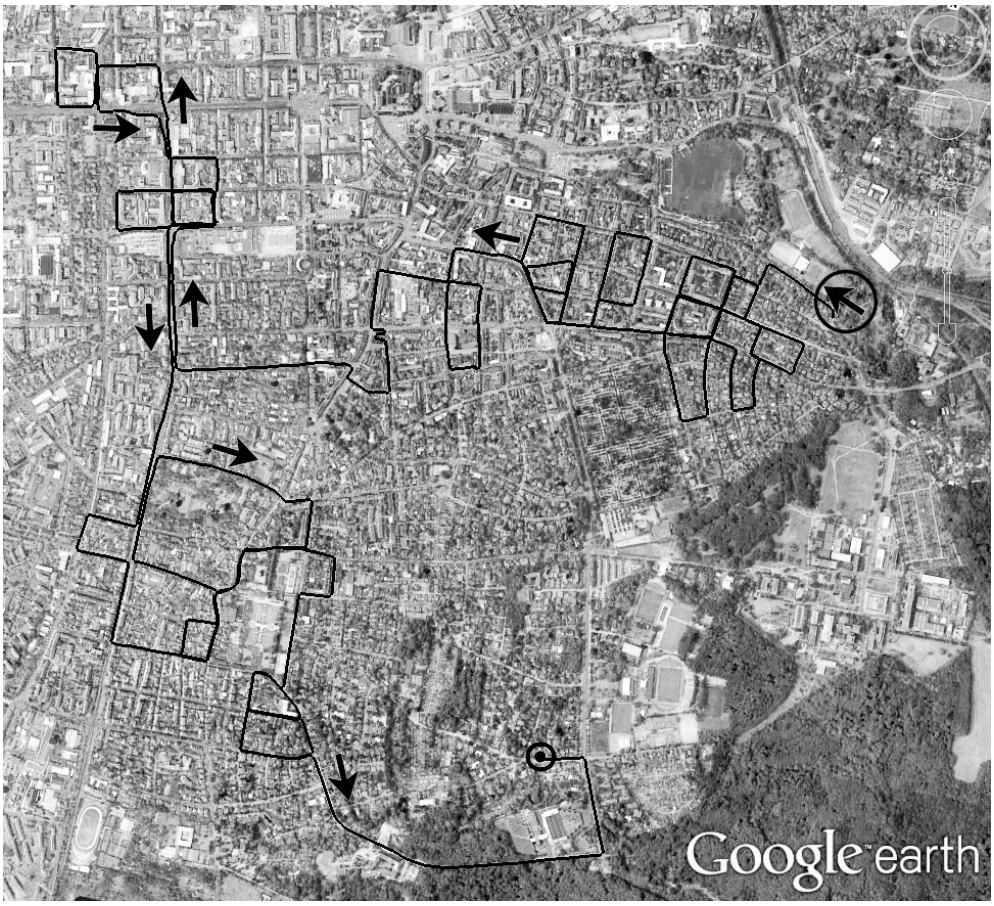

Figure 4-9: Test Route[119]

4.4.4 Test Subjects

The main task in selecting test subjects is to achieve a representative group in relation to the population. According to Bubb[120] distinguishing criteria need to be formulated that the test group has to fulfill. In this work, no focus is put on a special group of drivers. Following the test subject selection used by Hohm,[121] test subjects are selected to fulfill equal ranges of gender, age and driving experience. The definition of age groups used here is based on age groups defined by the German accident statistics:[122] Driver age is divided in three classes: $age < 25$, $25 \leq age < 55$ and $55 \leq age$. Male and female drivers are considered in equal parts. Driver age varies between 20 and 71 years. Figure 4-10 shows the cumulated distribution of the test subjects age.

[119] Image created using Google Earth 7.1.5.1557, access: 28.08.2016.

[120] Bubb, H.: Wie viele Probanden braucht man (2003), pp. 26–39.

[121] Hohm, A.: Diss., Überholassistenzsystem (2010), pp. 46–47.

[122] Statistisches Bundesamt: Unfallentwicklung auf deutschen Straßen 2012 (2013), pp. 29–36.

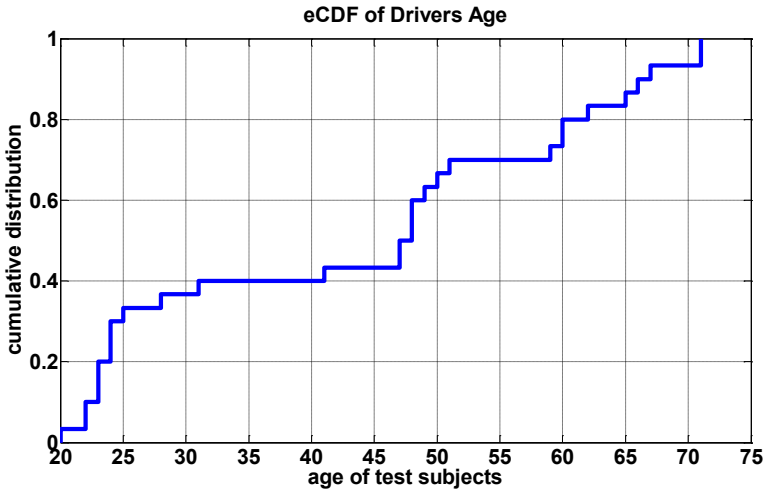

Figure 4-10: Test Subjects

A survey of annual mileage of more than 23,000 German passenger car found that 47 % have an annual mileage of $\leq 10.000\ {}^{\mathrm{km}}/_{\mathrm{a}}$.[123] Thus, two groups are considered here: drivers with low driving experience $\leq 10.000\ {}^{\mathrm{km}}/_{\mathrm{a}}$ and with high driving experience $> 10.000\ {}^{\mathrm{km}}/_{\mathrm{a}}$.

According to Bubb,[120] the number of test subjects n needed for equal distribution is given for a total of k criteria and n_i classes by:

$$n \geq \prod_{i=1}^{k} n_i \tag{4-1}$$

Here, with $k = 3$, $n_1 = 3, n_2 = 2$ and $n_3 = 3$, a total of $n \geq 12$ test subjects is needed. As recommended by Bubb, n has to be multiplied by a factor of $w = [3 \dots 10]$. Because this work does not focus on evaluating differences between the classes of each criterion, $w = 2.5$ is selected here. Thus, a representative set of 30 test subjects (15 male and 15 female) is selected for the driving tests to reflect a cross-section of the population. The average age of the test subjects is 41.8 years, that is close to the average age of 46.2 years in Germany.[124]

With the predefined test route being approximately 22 km long, a database of 660 km of urban driving containing approximately 4,400 intersection approaches is recorded and used for the prototypical implementation of the intention detection system.

[123] N.N.: Jährliche Fahrleistung in Deutschland (2016).

[124] N.N.: Durchschnittsalter (2016).

5 Maneuver Prediction

Based on methods for maneuver detection introduced in section 2 and the basic methodology to assess the research questions presented in section 3.2, principal requirements for the maneuver prediction system are derived:

The prediction systems have to be able to deal with different types of input data, handle uncertain and noisy data, and create predictions based on varying number of input signals, even with partially missing values. Input data for the prediction system is used from different signal sources: driver's control inputs acquired via CAN bus, driver's behavior within the vehicle's cockpit, intersection-specific information and environmental perception information. Thus, data types of input signals vary from binary to continuous signals. The quality of input data varies and input signals are noisy due to measurement errors. For each intersection class, there is a subset of signals that is used for maneuver prediction while the remainder is ignored. The size of the subset varies among different intersection classes and even within an intersection class. For example, there are signals that are useful for maneuver prediction only if the ego-vehicle is close to the center of the intersection. Furthermore, due to limitations of sensor systems, pieces of the input data may be missing partly or completely. Measurement data from the video-based head tracking system is only available if the driver is within the sensor's field of view. When the driver leaves the field of view due to large head rotation angles or leans outside the field of view, tracking stops as long as the driver is not visible to the system. A prediction has to be carried out in this case as well.

In the following, the concept of indicator-based maneuver prediction is introduced that fulfills the requirements listed above. The basic principle of indicators is inspired by a work by Bonnin et al.[125]

Indicators use transfer functions to transfer any kind of input signal (measurement data) to maneuver likelihoods. Note that here a likelihood is calculated because contrary to probabilities, likelihoods refer to past events with known outcomes.[126] The prediction system consists of a total of N_{ind} indicators. The maneuver likelihood outputs of each indicator are combined into probabilities for each maneuver by an inference system as described in section 6.1. The maneuver corresponding to the highest probability is selected as maneuver prediction when the probability exceeds a defined limit γ.The structure of the system described is shown in Figure 5-1.

[125] Bonnin, S. et al.: General Behavior Prediction (2014), pp. 1478–1488.

[126] Weisstein; W, E.: Likelihood (2016).

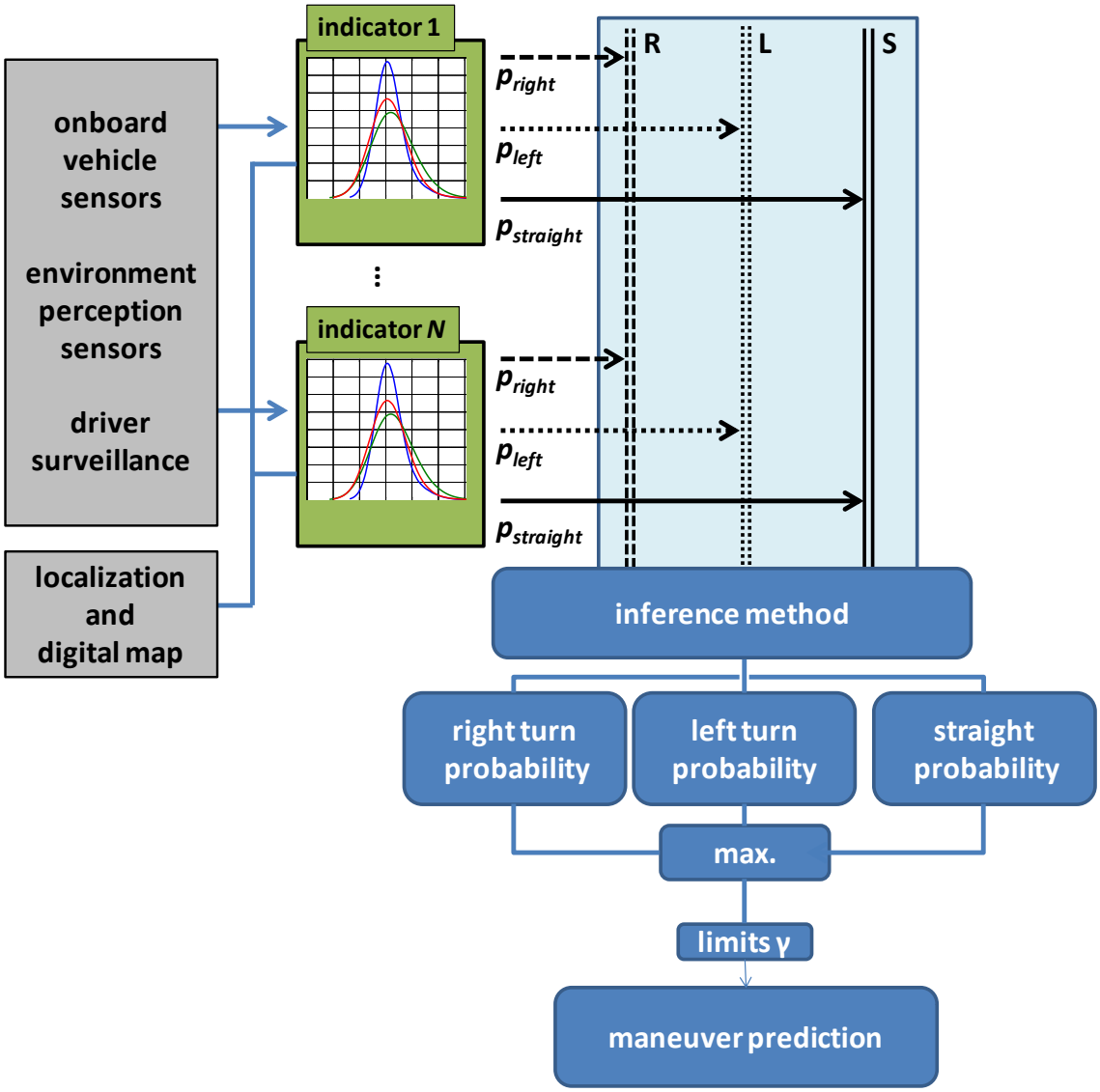

Figure 5-1: System structure

5.1 Indicator-based Maneuver Prediction

The indicator concept allows for the easy combination of all types of information mentioned above. By using transfer functions, arbitrary information can be used for maneuver prediction. Detected patterns in driver behavior can be integrated in the same way as direct measurement data from sensor systems. It is possible to add, remove, activate or deactivate indicators at any time without changing the overall system structure. Information from the ego-vehicle's environment is integrated in the maneuver prediction process in a simple and flexible way. Gathering contextual information from the environment has the major advantage that this information is available at an early phase of the intersection approach with several seconds remaining to maneuver initiation.

Key features of environmental context information are direction arrows on the road surface. A direction arrow in a lane is directly connected to the maneuver to be carried out when driving in that lane. For example, a right turn arrow detected in the ego-lane significantly raises the probability for the execution of a right turn. If there are arrows pointing in multiple directions (e.g. right and straight) within one lane, likelihoods for both maneuvers are raised. In this case, a direct inference of a maneuver is not possible and additional information is needed. Furthermore, in the example of the right and straight arrow, the probability for a left turn maneuver is reduced.

5.1.1 Description of Indicators

Indicators have at least one input signal. Input signals are either values directly measured by sensors or signals created by calculations based on multiple input signals. Each indicator is equipped with a total of N transfer functions deriving N outputs (one for each potential maneuver). Note that theoretically it is sufficient to calculate $N-1$ output values because the likelihoods of each indicator sum up to a total of one.

Each indicator has one output signal for each potential maneuver. Applying indicators to the case of intention detection at intersections results in 3 outputs of each indicator: a right turn likelihood, a left turn likelihood and a straight driving likelihood. For T-shaped intersections with only two potential existing maneuvers, the indicator's maneuver output connected to the non-existing road is set to zero, while the indicator's structure remains the same. The basic principle of indicators is depicted in Figure 5-2.

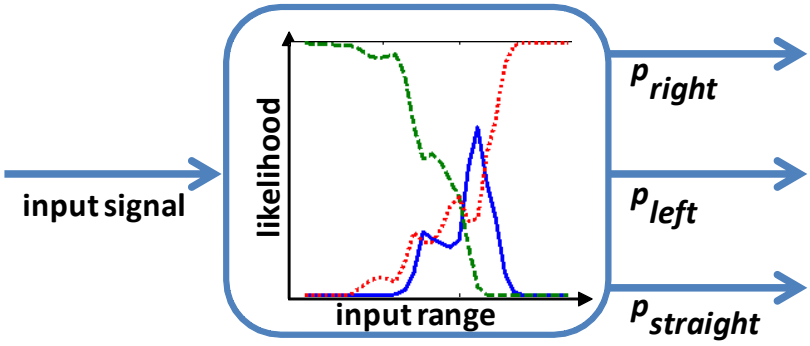

Figure 5-2: Indicator Principle

5.1.2 Transfer Functions

A crucial idea of the indicator concept is the definition of transfer functions. In general, arbitrary mathematical functions can be used to transfer input signals to maneuver likelihoods. Potential ways of determining the transfer functions are:

- Defining transfer functions based on expert knowledge
- Using a priori information
- Determining transfer functions by training data

When expert knowledge is used to create the transfer functions, this knowledge has to be modeled mathematically. An example is given in the following: A general rule used as expert knowledge here is that drivers perform a shoulder check before executing a turn maneuver. When a shoulder check is detected by sensor systems, a turn maneuver is assumed to start shortly. Thus, a transfer function f is defined with $sc_r = 1$ denoting a shoulder check to the right and $sc_l = 1$ to the left. The maneuver likelihoods p_r, p_l, p_s correspond to the maneuver options right turn, left turn and straight driving. Values for the parameter p_{act} are defined by expert knowledge as well. The likelihood vector P is given by:

$$P = \begin{pmatrix} p_r \\ p_l \\ p_s \end{pmatrix} \begin{cases} p_r = p_{act},\ p_l = 1 - \dfrac{p_{act}}{2}, p_s = p_l; \text{ for } sc_r = 1, sc_l = 0 \\ p_l = p_{act},\ p_r = 1 - \dfrac{p_{act}}{2}, p_s = p_r; \text{ for } sc_l = 1, sc_r = 0 \\ p_s = p_{act},\ p_r = 1 - \dfrac{p_{act}}{2}, p_l = p_r; \text{ for } sc_l = 0, sc_r = 0 \end{cases} \tag{5-1}$$

Note that this example only demonstrates the process of modeling transfer functions based on expert knowledge in general. The choice of the parameter p_{act} is arbitrary and the prediction results achieved with this transfer function depend on the parameter. Using a priori information for generating transfer functions follows the same approach. A priori information is any kind of information that is available prior to an intersection approach. For example, a priori information is provided by the vehicle's navigation system. Under the assumption the driver follows to the routing instructions of the navigation system, a likelihood vector P depending on driving instructions dri is used as a transfer function analogous to (5-1):

$$P = \begin{pmatrix} p_r \\ p_l \\ p_s \end{pmatrix} \begin{cases} p_r = p_{act},\ p_l = 1 - \dfrac{p_{act}}{2}, p_s = p_l; \text{ for } dri = R \\ p_l = p_{act},\ p_r = 1 - \dfrac{p_{act}}{2}, p_s = p_r; \text{ for } dri = L \\ p_s = p_{act},\ p_r = 1 - \dfrac{p_{act}}{2}, p_l = p_r; \text{ for } dri = S \end{cases} \tag{5-2}$$

Again, the selection of the parameter p_{act} is arbitrary and directly effects the likelihoods generated by the indicator. To avoid having to select parameters arbitrarily, another method of generating transfer functions is applied in this work: Transfer functions are created by using training data acquired in test drives. Using training data, discretized transfer functions are generated automatically and no arbitrary parameter selection is needed. The process of generating transfer functions by training data is described in detail in the following.

5.1.3 Training Data

The generation of transfer functions by training data depends on the type of input signal. A survey of using different types of signals is given below.

Discrete transfer functions

In the first step, the range of the input is determined and discretized in a number of N_b bins, referred to as intervals in the following. Afterwards, a training dataset containing intersection approaches for each potential maneuver is analyzed. The absolute frequency of each interval in training data is checked for each maneuver. The result of this step is histograms for every potential maneuver with N_b bins. Following the basics of the Maximum-Likelihood calculation,[127] relative frequencies (in percentage) are generated for each interval. An exemplary calculation of the transfer function for longitudinal acceleration a_{lon} is given in the following:

The sensor's measurement range is $-1\ g \leq a_{lon} \leq\ 1\ g$. Thus, the intervals are defined within a range of $r_{a,lon} = \left[-10\ \frac{\mathrm{m}}{\mathrm{s}^2}, 10\ \frac{\mathrm{m}}{\mathrm{s}^2}\right]$. The signal's range is discretized in N_b equally spaced intervals. Table 5-1 shows an extraction of the number of occurrences of intervals separated by maneuver created using training data.

Table 5-1: Frequency in training data

acceleration in m/s² / maneuver	...	$-5 < a_{lon} \leq -3$	$-3 < a_{lon} \leq -1$	$-1 < a_{lon} \leq 0$	...
right		13	1436	1091	
left		11	1197	1636	
straight		0	25	1548	

In the example of Table 5-1, accelerations $-3\ \frac{\mathrm{m}}{\mathrm{s}^2} < a_{lon} \leq\ -1\ \frac{\mathrm{m}}{\mathrm{s}^2}$ occurred 1436 times in training data for right turns, while values within this interval occurred 1197 times for left turns and 25 times for straight driving. Table 5-2 shows the relative frequencies for each interval that represents the transfer function. E.g., for interval -3 $\frac{\mathrm{m}}{\mathrm{s}^2} < a \leq$ -1 $\frac{\mathrm{m}}{\mathrm{s}^2}$, the total amount of training entries is:

$$n_{total} = n_r + n_l + n_s = 2658. \tag{5-3}$$

[127] Blobel, V.; Lohrmann, E.: Datenanalyse (1998), pp. 183–200.

The corresponding relative frequencies are:

$$\frac{n_r}{n_{total}} = \frac{1436}{2658} = 0.54 \quad \frac{n_l}{n_{total}} = \frac{1197}{2658} = 0.45 \quad \frac{n_s}{n_{total}} = \frac{25}{2658} = 0.01 \tag{5-4}$$

Table 5-2: Relative Frequencies

acceleration in m/s² / maneuver	...	$-5 < a_{lon} \leq -3$	$-3 < a_{lon} \leq -1$	$-1 < a_{lon} \leq 0$	...
right		0.54	0.54	0.26	
left		0.46	0.45	0.38	
straight		0.00	0.01	0.36	

Continuous transfer functions

Instead of using discretized transfer functions relying on bins, continuous transfer functions can be used. Continuous transfer functions are derived from the empirical cumulative density function (eCDF) of training data that is fitted with a predefined function. Typically, fitting functions are either based on polynomials or splines. Because the quality of using a polynomial fit varies with the shape of the eCDF curve, polynomial fits can lead to non-negligible fitting errors. For example, using a cubic spline interpolation results in an interpolation of the eCDF curve based on $N_{tr} - 1$ splines using all N_{tr} values provided in the training data as breakpoints.[128] Because all data elements of the eCDF are used as knots of the cubic splines, the eCDF is represented without fitting errors. However, due to using $N_{tr} - 1$ cubic splines, the derivation of the spline is very noisy. To avoid this issue, a spline interpolation based on least-squares approximation can be used. This approximation computes an approximating spline consisting of a predefined number of splines and is not error-free. In the example below, 4 splines are used to interpolate the eCDF. The advantage of the least-squares approximation is that the first derivation of the spline is a smooth curve. The slope of the eCDF represents the density of values in the input signal. Using M density functions according to M potential maneuvers describes the relation between potential maneuvers. This relation between the density measures is used to create the indicator's output by calculating relative percentages of the density values. An example is given in the following to clarify the calculation principle.

[128] Note that cubic spline interpolation is only selected here as an example and other methods are applicable as well.

Figure 5-3 shows the eCDF of the ego-vehicle's speed values for a selected maneuver and the cubic spline interpolation using $N_{tr} - 1$ cubic splines. As discussed above, the first derivation shows a lot of noise.

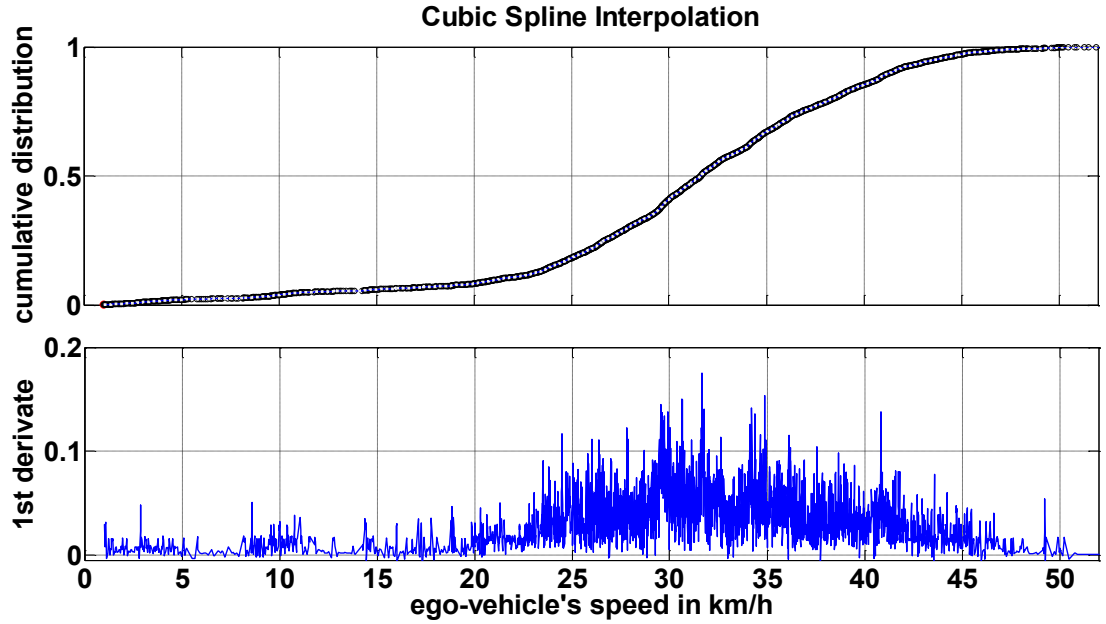

Figure 5-3: Cubic spline interpolation using $N_{tr} - 1$ splines

In contrast, Figure 5-4 shows the least-squares approximation of the same data using four cubic splines and the corresponding derivations. The breakpoints determined in the approximation are marked by vertical grey lines.

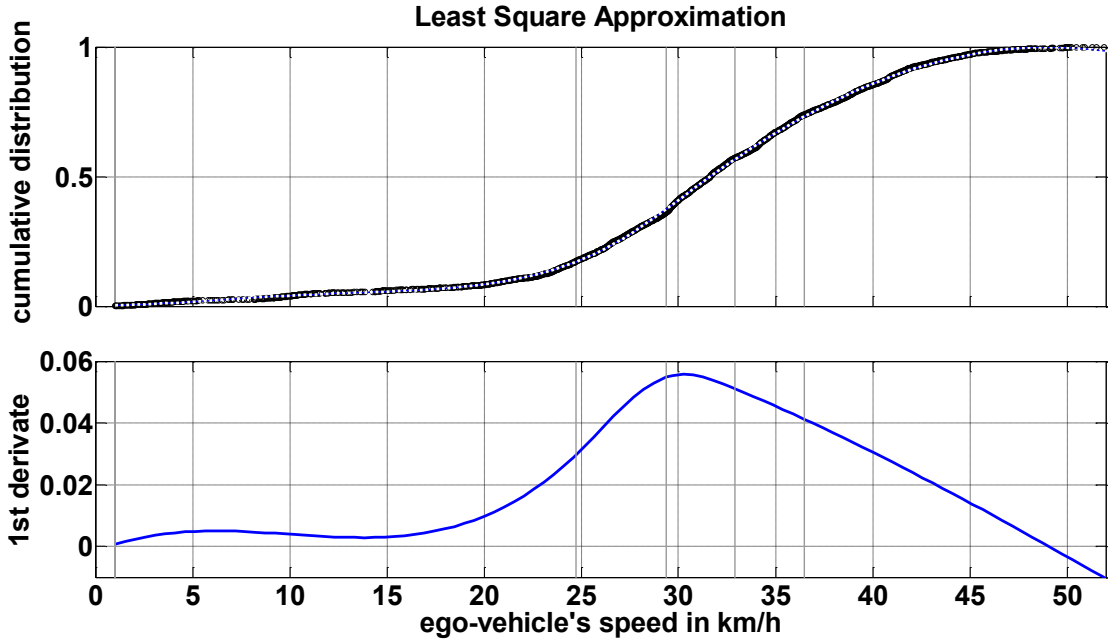

Figure 5-4: Cubic spline approximation using 4 cubic splines

Following this approach, Figure 5-5 shows the resulting continuous density functions based on four cubic splines for all three potential maneuvers. The density values are used to calculate the maneuver likelihoods analogue to the discretized transfer functions.

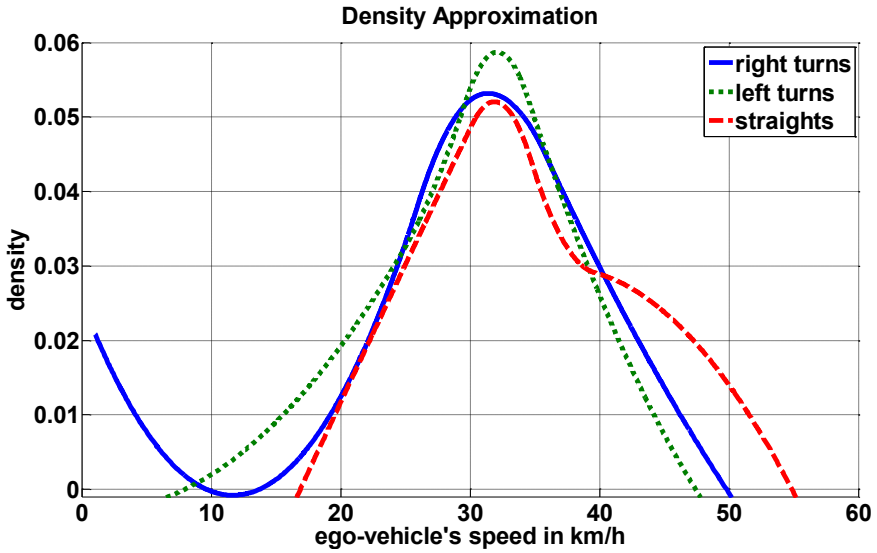

Figure 5-5: Density functions

Comparison of discrete and continuous transfer functions

At first glance, it seems beneficial to use continuous transfer functions generated by fitting training data with predefined functions. The advantage of continuous functions is that the functions are derived analytically and therefore are free of quantization errors. However, the disadvantage of this method is that this procedure creates fitting errors between the training data and the fitting function. Fitting errors are likely to influence the transfer function, especially at peripheral areas of the input signal with sparse occupancy. The result acquired with this method is dependent on the number of breakpoints and order of the splines used. Furthermore, using discrete values enables the identification of sparsely occupied areas. When sparse areas are identified, special considerations are needed with respect to the reduced reliability of these areas. Identifying sparse areas is not possible when using continuous functions.

Discrete states on ordinal or nominal scale

Calculating transfer functions for binary inputs using training data is similar to the process of creating discrete transfer functions for continuous and discrete inputs. The only difference is that for binary signals no discretization of the input is needed. When zero values correspond to the state "no detection", the amount of non-zero entries in training data can be counted directly for each maneuver.

Conditions and pattern matching

Adopting the principle idea of integrating expert knowledge as described above, conditions are formulated that the input signal has to fulfill. Here, the number of matched conditions in the training data is determined for each maneuver. The calculation of transfer functions is done analogously by determining relative percentages for each maneuver with fulfilled conditions. This allows for the integration of any kind of condition that is described mathematically. So, the main challenge here is to model expected driver behavior and behavior patterns. For example, an indicator relying on this principle is the predicted stop distance indicator described in section 5.4.4. Here, the expected behavior is that drivers will slow down from normal cruising speed to a comfortable turning speed. This behavior pattern is modeled by extrapolating the ego-vehicle's motion state. The condition is formulated that a stop of the ego-vehicle is predicted at a distance of $\pm\, d_{int}$ from the intersection center. This condition is applied to the training data and the frequency of the occurrence of predicted stops is determined for turn maneuvers and for straight drives.

5.2 Influence of Distance to Intersection

A typical intersection approach for a turn maneuver is shown in Figure 5-6. The figure shows that the driver slows down from regular cruising speed when approaching the intersection. Thus, to evaluate the vehicle's speed, the relative position of the ego-vehicle to the intersection needs to be considered for maneuver prediction.

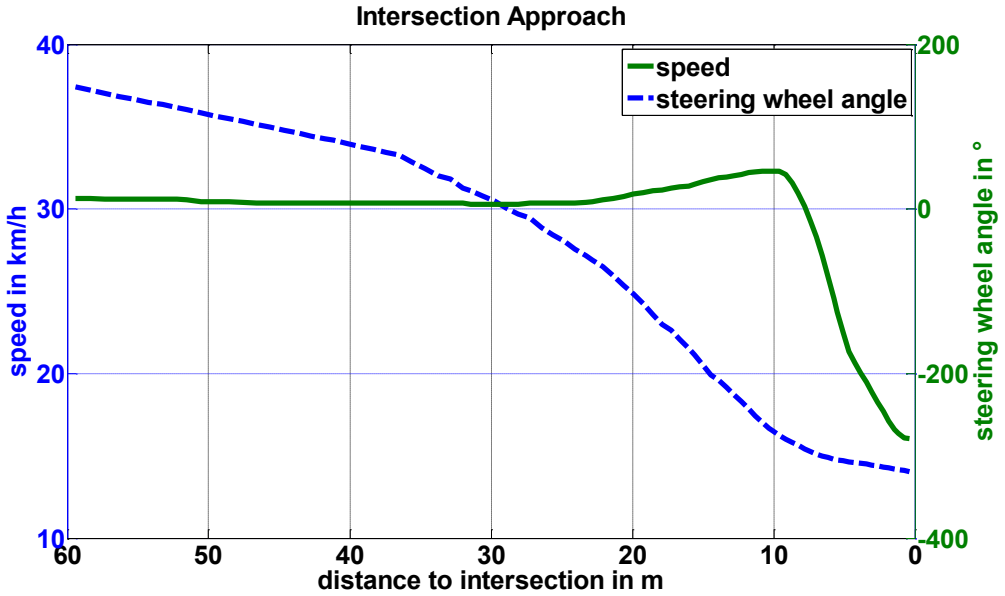

Figure 5-6: Exemplary intersection approach

The same applies to the driver's behavior and driving inputs as well as all further data based on driving physics. All information that is not distance-invariant has to be evaluated in relation to the vehicle's position.[129] In general, this can either be done by evaluating the distance remaining between the vehicle and the next intersection or the estimated time to intersection tti. Predicting an estimated time until the ego-vehicle reaches the intersection is done by extrapolating the vehicle's motion state. Here, the vehicle's speed and longitudinal acceleration as well as the actual distance between the vehicle and the intersection is needed for the calculation. Furthermore, an assumption has to be made for the vehicle's future motion state. For example, assuming constant acceleration is a common method of motion prediction.[130] The disadvantage of using tti is that the prediction becomes less accurate with increasing distance. Aside from inaccuracies in the estimation of distance to the intersection, the driver's approach behavior for the maneuver planned by the driver influences the prediction quality. These disadvantages are avoided by using the distance remaining between the ego-vehicle and the next intersection to classify driver's behavior during the phases of intersection approach. The distance is determined using a digital map as described in section 4.2.2.

For training purposes, sections of the test drives have to be defined as intersection approach training data. These sections are referred to as intersection specific "relevant areas" in the following. The relevant areas for intersection approach start at a distance d_{re} to the intersection on the road the ego-vehicle is approaching the intersection and end at the intersection center defined by the digital map. The distance d_{re} is determined following basic motion equations. The distance needed to stop is given by:

$$d_{st} = \frac{v_{ego}^2}{-2a_{lon}}; a_{lon} < 0 \tag{5-5}$$

Assuming a constant comfortable acceleration of $a_{lon} = -2\ \frac{m}{s^2}$ and a starting velocity of $v_{ego} = 50\ \frac{\text{km}}{\text{h}}$ leads to a stopping distance of $d_{st} = 48.2$ m. Considering that braking to standstill is not necessary, this lowers d_{re} to $d_{re} < d_{st}$. Assuming drivers don't apply constant deceleration while braking and that turn maneuvers may be started before reaching the intersection center raises the value of d_{re} to $d_{re} > d_{st}$. With respect to these effects, the length of the relevant area is set to $d_{re} = 60$ m. With defined limits of the relevant area, the concept of distance intervals is introduced:

The relevant area is divided into M_{di} equally spaced intervals, referred to as "distance intervals" (di) afterwards. The number of distance intervals used can be varied. Higher

[129] Distance-invariant signals are information that do not change within an intersection approach at all. For example, the number of potential driving directions at an intersection is distance-invariant.

[130] Hermes, C. et al.: Long-term vehicle motion prediction (2009), pp. 656–657.

number of intervals results in lower amount of training data within each distance interval. A total of $N_{di} = 2$ distance intervals is the minimum value offering benefits as opposed to completely disregarding the ego-vehicle's distance to the intersection. For the prototypic implementation done in this work, the length of each distance interval is set to 10 m. The resulting distance intervals are shown in Figure 5-7. Using distance intervals, indicators are set up with respect to the remaining distance to the next intersection. Indicator's transfer functions are calculated M_{di} times, each time only using training data from the corresponding distance interval. The concept of distance intervals is applied to all indicators that are distance dependent.

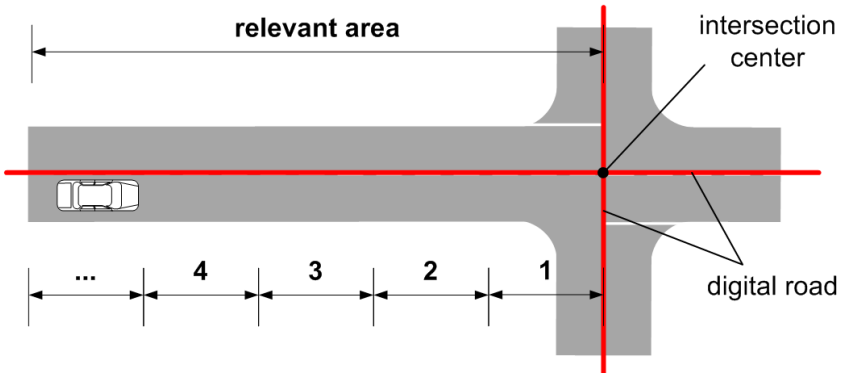

Figure 5-7: Distance intervals

5.3 Free Driving Conditions

Among the indicators used for maneuver prediction described in section 5.4, there are indicators that are only relevant in free driving conditions. These indicators are called free-driving-dependent hereafter. "Free driving" signifies that the driver's choice of speed is only dependent on the maneuver planned by the driver and the speed limit. Using information from the ego-vehicle's speed and acceleration as well as all driver inputs that effect the ego-vehicle's speed is only beneficial for maneuver prediction if the driver's behavior is not influenced by external conditions. External conditions here are priority regulations that require the driver to stop or slow down. This includes time-invariant traffic regulations like stop and give-way regulations as well as traffic lights demanding the driver to stop at red lights. Information about the actual state of traffic lights are either acquired in video format by a front camera[131] or by V2X communication devices if a traffic light sends out its state information.[132] Furthermore, other traffic

[131] Chiang, C.-C. et al.: Detecting and recognizing traffic lights (2011), pp. 6919–6934.

[132] Fuchs, H. et al.: Vehicle-2-X (2016), p.674.

participants may represent external conditions forcing the driver to adapt his speed when following a leading vehicle or approaching a stopped vehicle. While following another vehicle, the driver has to follow the speed profile of the leading vehicle in order to avoid collisions and to maintain a safe distance. In general, positions and motions of other traffic objects in the driving corridor of the ego-vehicle are acquired by environment perception sensors like radar, lidar, camera, or received via V2X, as well. In this work, radar sensors are used for the detection of other vehicles in the driving corridor because of their ability to directly measure an object's distance and relative velocity.

There are many car-following models known in literature, with most of them originating from the area of traffic flow simulation with varying complexity and calculation demands. Famous models are the Newell's car-following model,[133] Gipps' model[134] and the Intelligent Driver Model (IDM).[135] For example, the IDM calculates an acceleration demand due to following conditions and compares this acceleration demand to the actual acceleration. The main challenge in using a model is finding parameters for fitting the models to measurement data. Here, a simplified model is selected based on driving physics. To decide whether speed dependent indicators should be activated or not, the only relevant information needed is if the driver is following another vehicle or not. Thus, only binary information is needed without a calculation of speed or acceleration demand.

The model applied here is based on distances of objects detected by the front radar sensors d_{obj}, their relative velocities $v_{obj,rel}$, and the ego-vehicle's speed v_{ego}. The following values are calculated for each relevant object detected by the sensors:

- time gap τ for steady following without relative speed between the vehicles: $\tau = \frac{d_{obj}}{v_{ego}}$
- time to collision ttc for approaching a slower leading vehicle: $ttc = -\frac{d_{obj}}{v_{rel}}$
- time t_{obj} an object is tracked by the radar sensors: $t_{obj} = t_{obj,1st} - t_{obj,last}$

Objects detected by the radar sensors are considered relevant if they are detected within a range ε_{pp} in the longitudinal direction of the ego-vehicle's path and a lateral range $\pm \gamma_y$ to the ego-vehicle's path as shown in Figure 5-8. The path is estimated using

[133] Newell, G. F.: A simplified car-following theory (2002).

[134] Gipps, P. G.: Car-following model (1981), pp. 105–111.

[135] Treiber, M.; Kesting, A.: Elementary Car-Following Models (2013), pp. 187–191.

a linear single-track model.[136] All objects detected at distances $d_{pp} > \gamma_{pp,lim}$ or $|d_y| > \gamma_{y,lim}$ are ignored in follow behavior calculations, as well as objects that are only detected for a time span $t_{obj} < t_{min}$. This is done due to the increasing inaccuracy of path prediction by the single track model for increasing distances.

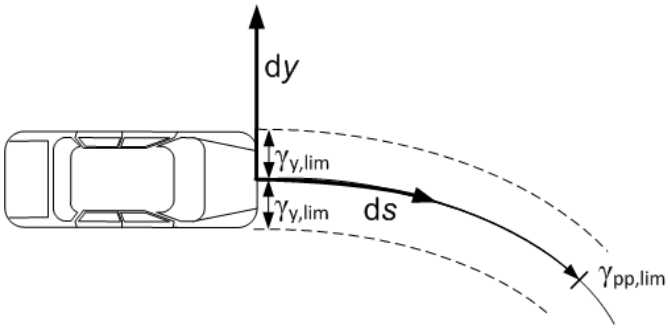

Figure 5-8: Relevant objects of environment perception sensors

In the intention detection system, vehicle follow behavior is activated if at least one of the following conditions is fulfilled within a discrete calculation step:

- $0 < -\frac{d_{obj}}{v_{rel}} < ttc_{lim}$
- $0 < \frac{d_{obj}}{v_{ego}} < \tau_{lim}$
- ego-vehicle has stopped ($v_{ego} = 0$) behind a standing object (stationary or leading vehicle detected braking to standstill)
- start up after standstill with $v < v_{lim}$

Values for the limits used above are found applying a two-step procedure:

In the first step, values of $\gamma_{pp,lim}$ and $\gamma_{y,lim}$ are determined by analyzing measurement data from real test drives. Ground truth for existence of relevant objects in the predicted path is determined by analyzing video data recorded with measurement data. Iteratively varying $\gamma_{pp,lim}$ and $\gamma_{y,lim}$ leads to a selection of values that offers the best compromise between true positives and false negatives. For determination of ttc_{lim} and τ_{lim}, a test group of five people was asked to classify and label vehicle following behavior by watching recorded video scenes from pre-tests. Time gaps τ and time to collision ttc for relevant objects are calculated for the scenes using the objects detected by the vehicle's radar sensors. Based on scenes classified as vehicle following behavior by the test group, values for ttc_{lim} and τ_{lim} are determined. To ignore outliers, the smallest and largest 5% of the values in the distribution of follow behavior are ignored. The value of v_{lim} is determined by analyzing the ego-vehicle's speed at the time the driver initializes

[136] Schramm, D. et al.: Vehicle dynamics (2014), pp. 223–226.

a turn after having stopped during the intersection approach. Figure 5-9 shows the share of speeds in the test drives when a maneuver is initialized after starting from standstill. Here, a value of $v_{lim} = 26\ \frac{\text{km}}{\text{h}}$, corresponding to 95 % of all events, is selected for the range where follow dependent indicators are ignored after stopping within an intersection approach. Note that turn initialization is determined according to section 6.3.2 and can therefore be at $v_{ego} = 0\ \frac{\text{km}}{\text{h}}$ as well.

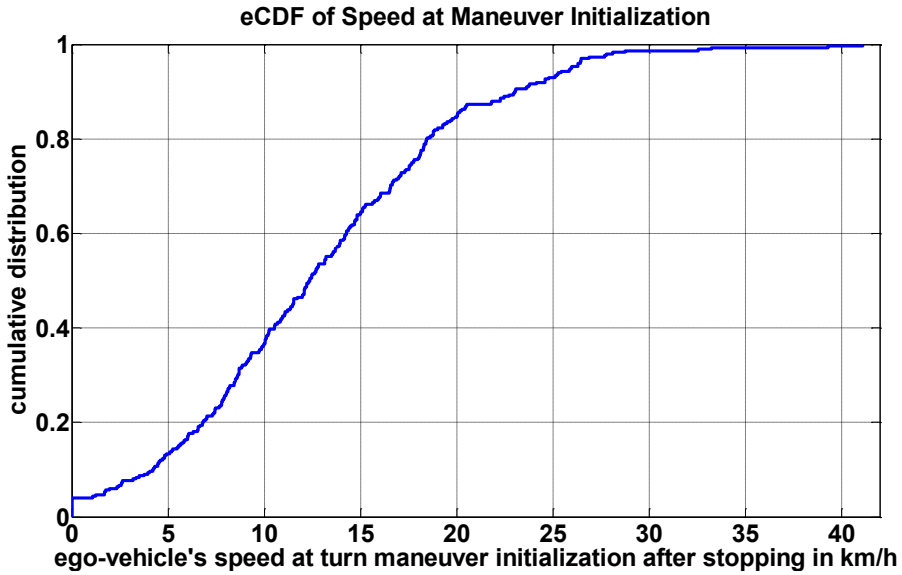

Figure 5-9: CDF of vehicle's speed initializing a turn maneuver

When vehicle following behavior, red traffic lights, or starting after stopping is detected, the free driving dependent indicators are not used in the inference system and the maneuver prediction is done solely with the remaining free driving independent indicators.

5.4 Indicators of the Prediction System

Based on the classification of information presented in section 2, the following section presents indicators that rely on the information and have been analyzed for their prediction capability. Indicators introduced in the following are grouped depending on their type of input data. Indicators of the first group described in section 5.4.1 are set up directly using measurement data acquired from driving dynamics and control inputs as described in section 5.1.3. The second group contains indicators that describe the driver's behavior within the vehicle. Indicators introduced here are based on the driver's head pose and gaze tracking. Indicators of the third group, using information from environment perception systems during intersection approach, are described in section 5.4.3. The fourth group introduced in section 5.4.4 contains indicators that evaluate the driver's approach behavior at an intersection and consist of information calculated

from the vehicle's motion in relation to the intersection. The difference to the first group is that data used here does not need to have physical counterparts and is not provided directly by the vehicle's sensor systems. Finally, the last group described in section 5.4.5 contains indicators based on general intersection information.

5.4.1 Driving Dynamics and Driver's Control Inputs

Indicators of this group are set up by analyzing the number of occurrences of the corresponding values for each maneuver. All indicators related to the vehicle's speed are only considered while the vehicle is in free driving conditions.

- Ego-vehicle's Speed Indicator
  The ego-vehicle's speed curve is directly connected to the maneuver to be executed under the following conditions: The ego-vehicle is in free driving and the intersection's priority regulations do not demand the vehicle slow down for any maneuver. Under these conditions, if the vehicle approaches an intersection with regular urban cruising speed (40 - 50 km/h) and slows down, this behavior is directly connected to a turn maneuver as shown by measurement data in Figure 5-10. Thus, the ego-vehicle's speed is analyzed directly in an indicator.

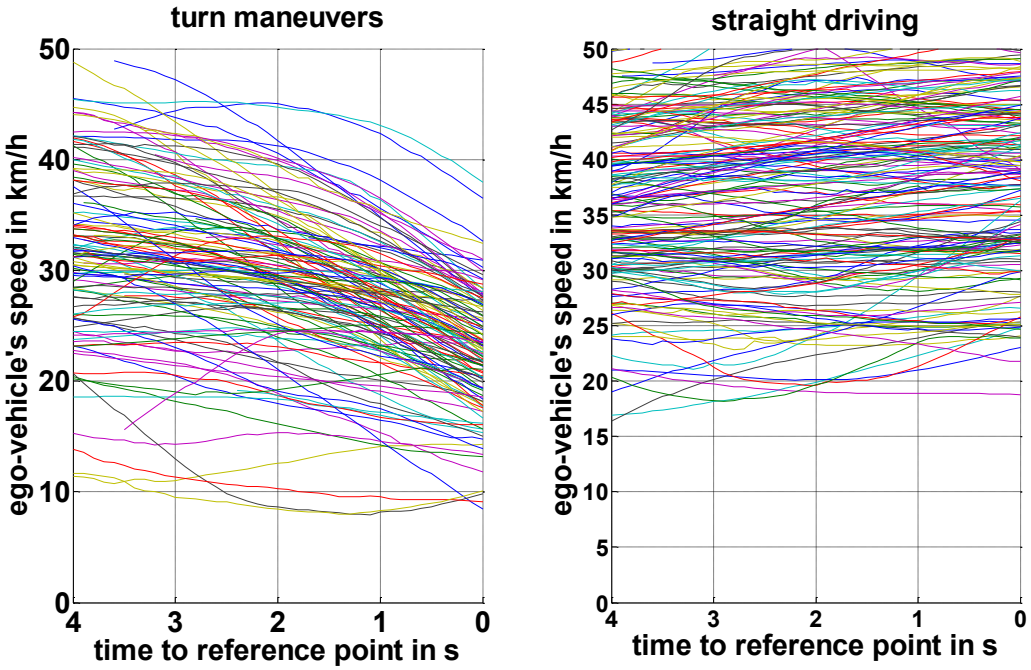

Figure 5-10: Speed profiles in free driving conditions

- Longitudinal Acceleration Indicator
  Analogous to the ego-vehicle's speed, the vehicle's longitudinal acceleration is analyzed in a separate indicator. Although both values are related to each other, the acceleration indicator is set up for means of performance comparison with the speed indicator.

- Accelerator and Brake Pedal Operation
  The control inputs to modify the vehicle's speed are mainly given by the accelerator and brake pedal. Thus, both operations are analyzed in separate indicators.
- Current Gear
  For vehicles equipped with a manual transmission, the current gear selected by the driver is analyzed in an indicator under free driving conditions.

5.4.2 Driver's Behavior in Vehicle

This group consists of indicators describing the driver's behavior and motions within the vehicle's cockpit. Here, data acquired via the head and gaze tracking system mounted inside the test vehicle is used to set up indicators. The frequency of occurrences is analyzed for each maneuver in the same way used to set up all other indicators.

- Head and Gaze Rotation Angle
  Several approaches to using the driver's viewing behavior during intersection approach can be found in the literature.[137] The same applies to the driver's head rotations in preparation for maneuver initialization.[138] Thus, the driver's gaze rotations and head rotations are analyzed in separate indicators. This is done with respect to the vehicle's motion state. While the gaze direction and head rotation are supposed to be related to the driver's intentions while the vehicle is moving, this assumption cannot be maintained during standstill. Here, driver's attention might be occupied by arbitrary objects outside or inside the vehicle unrelated to the driving task.
- Fixed Objects in the Vehicle's Cockpit
  A virtual model of the vehicle's cockpit is set up containing positions of selected elements of the real vehicle's cockpit. Among others, the vehicle's side and center rear-view mirrors are of interest for maneuver prediction. The frequency of driver's mirror fixations is analyzed in the underlying indicator.
- Patterns in Head and Gaze Motion
  Aside from direct analysis of the input signal in each discrete calculation step, the indicator concept also allows for the recognition of patterns in input signals (e.g. repeated changes from left to right).

---

[137] A recent survey is given in: Liebner, M.; Klanner, F.: Driver Intent Inference and Risk Assessment (2016), pp. 891–915.

[138] Land, M. F.: Predictable eye-head coordination (1992), pp. 318–320.

5.4.3 Environment Perception

Indicators of this group use data from sensor systems for perceiving the surroundings outside the ego-vehicle. In principal, this can be any kind of sensor such as radar, camera, lidar, etc. The prototypic implementation done here is based on environment perception by radar and camera sensors.

- Direction Arrows on Road Surface
  All direction arrow indicators are set up in the same way. The indicators only differ in the type of direction arrow detected and the position of the arrows in relation to the ego-vehicle. Direction arrows on the road surface dictate the maneuver that is allowed while driving in the current lane. Theoretically, the likelihood of the maneuver related to the detected direction arrow can be assumed to be one, while all likelihoods of alternative maneuvers are set to zero. This approach is not applicable in real driving due to several reasons:

  Information from detected direction arrows is saved until another arrow is detected or the intersection is traversed. Using the save functionality, lane changes of the ego-vehicle may lead to false maneuver likelihoods if the lane changes are not detected.[139] Furthermore, deriving the predicted maneuver directly from the direction arrow implies an ideal perception. Considering real driving conditions, direction arrows that are partly damaged or worn-out exist, which lead to false detections. Further reasons for imperfect detections are road works with changed traffic routing or arrows not visible due to other traffic participants as shown in Figure 5-11. Here, the straight arrow on the right lane is hardly noticeable due to other traffic participants obstructing the view.

Figure 5-11: Example of imperfect environment perception

[139] See Annex D for more details.

The calculation of likelihoods is done by calculating relative frequencies for each arrow in each lane according to section 5.1.3. For lanes adjacent to the ego-lane, some boundaries arise: Arrows indicating the driving direction of an adjacent lane limit potential maneuvers for vehicles in the ego-lane: Multiple lanes have to be collision free. This means, that no maneuver from any lane may lead to crossing an adjacent lane heading in the same direction. An exception from this rule is only applied in the case of hook turns.[140]

- Existence and Traffic Directions of Adjacent Lanes
  Information from the existence of additional lanes next to the ego-lane are used to limit the ego-vehicle's potential maneuvers. Following the principle of collision free lanes, a detected adjacent lane to the ego-vehicle precludes a turn maneuver on the side the lane is detected.[141] Thus, the information needed here is the existence of adjacent lanes to the left and right and their traffic directions. While in right hand traffic adjacent lanes to the right are required to have the same traffic direction as the ego-lane, an adjacent lane to the left can either be heading the same direction or oncoming. This information can either be acquired via V2X communication or environment perception sensors. Here, an implementation based on radar sensors is applied. To determine the traffic direction of other traffic participants (same direction or oncoming), their relative velocities and the ego-vehicle's speed are needed. In general, radar sensors perform well in measuring relative speeds of detected objects using the Doppler effect.[142] In addition, the implementation based on radar sensors is independent of influences of weather and illumination. The radar based approach also detects static objects and uses them to calculate the likelihood that an adjacent lane is nonexistent. The functional principle of the radar based lane detection model is given in annex B. If a lane with oncoming traffic to the left of the vehicle is detected, the lane is not accessible for the ego-vehicle and no information for maneuver prediction is acquired. The calculation of transfer functions is done accordingly with the other indicators described above by statistical evaluation of the training data.
- Maneuver Detection of Leading Vehicle
  The indicator is based on detecting the maneuver a preceding object O is performing. This can be either done by V2V communication or by environment

[140] Currie, G.; Reynolds, J.: Hook Turns (2011), pp. 10–19.

[141] Note that this is only valid for roads with no more than one turning lane for each direction. However, intersections with multiple lanes turning the same direction can be identified via digital map data. If the ego-vehicle approaches such an intersection, the indicator introduced here is not applied.

[142] Winner, H.: Automotive RADAR (2016), pp. 332–333.

perception systems. The assumption used in this indicator is that the ego-vehicle will perform the same maneuver as the leading vehicle. Figure 5-12 shows the basic principle of the indicator.

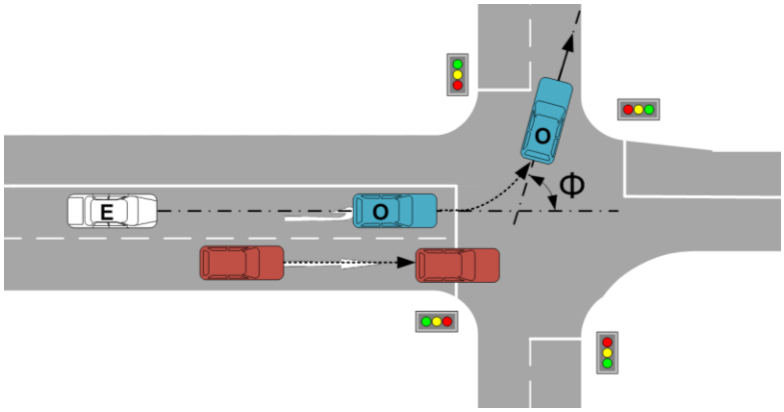

Figure 5-12: Angle of leading vehicle

This assumption is only valid in cases where intersections are equipped with separate lanes for each maneuver. For example, this information could be provided by localization on a digital map. The implementation selected here is based on tracking other traffic participants detected by the ego-vehicle's radar sensors. The leading vehicle in the ego-vehicle's lane is distinguished from all detected objects. The path the leading vehicle takes is analyzed during intersection approach. The relative angle ϕ between the ego-vehicle's heading and the leading vehicle's heading is evaluated. If a deviation $|\phi| > \phi_{\text{lim}}$ between both headings is determined for a minimum time span Δt, the lead vehicle is considered to be turning. By definition, this indicator is only applicable if a leading vehicle is present. Although separate direction lanes are marked with direction arrows in most cases, this indicator raises the prediction performance if direction arrows on the road surface have not been detected.

5.4.4 Intersection Approach Behavior

The vehicle's speed curve in correlation with the distance remaining to the intersection is used to calculate further values of the driver's intersection approach behavior. Indicators of this type are only applied to intersection classes without demands to slow down for any maneuver. Some of the indicators introduced here rely on a predicted lateral acceleration when turning. Thus, a maximum radius R for a potential turn maneuver at the intersection is estimated. The radius is determined using a a circle with radius R and tangential transitions between straight parts and the circle as shown in Figure 5-13. The distance d_{act} between the ego-vehicle and the intersection's center as well as the angle α between the roads are extracted from the digital map and the localization of the ego-

vehicle. The line between the circle's center and the intersection center is the bisector of the angle α between the two roads. Basic geometry results in:

$$R = \frac{d_{act}}{\tan \varphi} \tag{5-6}$$

$$\varphi = \frac{\pi - \alpha}{2} \tag{5-7}$$

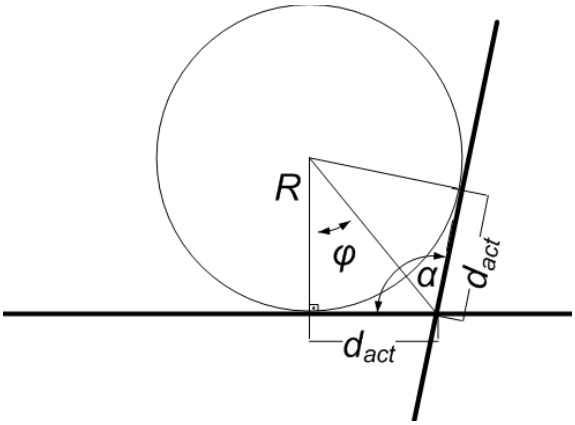

Figure 5-13: Radius estimation

Thus, the max. radius R of a turn the ego-vehicle can perform from its current position is given by:

$$R = \frac{d_{act}}{\tan\left(\frac{1}{2}(\pi - \alpha)\right)} \tag{5-8}$$

In cases of intersections allowing turn maneuvers to either the left or the right, radii for both options are calculated and evaluated independently.

Using R, the predicted lateral acceleration $a_{y,R}$ for potential turn maneuver is given by:

$$a_{y,R} = \frac{{v_{ego}}^2}{R} = \frac{{v_{ego}}^2}{d_{act}} \cdot \tan\left(\frac{1}{2}(\pi - \alpha)\right) \tag{5-9}$$

The acceleration $a_{y,R}$ is compared to maximum lateral accelerations $a_{y,max}$ tolerated by drivers in urban turn maneuvers. Data from the test study of this work shows that $|a_{y,max}| = 2.2\ \frac{m}{s^2}$ for right turns and $|a_{y,max}| = 1.7\ \frac{m}{s^2}$ is not exceed in 95 % of all turns in test drives. The share of predicted accelerations $a_{y,R}$ on priority roads is given in Figure 5-14. Here, each curve shows $a_{y,R}$ for all intersection approaches of the same maneuver (right/left/straight) one second prior to initialization. The figure also shows $|a_{y,max}|$ as dash-dotted vertical lines.

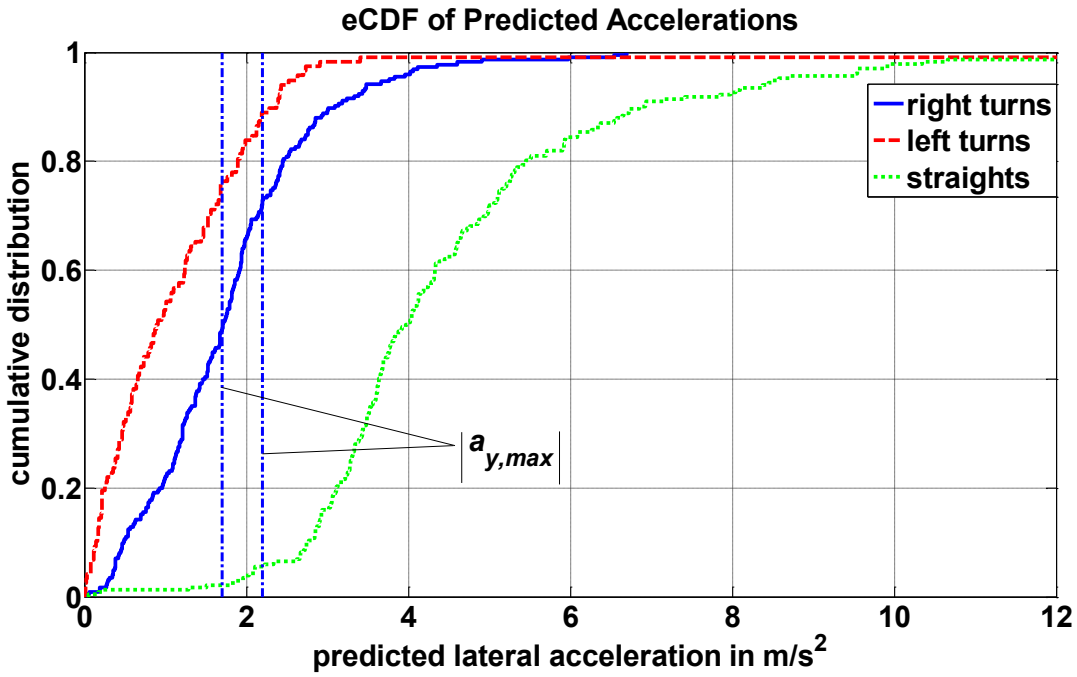

Figure 5-14: Share of predicted lateral acceleration

Figure 5-14 shows that $|a_{y,R}|$ exceeds $|a_{y,max}|$ in 26.7 % of all right turns as well as in 23.7 % of all left turns. This is caused by two effects: R is dependent on the localization and map accuracy. Furthermore, R is calculated using a circle for ego-vehicle's turning trajectory. Analyzing real trajectories shows that driver's turn trajectories aren't circles with constant radius. For example, turning can be modeled as a phase of constant curvature and a transition phase at the beginning and the end.[143] In addition, analyzing data from test drives shows that in 96.6 % of all recorded right turns, drivers enter the transition phase at higher speeds compared to the speed at the turns' apex.

- Estimated Lateral Acceleration for Turn Maneuvers
  Figure 5-14 shows that the majority of straight drives (> 94 %) result in estimated lateral accelerations $|a_{y,R}| > |a_{y,max}|$ one second before a maneuver is initialized. Thus, the predicted acceleration $a_{y,R}$ is beneficial for discriminating straight driving from turn maneuvers. The indicator's transfer function is calculated by statistical evaluation of discretized values of $a_{y,R}$ using N intervals as described above.

[143] Alhayaseen, W. et al.: Variation of Left-turning Vehicle (2011), p.1550.

- Braking to Maintain Maximum Lateral Acceleration
  Based on $a_{y,R}$, the necessary speed reduction for comfortable turning speeds is calculated. If $|a_{y,R}| > |a_{y,max}|$, the potential speed reduction Δv_{turn} needed for turning with $|a_y| < |a_{y,max}|$ is calculated by:

$$v_{comf} = \sqrt{a_{y,max} \cdot R} \tag{5-10}$$

$$\Delta v_{\text{turn}} = v_{ego} - v_{comf} \tag{5-11}$$

  The amount Δv_{turn} is evaluated statistically by discretizing Δv_{turn} to a number of N predefined intervals covering the range of Δv_{turn} for all potential maneuvers.
- Predicted Stop Distance
  An alternative method that does not use an estimated radius of potential turn maneuvers is based on predicting a (theoretical) stop near the intersection center. Extrapolating the ego-vehicle's actual speed v_{ego} and acceleration a_{lon} under the assumption of constant acceleration in longitudinal direction, the distance needed for braking to stop is given by:

$$d_{brake} = -\frac{v_{ego}^2}{2a_{lon}}; a_{lon} < 0 \tag{5-12}$$

  Due to the relevant area at the intersection (see section 5.2), d_{brake} is limited to $0 < d_{brake} < 60$ m. Using the remaining current distance to the intersection center, the predicted stopping distance d_{pre} in relation to the intersection center is calculated:

$$d_{pre} = d_{brake} - d_{act} \tag{5-13}$$

  Figure 5-15 shows an exemplary calculation of d_{pre} based on measurement data of an approach sequence with a consecutive right turn maneuver.
  A stop of the ego-vehicle near the intersection center is predicted if $\dot{d}_{pre} \leq \gamma_{lim}$ is detected for a minimum time t during the intersection approach. The derivation $\dot{d}_{pre}$ resulting from Figure 5-15 is shown in Figure 5-16.

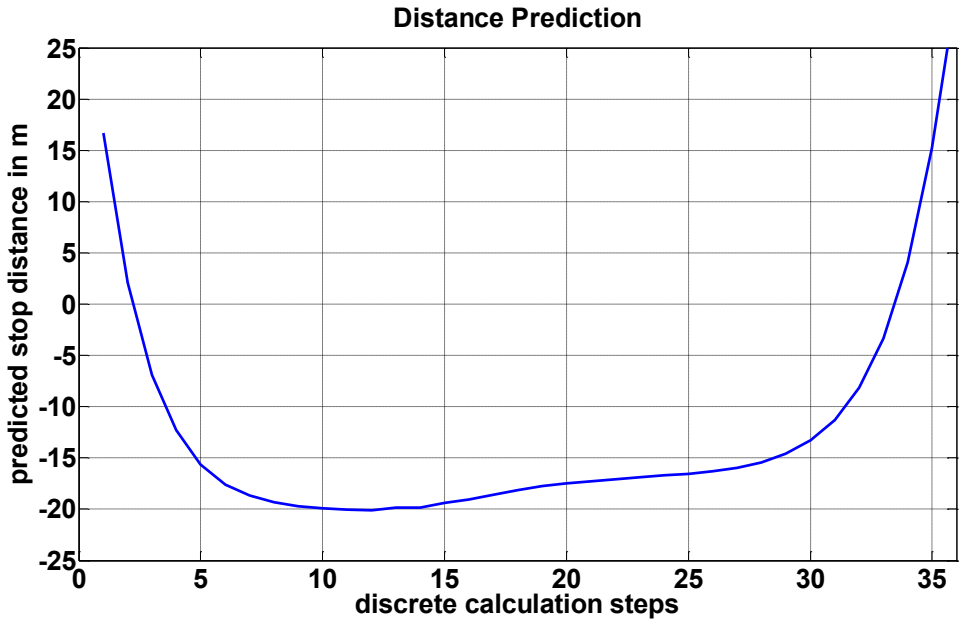

Figure 5-15: Exemplary predicted stopping distance

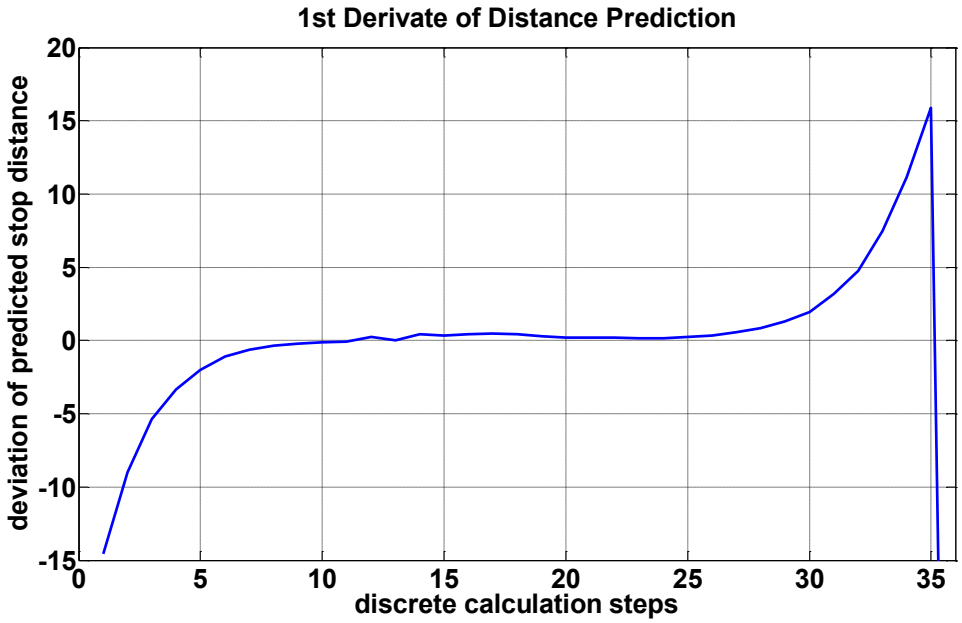

Figure 5-16: $\dot{d}_{pre}$ of exemplary approach

Note that this does not mean that the vehicle will come to a stop in reality. Figure 5-17 summarizes the predicted stops calculated for priority roads. The figure shows that numerous stops are predicted during the intersection approach for right and left turn maneuvers. Note that in accordance with the definition of d_{pre}, values $d_{pre} < 0$ correspond to predicted stops of the ego-vehicle before the intersection center and vice versa. While this indicator is not capable of discriminating right and left turn maneuvers, it performs well in separating turn

maneuvers from straight drives. Aside from few outliers, no stops are predicted for straight driving maneuvers within the range of ±30 m. Reviewing the straight driving maneuvers resulting in the outliers shows that two of the outliers are generated due to failed detection of vehicle follow conditions. The third outlier was generated by the driver's behavior in free driving conditions. The test subject did not correctly interpret the priority regulation and slowed down to give way to a vehicle from the right, even though the ego-vehicle was driving on a priority road.

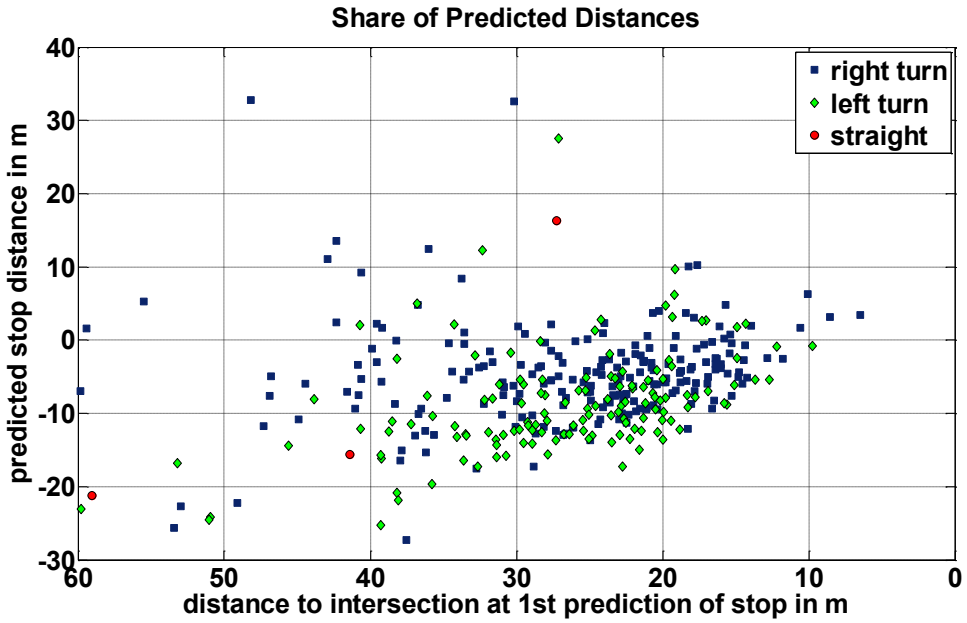

Figure 5-17: Predicted stopping distance

Using test drive data, the occurrence of predicted stops near the intersection center $(d_{pre} \leq d_{pre,lim})$ is summed up for each turn maneuver and straight driving. These sums are used to calculate the indicator's transfer functions.

The benefit of this indicator is its availability in an early phase of the intersection approach. Figure 5-18 shows the share of distances where a stop is predicted during intersection approach sequences. The plotted line shows that less than 10 % of all predicted stops are detected at distances $d < 16$ m to the intersection center.

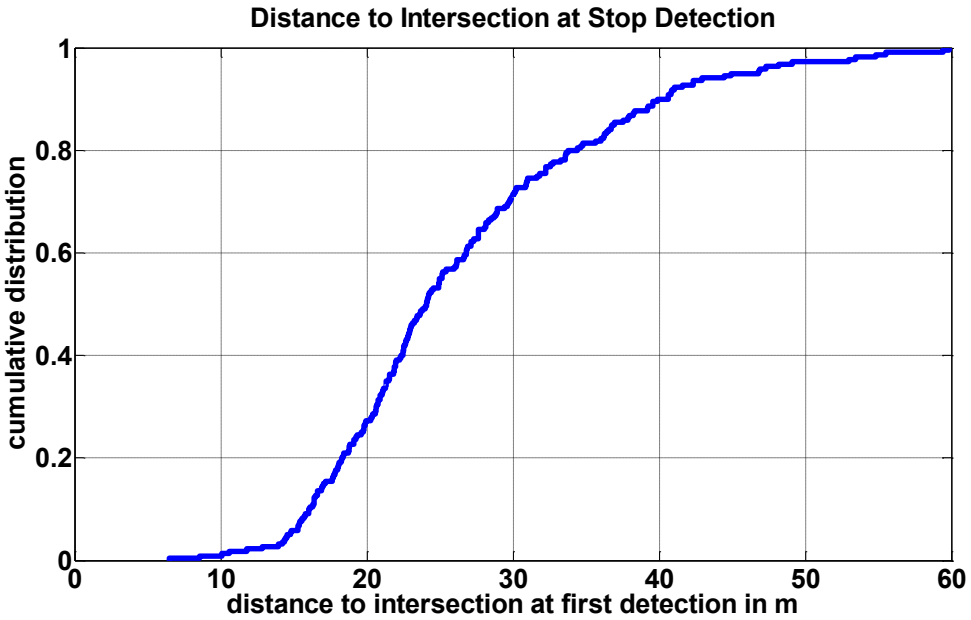

Figure 5-18: eCDF of predicted stopping distance

- Lane Change Maneuver (Ego-Vehicle)
  At intersections with multiple lanes heading towards the intersection, lane change maneuvers performed during intersection approach might be related to the maneuver intended by the driver, but don't have to be. On the one hand, lane change maneuvers are done to get into dedicated lanes for a maneuver intended by driver. In this case, the information is beneficial for maneuver prediction. On the other hand, lane change maneuvers are executed in preparation for maneuvers pending at the intersection after the current one, or just due to traffic conditions. Thus, aside from the challenge of detecting lane change maneuvers in urban conditions, a lane change maneuver cannot be used for reliable maneuver prediction at the intersection.

5.4.5 General Information

- Road Existence

  The road existence indicator is based on the number of potential traffic directions at the intersection the ego-vehicle is heading to. During intersection approach, the upcoming intersection is checked for the existence of roads for each potential maneuver (right or left turn or straight driving) and turning restrictions. If a road corresponding to a potential maneuver is found at the intersection, the legality of the maneuver is checked. If the related maneuver is allowed for vehicles on the road the ego-vehicle is using (no entering a one-way road from the wrong direction, no turn restrictions), the potential maneuver is considered as valid. Taking a number of M valid potential maneuvers into account, the road

existence indicator is set to $p_{ex} = \frac{1}{M}$ for each valid maneuver. For the intersections considered in this work, M is within the range of one and three. Although it is not possible to predict the maneuver to be executed if more than one maneuver is valid, the overall likelihood of non-valid maneuvers can be reduced by setting p_{ex} to zero for these maneuvers or excluding the maneuver options completely. In cases of M valid potential maneuvers, the road existence indicator does not affect the overall prediction performance.

- Priority Regulation
  Indicators' transfer functions are swapped depending on the priority regulation of the intersection the vehicle is heading to, as described in section 4.4.2. Thus, the priority regulation is not an indicator itself, but is used to select the transfer functions corresponding to the actual priority regulation. Furthermore, depending on the priority regulation, indicators are enabled or disabled if they do not hold information for the prediction of the pending maneuver. For example, for priority regulations demanding the driver to slow down or stop for any maneuver, all speed-related indicators are ignored.

5.5 Indicator Quality Assessment

In order to decide which indicator is beneficial for each intersection class, a method for assessing the indicators' quality is needed. General requirements for an indicator quality measure are:

- true positive detection rate
- quality of discrimination among alternatives (sensitivity)
- availability of indicator

All factors have to be considered for assessing an indicator and selecting indicators to be used for maneuver prediction. The indicator assessment is done independently for each intersection class allowing for the selection of indicators according to their quality.

5.5.1 Indicator Quality Measure

Following the basics of likelihood calculations as introduced above, the indicators' quality of discrimination among several alternatives is considered. If an indicator outputs likelihoods being nearly the same for all maneuvers, the sensitivity is near zero (like in the left part of Figure 5-19). Otherwise, if an indicator outputs likelihoods that are clearly different for alternative maneuver options, the sensitivity is high (close to one) as shown in the right part of Figure 5-19. The sensitivity describes the "sharpness"

of the calculated maneuver likelihoods. Given that by the system's design and the method applied to calculate transfer functions, assessing the indicators' discrimination quality automatically contains the indicators' true positive detection rates.

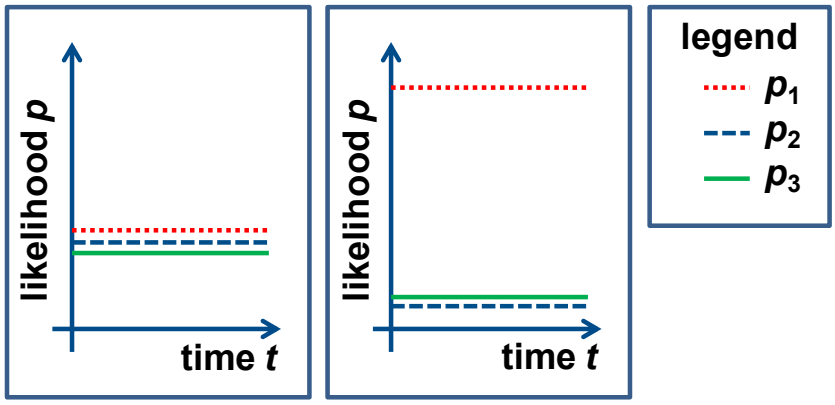

Figure 5-19: Sensitivity measure

The sensitivity measure SM evaluates the maneuver likelihoods in relation to a uniform distribution of likelihoods. Uniform distribution is given for : $p_1 = p_2 = \cdots = p_i = \frac{1}{M}$ for M maneuver options with $p_i = \frac{N_i}{N_{total}}$ representing maneuver likelihoods based on relative frequencies. Because maneuver likelihoods $0 \leq p_i \leq \frac{1}{M}$ lead to negative terms, squared differences are used instead, also known as geometric distances. Thus, the sensitivity measure is defined as:

$$SM = \sum_{i=1}^{M} \sqrt{\left(p_i - \frac{1}{M}\right)^2} \tag{5-14}$$

In case of $M = 3$ potential maneuvers, the sensitivity measure is given by:

$$S = \sqrt{\left(p_1 - \frac{1}{M}\right)^2 + \left(p_2 - \frac{1}{M}\right)^2 + \left(p_3 - \frac{1}{M}\right)^2} \tag{5-15}$$

Transforming equation (5-15) using $\sum_{i=1}^{M} p_i = 1$ leads to a simplified form:

$$SM = \sqrt{p_1^2 + p_2^2 + p_3^2 - \frac{1}{M}} \tag{5-16}$$

While SM in the given form returns $SM = 0$ in case of uniform distribution $p_i = \frac{1}{M}$, the maximum value returned in cases of optimal separation for $p = [1|0|0]$ is $SM = \sqrt{\frac{M-1}{M}} = \sqrt{\frac{2}{3}}$. Therefore, a linear transformation by the factor $w_{trans} = 1/\sqrt{(M-1)/M}$ is applied to SM, resulting in the quality measure QM_{org}:

$$QM_{org}(p_1, \dots, p_M) = \frac{1}{\sqrt{\frac{M-1}{M}}} \cdot \sqrt{\sum_{i=1}^{M} p_i^2 - \frac{1}{M}} \tag{5-17}$$

In the case $M = 3$ maneuver options, QM is given by:

$$QM_{org}(p_1, p_2, p_3) = \frac{1}{\sqrt{\frac{2}{3}}} \cdot \sqrt{p_1^2 + p_2^2 + p_3^2 - \frac{1}{M}} \tag{5-18}$$

Note that QM_{org} returns a sensitivity value in the range $0 \leq QM \leq 1$ that can be interpreted as percentage.

5.5.2 Sparsely Occupied Intervals

Using transfer functions to calculate maneuver likelihoods follows the basic assumptions that relative frequencies observed within one interval i correspond to the real (but unknown) share of data:

$$\begin{bmatrix} p_{obs,i,r} \\ p_{obs,i,l} \\ p_{obs,i,s} \end{bmatrix} = \begin{bmatrix} p_{real,i,r} \\ p_{real,i,l} \\ p_{real,i,s} \end{bmatrix} \tag{5-19}$$

The assumption is not valid when an interval is sparsely occupied and has only few entries N for each potential maneuver. In extreme cases, an interval occupied with $N_1 = 1, N_2 = N_3 = 0$ returns a quality measure $QM = 1$, but the information is useless due to $\sum_{i=1}^{M} N_i = 1$. Thus, sparsely occupied intervals need to be detected and treated in a special way. The simplest way to detect barren intervals is to apply a limit N_{lim} that the interval has to exceed: $\sum_{i=1}^{M} N_i \geq N_{lim}$. Arbitrary values for N_{lim} can be used without reasoning for the selection of N_{lim}.

A more sophisticated way introduced here is based on a trust in the sensitivity determined for each interval. The trust in the observed distribution is based on the sensitivity of the quality measure to changes in the input values. The trust tr is calculated based on a total of $M + 1$ quality measures. In addition to $QM_{org}\left(p_{1,} \dots p_M\right)$ based on the input values $N_1, \dots N_M$, a total of M modified values $QM_{mod,i}$ is calculated with either the i-th likelihood p_i being replaced by:

$$p_{i,mod} = \frac{N_{i,mod}}{N_{total}} = \frac{N_i + \chi}{N_{total}} \tag{5-20}$$

Aside from the frequencies of the occurrence of N_i , $\chi \in \mathbb{N}$ is used to modify N_i to analyze the sensitivity of QM.

$$QM_{i,mod} = \frac{1}{\sqrt{\frac{M-1}{M}}} \cdot \begin{cases} \sqrt{p_{1,mod}^2 + \cdots + p_M^2 - \frac{1}{M}} \; ; & \text{for } i = 1 \\ \sqrt{p_1^2 + \cdots + p_{i,mod}^2 + \cdots + p_M^2 - \frac{1}{M}}; & \text{for } 1 < i < M \\ \sqrt{p_1^2 + \cdots + p_{M,mod}^2 - \frac{1}{M}} \; ; & \text{for } i = M \end{cases} \quad (5\text{-}21)$$

Based on the $M+1$ quality measures ($QM_{org} + M\ QM_{mod,i}$) a mistrust value $\overline{tr}$ is calculated by the differences of $QM_{mod,i}$ and QM_{org} , representing the gradient of the sensitivity measure QM_{org}:

$$\overline{tr} = \sum_{i=1}^{M} \left| QM_{org} - QM_{mod,i} \right| \quad (5\text{-}22)$$

For the example of $N_1 = 1, N_2 = N_3 = 0$, $\overline{tr}$ returns a value of $\overline{tr} = 1$, representing the highest possible distrust in the quality measure. Otherwise, intervals with $N_i \to \infty$ observations result in $\overline{tr} \to 0$. Thus, the trust tr in the calculated sensitivity measure is given by:

$$tr = 1 - \overline{tr} \quad (5\text{-}23)$$

Finally, the trust tr is combined with the interval's quality measure by multiplication:

$$QMT = QM \cdot tr \quad (5\text{-}24)$$

Only intervals with a high quality measure QM_{org} and sufficient number of observations N_i result in a highly trusted quality measure QMT. Thus, QMT can be used to assess the suitability of an indicators' interval for maneuver prediction.

The process of selecting indicators according to their quality is described in section 6.5. Furthermore, the QMT value is used for optimization of indicators as described in the following section. Taking sparsely occupied intervals into account as demonstrated above automatically contains an assessment of the indicators availability. Indicators based on conditions only available at seldom occurring events result in sparsely occupied intervals. Applying the quality measure of QMT identifies these indicators as well.

5.6 Optimization of Indicators

The prediction performance of indicators with transfer functions created by the range of input signals being discretized into N_b bins depends on the selected value of N_b. By the system's design with discrete bins, N_b has to be a natural number. The range of potential values of N_b is given by:

$$1 < N_b \leq \frac{r_{\max} - r_{\min}}{Res} \tag{5-25}$$

Here, r represents the range of the input signal and Res the resolution of the input signal. Using $N_b > N_{max} = \frac{r_{\max} - r_{\min}}{Res}$ bins results in empty bins. Selecting $N_b = 1$ is obviously not suitable for maneuver prediction: With a total of one bin used for the range of the input signal, transfer functions result in $p = \frac{1}{M}$ for each of the M potential maneuvers. Thus, $N_b > 1$ has to be selected. Using a high number of bins (e.g. $N_b = N_{max}$) results in sparse occupation of bins. The less samples are contained in each bin, the higher the dependency on the training data is and the risk of overfitting increases. The optimization is carried out as follows: N_b is varied within the range $1 < N_b \leq N_{max}$ with the training data separated accordingly into N_b intervals. The quality measure QMT is calculated separately for each interval. To determine the quality of the variation of N_b, a measure to assess the share of all QMT is needed. Thus, an empirically cumulated distribution function of all trusted quality measures QMT of all training entries is calculated. The quality Q_{var} of the variation N_b is described by the arithmetic mean of all N_b QMT:

$$Q_{var} = \sum_{i=1}^{N_b} QMT_i \tag{5-26}$$

An example is given in the following for demonstration purposes: For the speed indicator introduced in section 5.4.1, input values are within $0\,\frac{\text{km}}{\text{h}} \leq v_{ego} \leq v_{max}$ with $v_{max} = 50\,\frac{\text{km}}{\text{h}}$ in urban conditions. The speed signal is recorded with a resolution of $Res = 0.1\,\frac{\text{km}}{\text{h}}$. Potential values of N to be analyzed in the optimization process are within the range $1 < N_b \leq 500$. The sensitivity calculation is carried out as described above. Figure 5-20 shows the resulting Q_{var} for all variations of $1 < N_b \leq 500$.

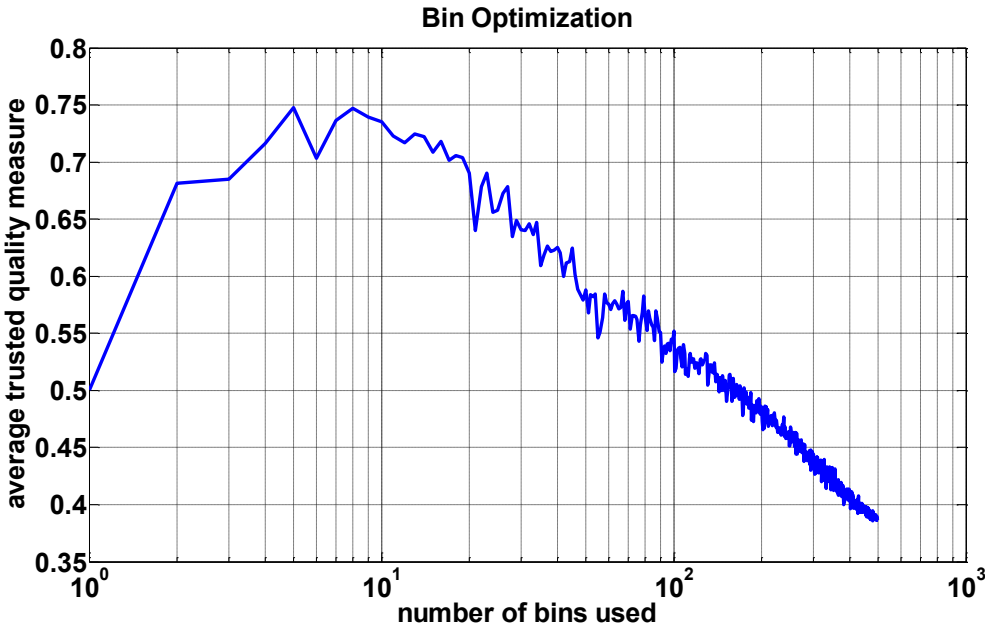

Figure 5-20: Quality Measures Q_{var}

The figure shows that in this example Q_{var} is the highest for $N_b = 8$ and is identified as best selection of N_b in the optimization process. The effect of the optimization process is demonstrated in Figure 5-21, comparing the eCDF of trusted quality measures for $N_b = 8$ bins and $N_b = 500$. The solid curve created with $N_b = 8$ bins clearly shows better performance than the dashed curve for $N_b = 500$ bins.

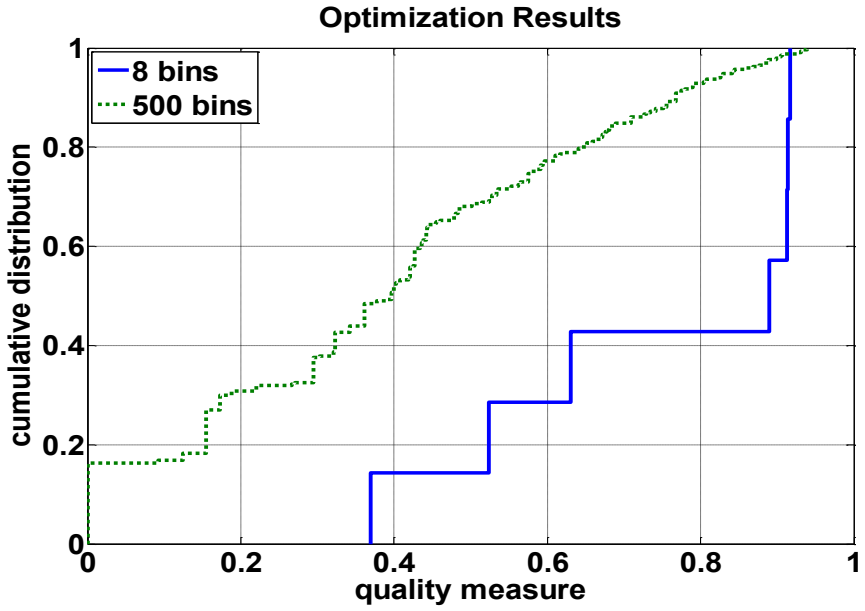

Figure 5-21: Effect of interval optimization

The optimization procedure to find the best number of intervals N_b as introduced above has to be carried out independently for each of the N_{di} distance intervals resulting in a total of N_{di} optimal values of N_b for each indicator.

5.7 Accuracy of Input Signals

This work analyzes the maneuver prediction capability by using automotive series sensor systems. Thus, the input signal inaccuracies and their effects on the maneuver predictions are analyzed. A detailed survey including which inaccuracy affects the calculation of which indicator is given in annex G. According to the calculations provided in the annex, neither inaccuracies in the steering wheel angle measurement, nor inaccuracies in the determination of the vehicle's speed affect the indicator calculation. Therefore, they are neglected here. The same applies to inaccuracies in the measurement of the vehicle's lateral acceleration, yaw rate and driver's pedal operations. Analyzing the accuracy of the head- and gaze tracking system shows that a maximum error of one interval can occur due to measurement inaccuracies and the detection of fixated objects on the vehicle's dashboard is not affected. None of the indicators based on radar sensors detecting environmental objects is affected by the measurement inaccuracies of state of the art radar sensors in any way. The precision the sensors offer in determining distance, relative velocity, and azimuth measurement is sufficient for all calculations done here. In contrast to data from sensors mentioned above, inaccuracies arising from the wrong or missing detections of road markings (especially direction arrows) clearly have an influence on the calculation of indicators and maneuver likelihoods. That is why imperfections in the perception of road markings are taken in account by using training data created statistically instead of directly deriving the maneuver from the direction arrow detected.[144] The accuracy of the ego-vehicle's position determined by the GNSS receiver does affect the calculation of indicators either directly (predicted stop distance, predicted lateral accelerations, e.g.) or indirectly by the distance intervals. All indicators relying on the distance remaining to the intersection center and using multiple transfer functions depending on the distance are affected by positioning errors. In the prototypic implementation used here, a total accuracy of $\varepsilon_{comb} = \pm 7.2$ m root mean square error (RMSE) is determined.[145] In reality, the road layout of urban intersections varies even within one intersection class depending on the features of each location, available space for the intersection, type of roads connected by the intersection, and amounts of traffic using the road.[146] Thus, a variety of intersection geometries exist even within one intersection class, resulting in different trajectories. Using the intersection center is an inaccuracy in itself because the layout of the intersection is not considered. However, the approach applied in this project deals with this inaccuracy by using training data acquired from a large set of intersections with varying geometry.

[144] See Section 5.4.3.

[145] See Annex G.

[146] Baier, R.: Richtlinien für die Anlage von Stadtstraßen (2007), p.109.

6 Evaluation

6.1 Inference Methods

The intention prediction system used here is set up by a total of n_{ind} independent indicators. For means of maneuver prediction on guidance level with a maximum of three potential maneuvers, each indicator generates three maneuver likelihoods. In case there is more than one indicator used in the prediction system, an inference method is needed to combine the results of the n_{ind} indicators. The inference method uses the 3 x n_{ind} indicator output values as inputs and calculates three probabilities for maneuver prediction: a probability for right turns, a probability for left turns, and a probability for straight driving. For means of maneuver prediction, the maneuver with the highest probability is selected as the most probable maneuver planned by the driver. Depending on the inference method, limits γ_{min} are integrated in the prediction process. Only in cases where the predicted maneuver has a probability that exceeds γ_{min}, is it considered a valid maneuver prediction. In general, integrating the limits γ_{min} lowers false-positive detection rates, but true-positive rates are likely to be lowered as well. In cases where the maneuver with the highest probability does not exceed γ_{min}, no maneuver is predicted by the system. Several inference methods are analyzed for combining indicator likelihoods into maneuver probabilities:

- Average Calculation

  Using the average function as an inference method is the simplest way of combining the indicator likelihoods into probabilities. Here, the average function is either applied to all right turn likelihoods $p_{i,right}$, to all left turn likelihoods $p_{i,left}$, or all straight driving likelihoods $p_{i,straight}$. The average probability AP for each maneuver m is given by:

  $$AP_m = \frac{1}{n_{ind} - n_{NaN}} \cdot \sum_{i=1}^{n_{ind}} p_{i,m} \tag{6-1}$$

  Likelihoods of non-applicable indicators due to the current intersection class or non-available indicators due to missing input data are ignored by the average function. The amount of non-available indicators n_{NaN} is subtracted from n_{ind} to avoid effects on the calculation of AP_m. Due to the computationally low complexity, the average function is a fast and flexible inference method. Further-

more, the average probabilities are output within the range [0,1]. Thus, limits γ_{min} can be directly integrated in the prediction process.

- Product Calculation

  The product approach is similar to the average calculation introduced above, but relies on using the product function instead of the average function. Thus, the compound probability for each maneuver $P_{cp,m}$ is given by the product of all indicator likelihoods p_i for one maneuver:

$$P_{cp,m} = \frac{1}{n_{ind} - n_{NaN}} \cdot \prod_{i=1}^{n_{ind}} p_{i,m} \tag{6-2}$$

  Likelihoods p_i of non-applicable indicators due to intersection classes or non-available indicators are ignored here as well by correcting n_{ind} with n_{NaN}. Comparing the product function to the average function shows the following differences: Using the product function as an inference method "penalizes" probabilities containing small likelihood values (e.g. $p_i < 0.1$). The computational needs and flexibility in the number of indicators is similar to the average function. However, integrating limits γ_{min} in the overall maneuver prediction is not directly possible. Although $P_{cp,m}$ still is within the range [0,1], it varies widely with the number of n_{ind} indicators used for the calculation. The more indicators with likelihoods $p_{i,m} < 1$ are used, the smaller $P_{cp,m}$ gets. For example, applying the average function to $n_{ind} = 1 \ldots 5$ indicators with $p_{i,m} = 0.5$ always results in the overall likelihood of $LH_m = 0.5$. In contrast, applying the product function returns $P_{cp,m} = 0.25$ for $n_{ind} = 2$, $P_{cp,m} = 0.125$ for $n_{ind} = 3$ and so on. Thus, limits γ_{min} have to be defined and selected based on the number of active indicators $n_{ind} - n_{NaN}$.

Instead of using an inference method and selecting the maximum probability provided by the inference method's output, a classifier can be used alternatively. Although a classifier uses the same inputs as an inference method, it directly returns a classification result based on the inputs. In the literature review, numerous systems based on machine learning approaches such as Bayesian networks, hidden Markov models, neuronal networks, and decision trees are identified. According to the guideline of classifier selection given by Pedregosa,[147,148] a Bayesian network is implemented and used as classifier. Bayesian networks have proven to be well performing classifiers in cases of noisy

[147] Pedregosa, F. et al.: Scikit-learn: Machine Learning in Python (2011).

[148] scikit-learn developers: Choosing the right estimator (2014).

data and inaccuracies in input data.[149] In general, Bayesian networks are represented by directed acyclic graphs and consist of nodes and edges. Each node represents a variable with probabilities according to the conditional probability table of each node. A detailed introduction to Bayesian networks is given by Jensen.[150]

6.2 Training and Test

To determine the prediction performance of a classifier in general, the classification performance of data not already known to the classifier is of interest.[151] If large amounts of data are available to train a classifier, the data provided is split into training data (to train a classifier and to set up the structure), validation data (to optimize classifiers parameters), and test data (to calculate the error rate). If only a limited amount of data is available, best practice is to split data into training and test datasets.[152] This procedure is selected in this work. While training data is used for the calculation of transfer functions, test data is used only for evaluation. Aside from achieving realistic performance results, separating training and test data ensures that the prediction system is able to deal with data not known to the system a priori. Here, a dilemma arises: To have as much training data as possible, the amount of unused data in the training process should be as small as possible. In contrast, the smaller the amount of test data becomes, the lower the confidence in the test results is and the higher the risk that the holdout (data not used in training and left for testing) is not representative for the entire collection of data.[151] In addition, test data should be stratified: The relation of test samples within the holdout should be equivalent to the relation of samples in the overall amount of data. There are several methods known in the literature to overcome this dilemma. A survey of existing methods is given by Nordman.[153]

Here, the *k*-fold cross-validation is applied by splitting all data available in *k* disjoint and stratified subsets. The classifier error rate is calculated *k* times. In each calculation, the *k*-th subset is used for testing and all remaining data is used for training. After performing *k* calculations, the average error rate of the classifier is known. According to Steinlein[153] and Witten[154], the most common method for evaluation in machine learning

[149] Rüdenauer, J.: Diplomarbeit, Probabilistische Verfahren zur Entscheidungsfindung (2003), p.29.

[150] Jensen, F. V.: An introduction to Bayesian networks (1996).

[151] Witten, I. H.; Frank, E.: Data Mining (2001), pp. 128–130.

[152] Steinlein, U.: Data Mining (2004), pp. 53–54.

[153] Nordman, A.: Data Mining - Evaluation (2011), pp. 3–6.

[154] Witten, I. H.; Frank, E.: Data Mining (2001), p.135.

applications has become a stratified ten-fold cross-validation. Indeed, ongoing research points out that a ten-fold cross-validation is the best selection method for evaluation classifiers.[155] Thus for the work presented here, a stratified ten-fold cross-validation is selected. The classifier used here predicts maneuvers (right/left/straight) and classification errors correspond to false predictions.

6.3 Reference Points

In order to evaluate the prediction performance of the approach introduced above, reference points need to be defined. These points represent the initialization of a maneuver and correspond to $t = 0$ s prediction time. All results shown in section 7 and 8 refer to the reference points defined here. In terms of maneuver prediction at intersections, various reference points are used in the literature. For instance, exemplary reference points are intersections centers or positions of artificial or real stopping lines.[156] Results referring to different reference points impede the comparison among other related prediction performance work and the approach used here. Furthermore, depending on the type of reference point that is used, inaccuracies arise.

6.3.1 Location Based Reference Points

For defining location based reference points at intersections, reference points are selected based on the area of potential collisions with other traffic participants. This area is given by the overlap of crossing roads at an intersection as shown in the left part of Figure 6-1. The point where the ego-vehicle enters the potential collision area generally corresponds to a stopping line in cases of stop sign or give-way regulated intersections.

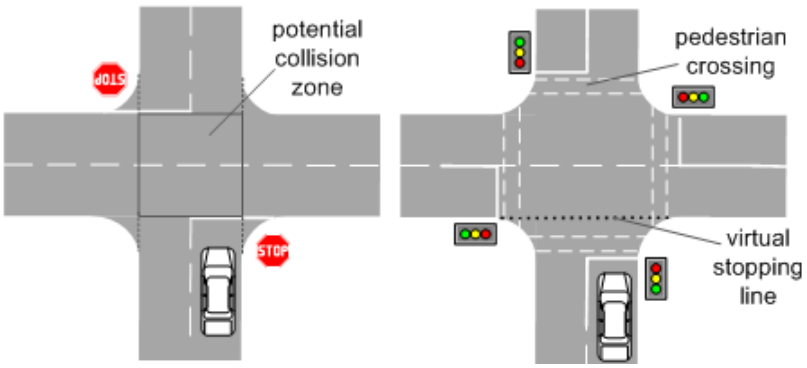

Figure 6-1: Potential collision area

[155] Markatou, M. et al.: Variance of Cross-Validation Estimators (2005), pp. 1127–1168.

[156] Mages, M.: Diss., Einbiege- und Kreuzenassistenten (2009), p.33.

If no stopping lines exist (e.g. priority to right regulations) or the stopping line marked on the road is set back due to pedestrian crossings, a "virtual stopping line" can be used as introduced by Mages.[156] This virtual line is acquired by an interpolation of the crossing road's lane marking next to the ego-vehicle, as depicted in the right part of Figure 6-1. The position of a (virtual) stopping line that serves as reference point for straight driving can be determined as follows: The position of the stopping line can either be determined directly by using GNSS localization and storing the position of stopping lines in the digital map. An approach following this principle and using many recorded trajectories from the same intersection to deal with inaccuracies arising from GNSS localization is presented by Ruhhammer et al.[157] However, using location based reference points at intersections has to face two main causes of errors: The inaccuracy of the vehicle's localization and the inaccuracy of the digital map used for determining the reference point. Especially with normal precision GNSS receivers, localization accuracy in urban areas varies within the range of several meters.[158] As shown in appendix G, the average positioning error of the localization used in this work is in the range of $\varepsilon_{loc} = \pm 7.2$ m. Taking a typical approach speed of $v_{ego} = 30\,\frac{\mathrm{km}}{\mathrm{h}}$ into account, the evaluation time inaccuracy created by inaccuracies in the reference point is within a range of $\Delta t = 1.7$ s. Hence, Δt is similar to the maneuver prediction time desired to achieve a prediction with the chance of collision avoidance. Within the example of an approach speed of $v_{ego} = 30\,\frac{\mathrm{km}}{\mathrm{h}}$, in order to reach a reference point induced time inaccuracy of $\Delta t < \pm 0.1$ s, a total localization error (positioning and digital map) $\varepsilon_{loc} < \pm 0.8$ m has to be maintained. Due to the selected system setup with normal precision navigation maps, neither the map nor the localization system offer sufficient precision to define location based reference points. In addition, selecting location based reference points does not take into account the beginnings of different maneuvers. In cases of right hand traffic and intersecting two-way roads, right turns are generally initialized at larger distances between the vehicle and the intersection center as compared to left turns. This is due to the fact that the target lane for right turns is closer to an intersection approaching vehicle than the target lane for left turns is, as illustrated in Figure 6-2. Using the same reference point for both maneuvers artificially adds extra time before a left turn is initialized.

---

[157] Ruhhammer, C. et al.: Crowdsourcing zum Erlernen von Kreuzungsparametern (2014), pp. 95–104.

[158] Modsching, M. et al.: GPS Accuracy in a medium size city (2006), p.214.

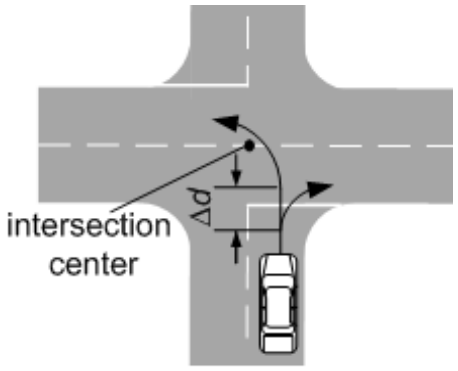

Figure 6-2: Maneuver initialization

6.3.2 Ego-motion-based Reference Points

In the following, an approach for the calculation of maneuver dependent reference points for turn maneuvers is introduced. The calculation is based solely on retrospective motion data measured by the ego-vehicle and is therefore free of inaccuracies arising from localization or a digital map. Reference points are calculated a posteriori for each intersection, depending on the maneuver executed and the trajectory the driver drove. This means that a unique reference point is calculated for every intersection approach sequence. The basic idea used here is to identify the apex of a turning motion and to relate the reference point to the apex of the turning trajectory.[159] The apex describes the center of the turning motion. The apex is reached at the point where half of the distance of the turn is travelled. The path driven while steering into the curve equals the path travelled while steering back to neutral. Figure 6-3 shows apex points for right and left turn maneuvers.

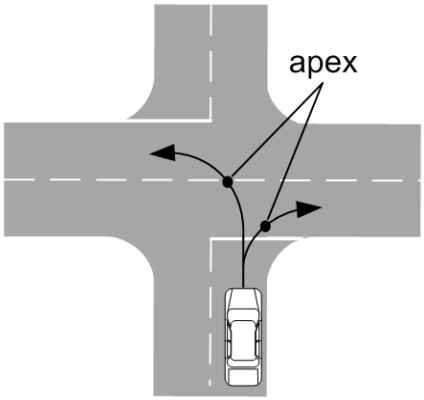

Figure 6-3: Reference points

[159] Rodemerk, C. et al.: Predicting Driver's Turn Intentions (2015), pp. 964–969.

Several approaches are known in the literature for curvature calculation. Following a survey given by Winner,[160] a hybrid curvature calculation based on the vehicle's yaw rate sensor $(\kappa_{\dot{\psi}})$ and the curvature calculation using the steering wheel angle (κ_δ) is applied. Details of the calculation are provided in annex H. The calculated curvatures $\kappa_{\dot{\psi}}$ and κ_δ are mixed in cases $v_{ego} < v_{trans}$ with v_{trans} being the transition speed. A speed dependent factor f_κ is defined using the transition speed of $v_{trans} = 20$ km/h:

$$f_\kappa = \mathrm{MIN}\left(1, \frac{v_{ego}}{v_{trans}}\right) \tag{6-3}$$

The total curvature κ_{total} is given by:

$$\kappa_{total} = \kappa_\delta \cdot (1 - f_\kappa) + \kappa_{\dot{\psi}} \cdot f_\kappa \tag{6-4}$$

Based on κ_{total}, the apex of the turn is determined using the area under the curvature versus travelled distance curve as shown in Figure 6-4. The area under the curve is calculated between κ_{start} and κ_{end} representing a curvature of $|\kappa| = 0.01\frac{1}{\mathrm{m}}$. The minimum value of $|\kappa| = 0.01\frac{1}{\mathrm{m}}$ is used to exclude noise in the curvature measured while straight driving resulting from steering activity for maintaining the lane.

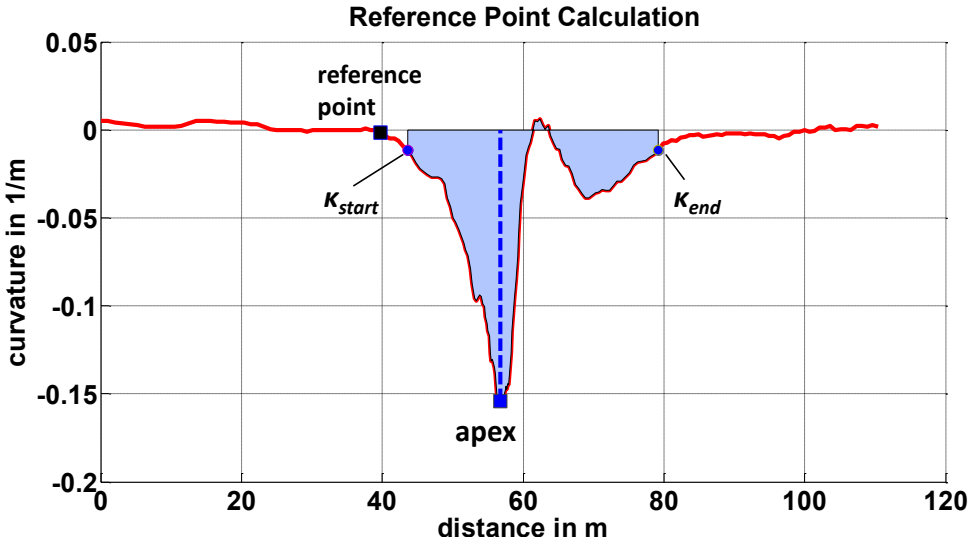

Figure 6-4: Apex

The reference point for turn maneuver initialization is defined according to 2 % of the apex's curvature.[161] The approach has proven its robustness and reliability even in challenging situations with the vehicle stopping during a turn or initializing the maneuver by steering in the opposite direction to enlarge the curve radius.

[160] Winner, H.; Schopper, M.: Adaptive Cruise Control (2016), pp. 1116–1117.

[161] Note that any other value can be selected as well without altering the general calculation principle.

However, the apex based method described above is not applicable to straight driving maneuvers. Thus, a location based reference point has to be used despite the inaccuracies arising from this method. Thus, for straight driving maneuvers, the (virtual) stopping line is identified at each intersection of the test route and used as reference point.

6.4 Evaluation Principle

The prediction system's structure is shown in Figure 6-5. First of all, the localization unit determines the next intersection in front of the ego-vehicle. Based on the intersection identified, the priority regulation (intersection class) is extracted from the digital map. The class selector selects the set of transfer functions corresponding to the intersection type and the list of indicators to be used. The transfer functions are handed over to the indicators along with all measurement data and the distance remaining between the ego-vehicle and the intersection center.

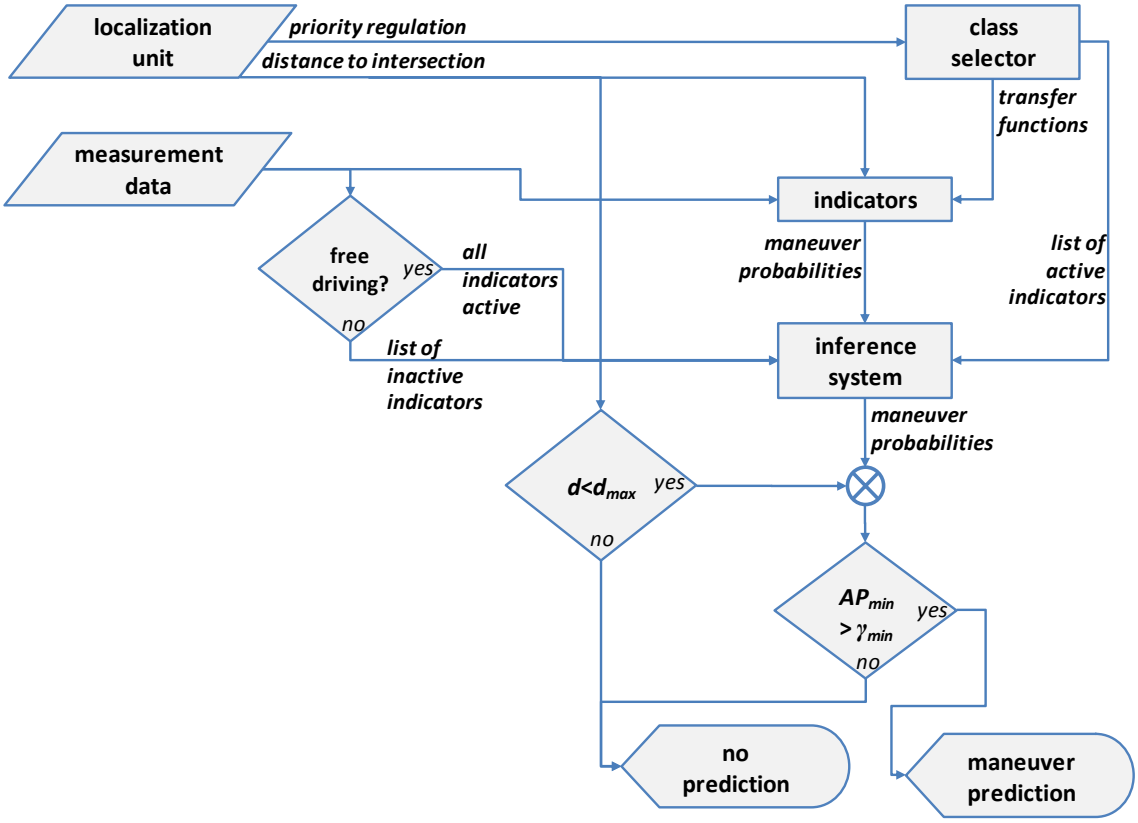

Figure 6-5: Evaluation structure

All measurement data acquired during an intersection approach sequence (starting with the ego-vehicle entering the relevant area before reaching an intersection and ending with the vehicle reaching the reference point) is sampled to discrete calculation steps. The actual values of the indicators' input signals are compared to the indicators' inter-

vals. Depending on the input value, the corresponding intervals are selected in each indicator. Furthermore, the actual distance interval inferred from the remaining distance of the ego-vehicle to the intersection center is determined. Thus, the input values and the distance interval are applied to a two-dimensional look-up-table containing the transfer functions to generate the indicators' output. In the implementation of the maneuver prediction system used here, each indicator contains three transfer functions, one for each potential maneuver. The indicators' outputs are connected to the inference system. The inference system receives the list of indicators to activate and deactivate due to the intersection class and the free driving conditions calculation. Note that the first list always has priority over the latter by system design. If the ego-vehicle is inside the relevant area before an intersection ($d_{act} < d_{re}$), the prediction done by the inference system is forwarded to the system's output if the limit γ_{lim} is exceeded. Otherwise, no calculation is completed at all and no maneuver is predicted.

6.5 Selection of Indicators

Depending on the intersection class, different sets of indicators are used by the inference system. To decide whether an indicator is used or not, all indicators introduced above are analyzed using the trusted quality measure QMT as described in section 5.5.2. Starting with the optimization of the number of bins, as described in section 5.6, a value of N_b resulting in the best performance is determined for each distance interval. In addition, an analysis of all intersection approach data originating from one intersection class and distance interval di[162] is done: QMT is calculated for each discrete calculation step i of each intersection approach sequence. Here, j is the number of calculation steps within one intersection approach and distance interval di and l is the number of intersection approach sequences available in training data. The result of this step is N_{QMT} quality values QMT:

$$N_{QMT} = \sum_{k=1}^{l} \sum_{i=1}^{j} QMT_{i,k} \tag{6-5}$$

To determine whether an indicator performs well in an intersection class, the average value $N_{QMT,me} = \overline{N_{QMT}}$ is calculated. Repeating this process for all distance intervals results in N_{di} values $N_{QMT,me,di}$. Exemplary results of $N_{QMT,me,di}$ for an indicator based on the ego-vehicle's speed in free flow are given in Figure 6-6. The figure shows $N_{QMT,me,di}$ for an exemplary selection of $di = 5$ distance intervals for intersection

[162] Distance intervals are defined according to section 5.2.

class 2 (priority regulated by traffic lights). Note that distance intervals are labeled ascending from the beginning of the relevant area at distance d_{re} to the intersection center. Note that $QMT_{i,k}$ is used only for discrete steps with inactive follow behavior.

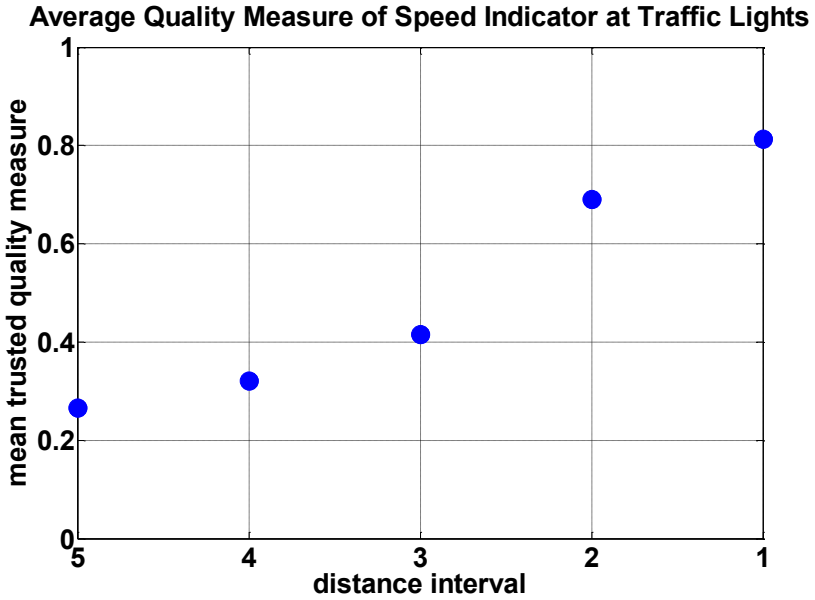

Figure 6-6: Average QMT of speed indicator at intersections with traffic lights

Figure 6-7 shows $N_{QMT,me,di}$ for the same indicator as in the previous figure. Here, the figure shows the same parameter for intersections regulated by stop signs (class 3).

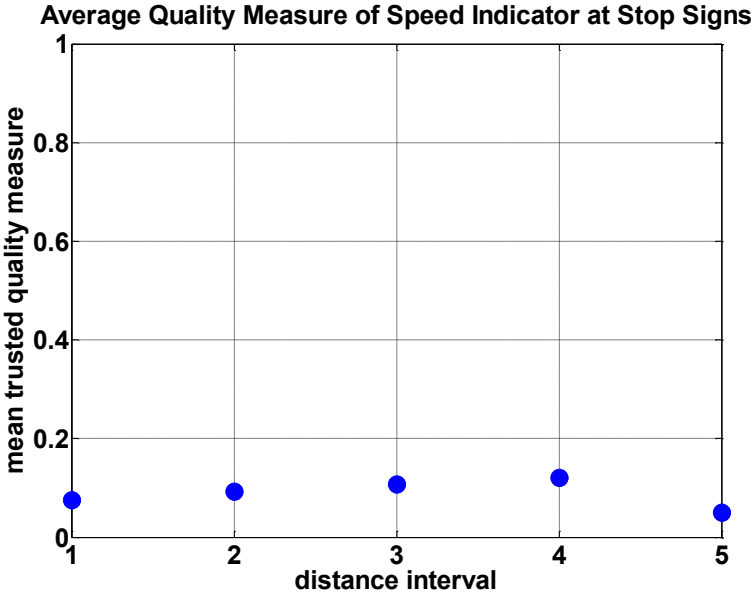

Figure 6-7: Average QMT of speed indicator at intersection with stop signs

The results are in line with expectations: $N_{QMT,me,5}$ in class 3 is clearly lower than $N_{QMT,me,5}$ in class 2. Because of the need to stop for any potential maneuver, the ego-vehicle's speed is hardly of any use for maneuver prediction at stop signs.

$N_{QMT,me,di}$ is calculated for all N_{ind} indicators analyzed in this work. The result of this step is a N_{ind} x di matrix containing $N_{QMT,me,di}$ values. This matrix enables the selection of the best performing indicators N_{act} of each distance interval di. In principle, the selection of indicators to activate can be done in two different ways.

- The first way is based on defining an arbitrary limit γ_{QMT}. All indicators with $N_{QMT,me,di} > \gamma_{QMT}$ are set as active, while the remainder are deactivated. The disadvantage of this method is that a fixed limit γ_{QMT} has to be defined arbitrarily for all indicators with the risk of excluding too many well performing indicators and including too many low performing indicators.
- Selecting active indicators using the second method avoids this problem. Here, the selection is done as follows: In each distance interval di, the N lowest performing indicators are selected out of N_{ind} and deactivated. Using the remaining $N_{ind} - N$ active indicators for maneuver prediction ensures that the best performing indicators are used in every distance interval di.

In addition to using the quality measures for indicator selection, correlations along the indicators' input signals are checked. If correlations are found, only the better performing indicator is used for maneuver prediction: Pearson correlation coefficients[163] are calculated among all indicators' input signals. If at least a significant correlation is found among two indicators, (corresponding to $p < 0.05$),[164] only the better performing indicator is used. A striking example is given in the following to demonstrate the process: Checking for correlations among the two obviously correlating indicators "Braking to maintain maximum lateral acceleration" and "Estimated lateral acceleration for potential turn maneuvers"[165] shows a strong correlation of $(R(1,1) = 0.9341)$ that is highly significant $(p(1,1) < 0.01)$.[166] Figure 6-8 shows a scatter plot of both indicators' input signals. This is in line with expectations because the calculations of both signals refer to the same physical value: a lateral acceleration in cases of a turn maneuver.

[163] Benesty, J.: Noise reduction in speech processing (2009), pp. 37–38.

[164] Fenton, N. E.; Neil, M.: Risk assessment and decision analysis (2012), pp. 12–13.

[165] A description of both indicators is given in section 5.4.4.

[166] N.N.: Correlation coefficients (2016).

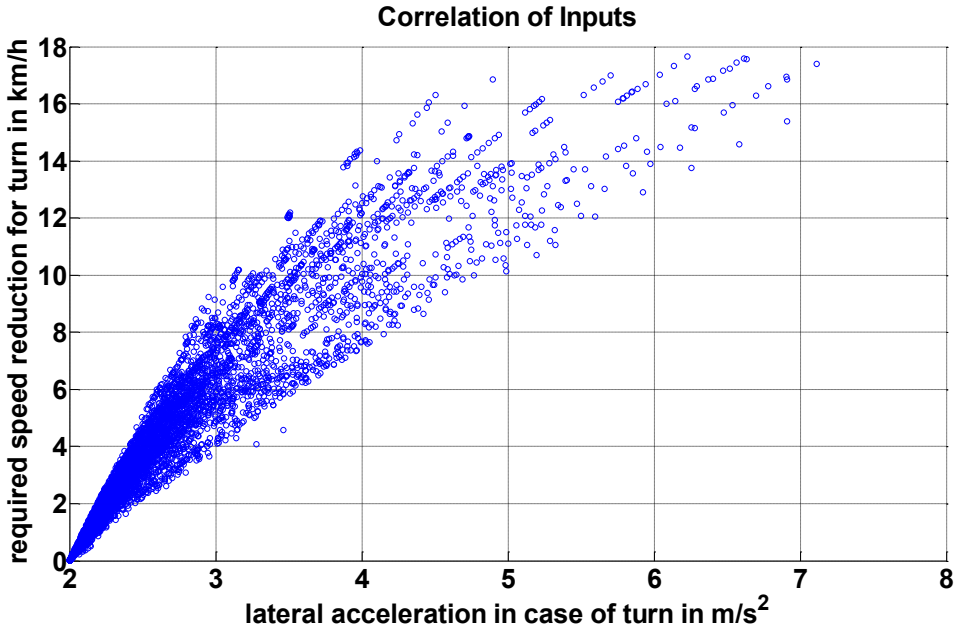

Figure 6-8: Scatter plot of correlations

Comparing the true-prediction rates of both indicators shows that predictions solely based on lateral accelerations result in higher true prediction rates as opposed to using the other indicator. Thus, the predicted lateral acceleration indicator is selected and the "Braking to maintain maximum lateral acceleration" indicator is discarded.

6.6 Exclusion of Alternative Maneuvers

6.6.1 Concept of Maneuver Exclusion

The evaluation introduced in section 6.4 is referred to as ”positive calculation method’’ in the following. The positive calculation method predicts a maneuver that the driver is about to perform by selecting the option with the highest maneuver probability. For example, this maneuver information can be used to predict a driving corridor and focus perception systems on this corridor. However, selecting potentially dangerous objects in the driving corridor is only possible if one maneuver is identified with a maneuver probability $AP_m \geq \gamma_{lim}$. To overcome this limitation, the concept of excluding alternative maneuver options is introduced here. The basic idea of the exclusion method is not to predict which maneuver is likely to be executed by the driver, but to predict what the driver is not going to do and to exclude this maneuver option.[167] The exclusion concept overcomes some general limitations of the "classic" positive calculation method: The

[167] Rodemerk, C. et al.: Exklusion alternativer Manöveroptionen (2015), pp. 119–128.

positive calculation method is dependent on the accuracy of the localization and only outputs maneuver predictions if the ego-vehicle is within the relevant area before an intersection. The exclusion method generates maneuver exclusions continuously and is not dependent upon the distance between the ego-vehicle and an intersection. In addition, the exclusion method is free of inaccuracies caused by localization. The localization unit is only needed for intersection class selection. The positive calculation method cannot predict a maneuver if two alternative maneuvers result in the same maneuver probability AP_m. The exclusion method is able to handle this situation regardless and excludes the third maneuver option. Hence, the exclusion generates additional information. With the information of an unlikely maneuver, objects within the driving corridor of the excluded maneuver can be ignored or tracked on a parallel and more unlikely path. Consequently, objects detected in critical zones according to the excluded maneuver do not trigger false alerts by collision warning systems.

6.6.2 Predictions on Multiple Exclusion Horizons

While the positive calculation method uses the intersection center as the reference for distance interval determination, the exclusion concept uses the ego-vehicle as the reference. Here, the reference for all calculations is the front end of the ego-vehicle as shown in Figure 6-9. Distance intervals di of the positive calculation method are replaced by prediction horizons that move along the road with the vehicle. All prediction horizons are evaluated in parallel resulting in a set of multiple exclusion statements in every discrete calculation step.

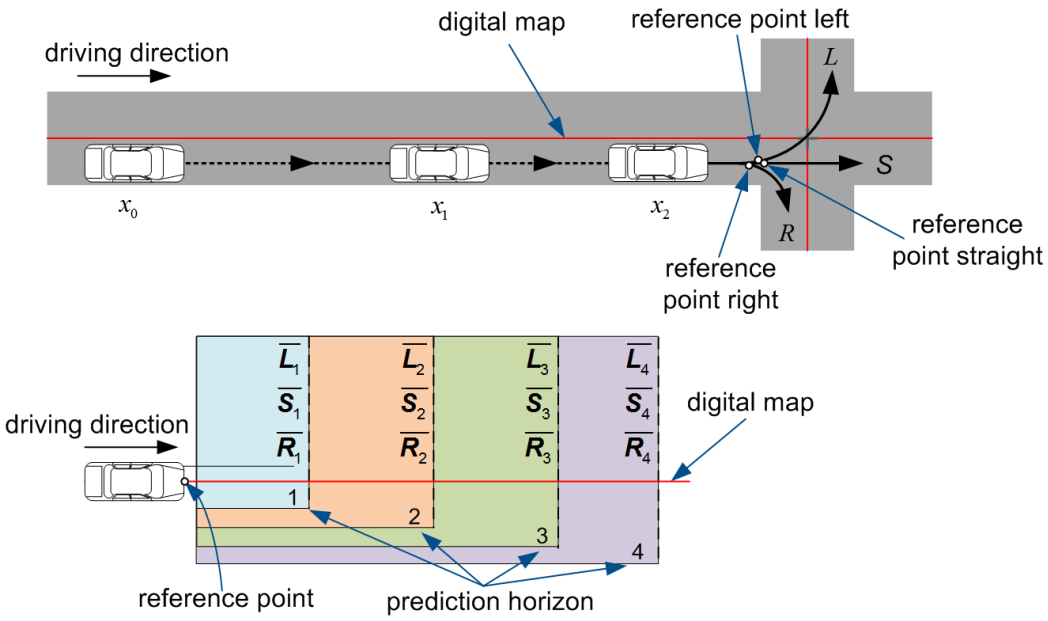

Figure 6-9: Comparison of reference points

6.6.3 Calculation

For the exclusion concept, the basic calculation of transfer functions introduced in section 5.1 has to be altered. In the positive calculation method, transfer functions are calculated based on the training data available for the corresponding maneuver. For instance, right turn training data is used to train right turns only. In the exclusion concept, all training data available from every maneuver is allocated into two groups: a maneuver group MG and a not-maneuver group MG'. The maneuver group MG contains data from the maneuver that is trained (approach sequences of right turns in the case of the example above). The not-maneuver group MG' contains all remaining data (all left turn approach sequences plus all straight driving sequences). Data from groups MG and MG' are used to generate transfer functions in the same way as the positive calculation method. Indicators used in the exclusion approach are the same as in the positive calculation method. However, some indicators cannot be calculated without using the distance between the ego-vehicle and the intersection. Because this information is not used in the exclusion approach, these indicators are left out.

Because of the different amount of training data in the groups created by the exclusion method (group MG' contains approx. twice the data of group MG), a weighting has to be done. The weighting factor w_{exc} is calculated for each interval by comparing the amount of data in the groups:

$$w_{exc,i} = \frac{\#MG_i}{\#MG'_i} \tag{6-6}$$

Taking the prediction horizon h into account, the occurrence of training data $\left(N'_{i,h}\right)$ in interval i in group MG' in relation to the overall occurrence of training data in the interval i defines the exclusion likelihood $p_{ex,h,m}$ for maneuver m:

$$p_{ex,h,m} = \frac{N'_{i,h}}{N_{i,h,w} + N'_{i,h}} \tag{6-7}$$

Note that $N_{i,h,w}$ is the weighted occurrence of training data in MG and unlike the positive calculation method, the m exclusion likelihoods of all maneuvers don't add up to a total of one.

6.6.4 Implementation

The implementation of the exclusion approach is done similarly to the positive approach. The basic structure of the concept is given in Figure 6-10. The difference to the structure of the positive calculation method is that the distance is not used and that indicators generate exclusion likelihoods from input signals.

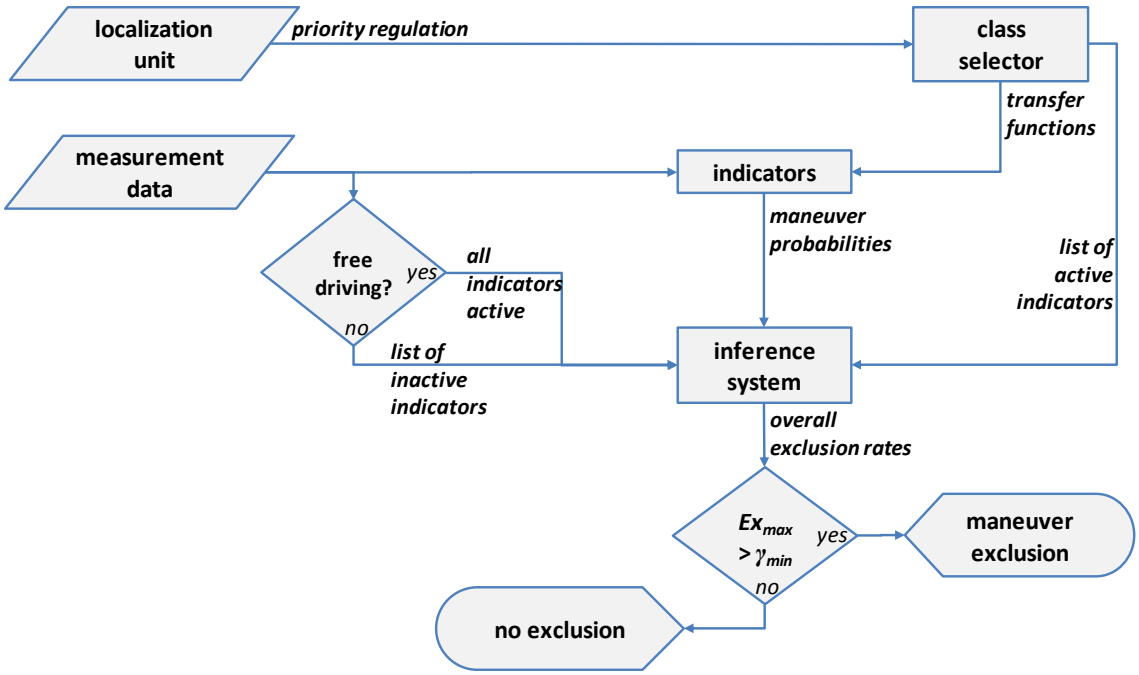

Figure 6-10: Exclusion structure

Based on the input data, all indicator exclusion likelihoods for either right turns, left turns or straight driving are summed up for each prediction horizon in the inference system. This results in h overall exclusion probabilities for either right turns $(p_{exc,total,r})$, left turns $(p_{exc,total,l})$ or for straight driving maneuvers $(p_{exc,total,s})$. For the selection of a maneuver to be excluded in a distance horizon h, the maximum value of $p_{exc,total,r}$, $p_{exc,total,l}$ and $p_{exc,total,s}$ is selected and the corresponding maneuver is excluded.

7 Results

This section gives a survey of the prediction performance achieved by applying the prediction system introduced in this work to measurement data from the test subject study carried out in this work. Note that all results presented in the following are generated without using the vehicle's turn indicator state at all. According to section 6.3, reference points for turn maneuvers are defined as using 2 % of the curvature's apex. The results presented in section 7.1 are generated using a selection of the indicators introduced and discussed above. The average function is applied here as an inference method for the calculation of maneuver probabilities. This is done to show that even this simple mathematical and computational method is able to detect intentions. In comparison, prediction results achieved by using a Bayesian network instead of the average function are presented in section 7.2.

7.1 Prediction Performance

In the evaluation, the maneuver with the highest probability is compared to the maneuver executed in reality in each discrete calculation step. True predictions are counted if the predicted maneuver is the same as the real maneuver executed by the driver. True prediction rates are shown for a time span of $t = 10\,\mathrm{s}$ prior to reference points. The figures present the results of a stratified 10-fold cross validation. True prediction rates of all classes considered here are summarized in Table 7-2 in section 7.3. Note that for all results shown here, standstill times during the intersection approach are removed so that the results present only predictions done while the ego-vehicle is moving.

7.1.1 Priority Roads

Figure 7-1 shows the true positive prediction rates for intersection class 5 containing all intersections the ego-vehicle approaches via a priority road not regulated by traffic lights, independent of the intersection's size and geometry. Best classification results are achieved for straight driving maneuvers with true positive predictions $tpr > 87\,\%$ at 1 second prior to the reference point. Right turn maneuvers are classified correctly with $tpr > 82\,\%$ at 1 second prior to the initialization of turn maneuvers. Left turn maneuvers are predicted correctly with $tpr > 78\,\%$ at 1 second prior to the initialization of a left turn maneuver.

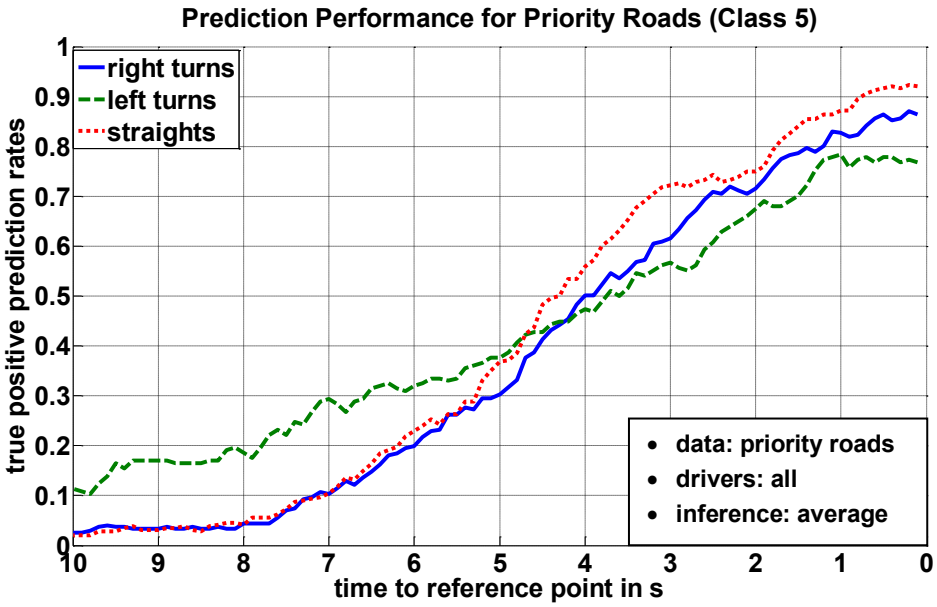

Figure 7-1: Results of class 5, priority roads

7.1.2 Traffic Lights

Figure 7-2 presents the true positive classification rate of intersection class 2 containing intersections operated by general traffic lights (traffic lights that show the same light at once for all legal maneuver options). The prediction performance is similar to *tpr* of class 5: Best classification performance is achieved for right turns $tpr > 83\ \%$ at 1 s prior to maneuver initialization, followed by left turns $tpr > 80\ \%$ and straight driving maneuvers $tpr > 76\ \%$. While the prediction performance at 1 s is similar, true prediction rates for higher times to maneuver initialization are higher than in class 5.

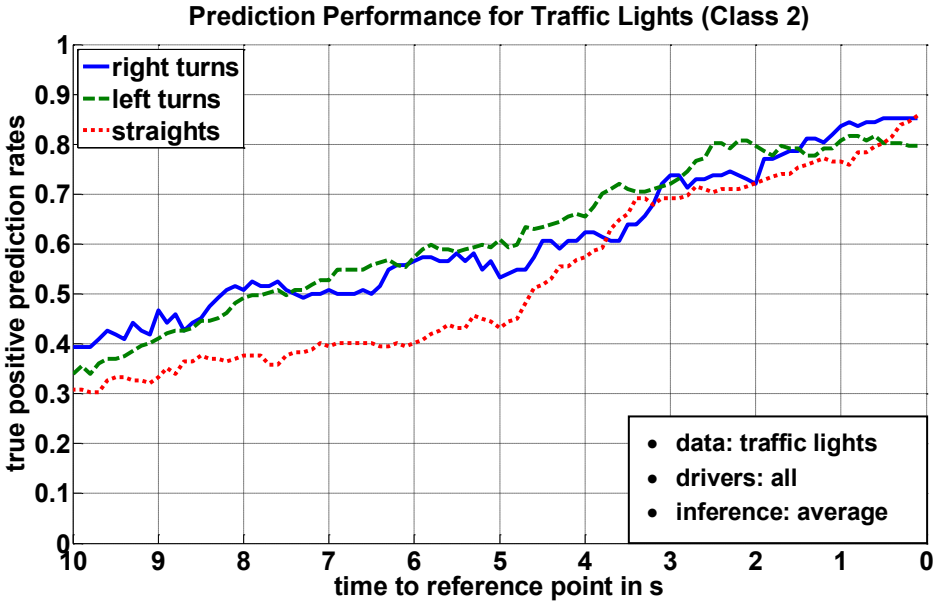

Figure 7-2: Results of class 2, traffic lights for all directions

Note that predicting the driver's maneuver intentions on priority roads regulated by maneuver specific traffic lights (class 1) is possible as well using the same calculation approach. However, the benefit of a maneuver prediction in this class is low. According to §37 StVO, [168] maneuver specific traffic lights (containing direction arrows within the traffic lights) are only used if the trajectories of vehicles are collision free with all other traffic's trajectories. This includes parallel traffic of pedestrians and cyclists, as well.[169] Thus, the prediction performance is not analyzed here.

7.1.3 Priority to Right Regulated Intersections

Figure 7-3 presents the prediction results of all priority to right regulated intersections of the test track. In comparison to the prediction performance above, detection rates are lower for priority to right intersections. This is caused by the features of the intersection class. If any traffic object from right is approaching the intersection, the ego-vehicle has to give way to the traffic object for straight driving and for left turns. Depending on the size of the intersection, slowing down or even completely stopping might be necessary even for right turns. The priority to right regulation is the standard regulation used especially in residential areas with narrow streets and speed limits of $v = 30$ km/h.[170] Furthermore, evasive maneuvers due to parked cars may be needed to enable other vehicles to pass in residential areas. This hampers the task of maneuver prediction.

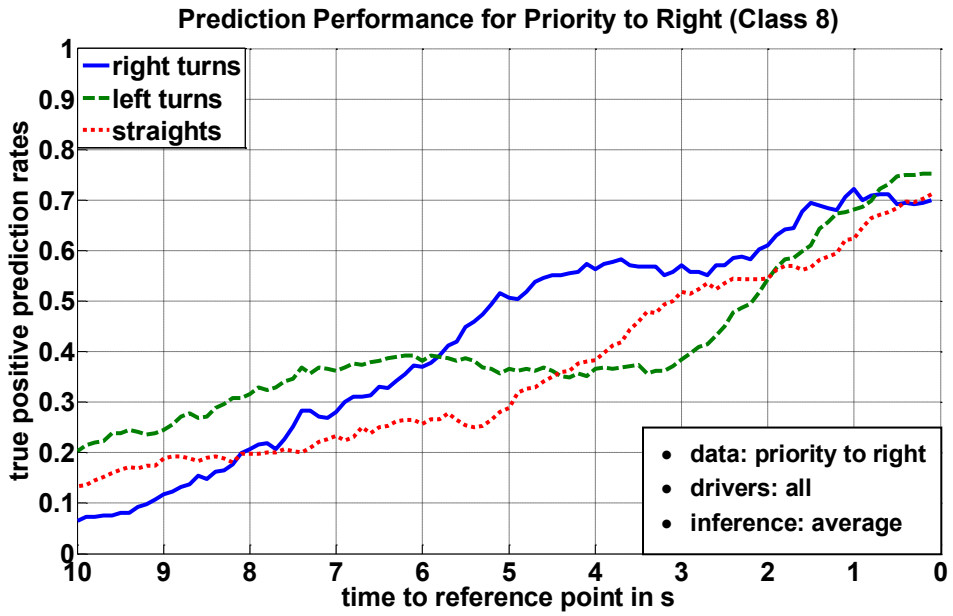

Figure 7-3: Results of class 8, priority to right

[168] Bundesministeriums der Justiz und für Verbraucherschutz: StVO (2015), p.19.

[169] Wissmann, M.: VwV-StVO (2015).

[170] Bundesministeriums der Justiz und für Verbraucherschutz: StVO (2015), Absatz 1c, p.25.

7.1.4 Give Way and Stop Sign Regulated Intersections

Prediction results achieved by the system for intersections operated by give way signs (class 4) are shown in Figure 7-4. The overall prediction performance is lower than for priority to right regulations. Predicting maneuvers in intersection classes 3 & 4 is the hardest task due to the demand to stop the vehicle or drive at low speeds in all cases and independent of maneuver. Thus, no speed-related indicators and no indicators based on driver's control inputs to affect the vehicle's speed are used at all. Driver's head- and gaze behavior is mainly dependent on the geometry of the intersections and view obstructions. In addition, typical driver behavior was observed in test drives that further exacerbated the difficulty of the prediction task: Having stopped the vehicle at line of sight, drivers turn their heads at large angles ($\delta_{HT} > 80°$) to the direction priority traffic is coming from. These angles are outside the field of view of the head tracking device used in this work. In order to track head and gaze rotations in these situations as well, more cameras and measuring devices with greater range would have to be used.

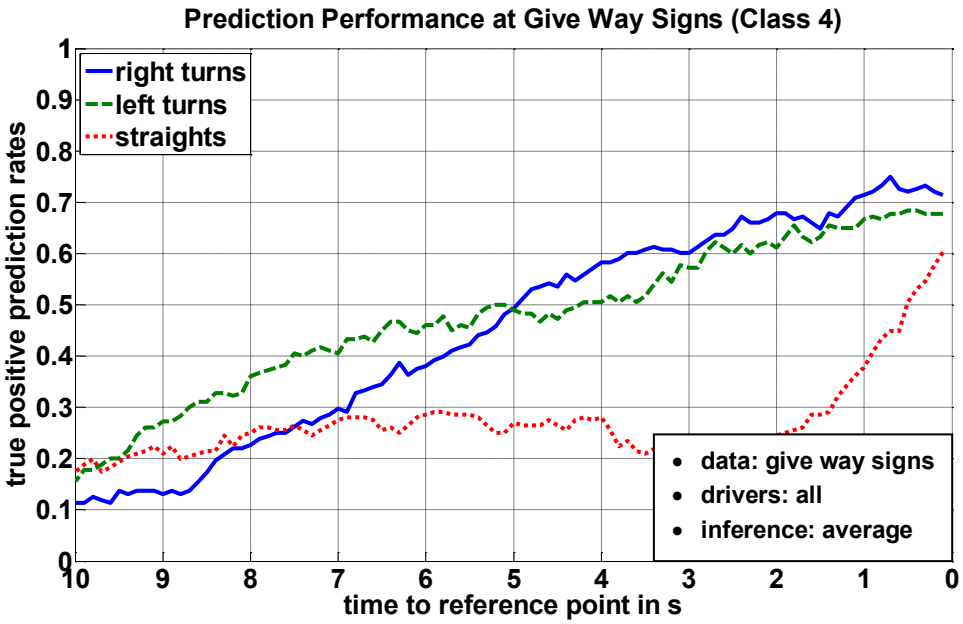

Figure 7-4: Results of class 4, give way sign

The same applies to the prediction results achieved at stop sign regulated intersections (class 3) shown in Figure 7-5, that are even lower than in class 4.

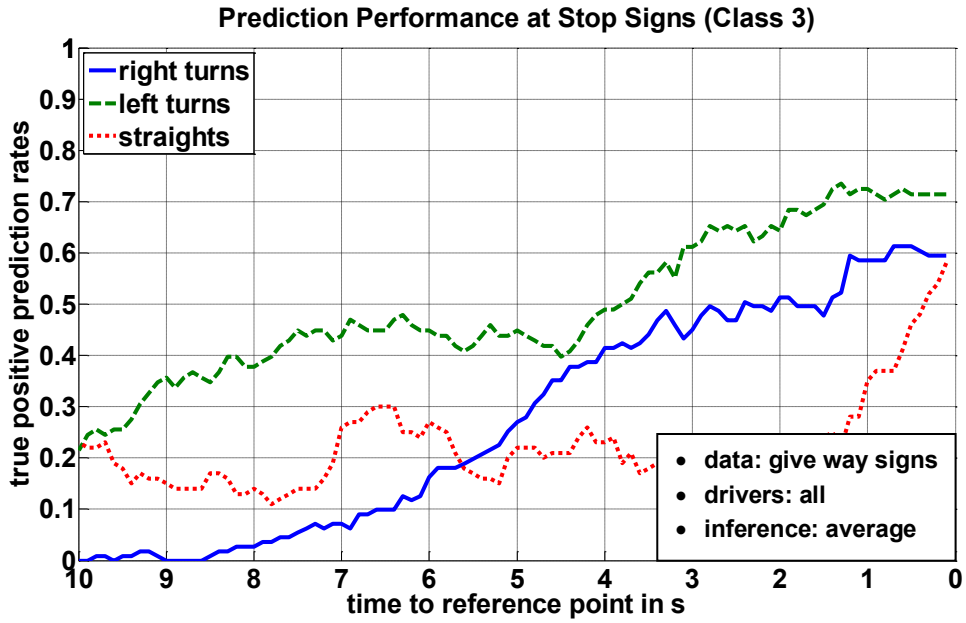

Figure 7-5: Results of class 3: stop sign

The low prediction quality achieved by the prediction system for straight driving maneuvers in both classes results from the trajectories used by drivers at stop sign and give way regulated intersections. A review of data recorded in the test drives for these two intersection classes shows a general pattern of trajectories: Trajectories for right turns clearly differ from the trajectories of the other two maneuvers at the same intersection. Intersection approach trajectories for straight driving and left turns lead straight to the stop line until the vehicle comes to a stop. Thus, approaching sequences for left turn maneuvers and straight drives are likely to be mistaken by the prediction system. Nonetheless, the intention prediction method is applicable to these two classes as well, even though the prediction performance is clearly lower than the performance achieved in other classes.

7.1.5 Robustness of Predictions

This section analyzes the frequency of dropped true predictions that are initially correct. Here, the entirety of true predictions at a time to maneuver initialization ($ttmi = 2$ s) is analyzed for consistency of consequent predictions. Figure 7-6 shows the variation of dropout rates for predictions at intersections regulated by traffic lights. The analysis is based on a total of 383 true predictions at $ttmi = 2$ s.

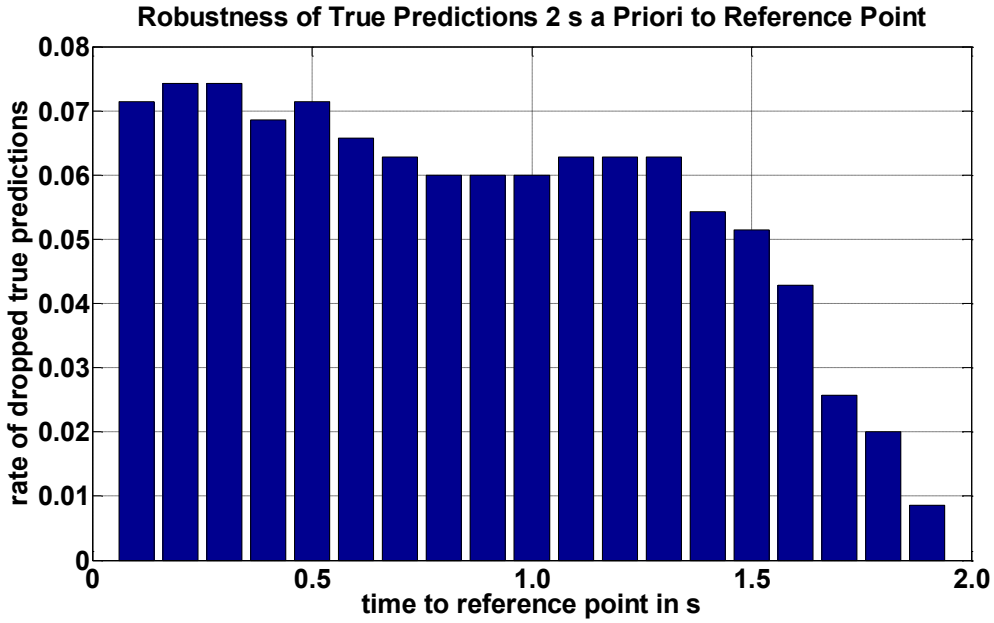

Figure 7-6: Robustness analysis

Dropout rates for all intersection classes analyzed here are given in Table 7-1 based on the total of true predictions at $ttmi = 2$ s.

Table 7-1: Comparison of prediction

intersection class	2	3	4	5	8
dropout rates at $ttmi = 1.5$ s	5.1	5.9	5.4	4.2	7.7
dropout rates at $ttmi = 1.0$ s	6.0	7.6	8.3	5.4	9.8
dropout rate at $ttmi = 0.5$ s	7.1	8.2	7.9	5.7	10.5

7.2 Bayesian Network

In addition to using the average or product function, a Bayesian network is set up in this work. The conditional probability table of each node in the network are learned using the same data that is used for generating the results in the previous section. The remainder of the evaluation is the same as in the previous section. The structure of the Bayesian network is shown in Figure 7-7.

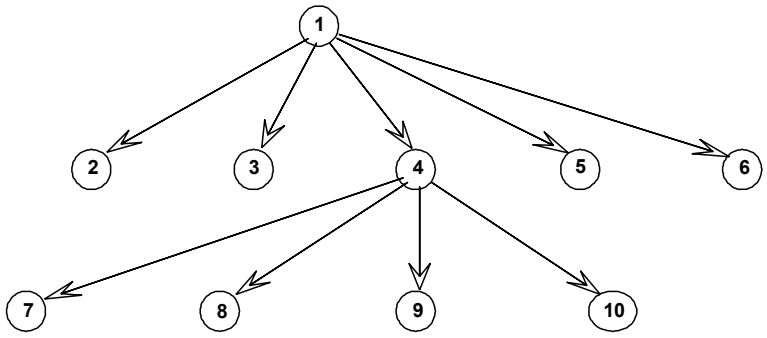

Figure 7-7: Bayesian network

Prediction results generated using the Bayesian network for class 2 and class 5 are shown in Figure 7-8 and Figure 7-9.

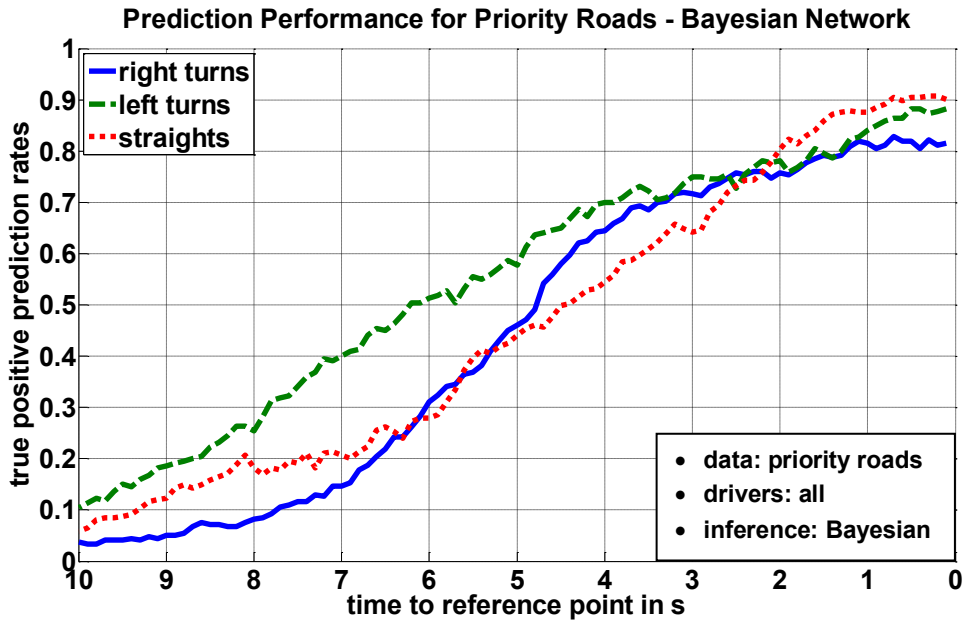

Figure 7-8: Results of class 5, priority roads, Bayesian network

As expected, true positive detection rates generated by the Bayesian network outperform the results generated by using the average function for left turns by 5.7 % ($tpr = 84.1\,\%$ at $ttmi = 1$ s). For straight driving maneuvers, the performance is nearly the same (+0.3 % at $ttmi = 1$ s). The true prediction rate of right turn maneuvers is even slightly lower ($tpr = 81.5\,\%$ at $ttmi = 1$ s). In intersection class 2 (traffic lights), using the Bayesian network results in $tpr = 82.0\,\%$ 1 s before maneuver initialization of left turns, $tpr = 91.3\,\%$ at $ttmi = 1$ s for right turns and $tpr = 91.5\,\%$ for straight driving. This corresponds to raised true prediction rates of +0.3 % for left turns, +7.7 % for right turns and +15 % for straight driving. In this class, using the Bayesian network clearly raises the prediction performance.

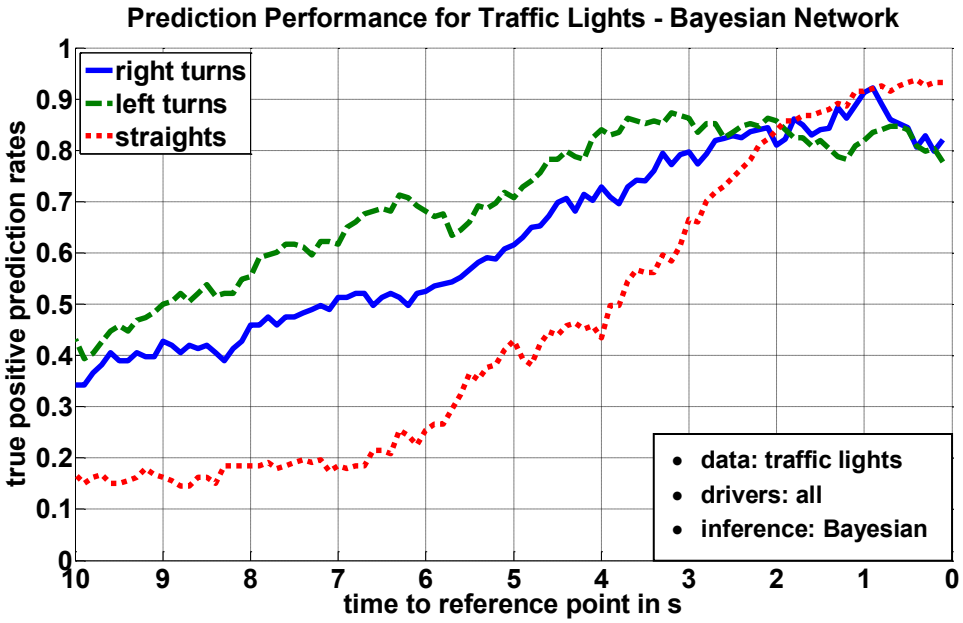

Figure 7-9: Results of class 2, traffic lights for all directions, Bayesian network

7.3 Neglecting Intersection Classes

In order to assess research question one introduced in section 3.1, the effect of the intersection classes on the prediction performance is analyzed. This is done by comparing two types of performance calculations: One type with respect to intersection classes (as introduced above) and one type neglecting intersection classes and using training data from all intersection approaches recorded in the test study. The figures given in annex I present the prediction performance for the latter calculation type. They are created based on the same conditions as in the previous section (average function as an inference system and 10-fold cross validation). Table 7-2 compares the prediction performance (tp=true positive rate) one second prior to maneuver initialization ($ttmi$ = 1 s).

Table 7-2: Prediction performance at *ttmi* = 1 s

int. class		2	3	4	5	8
ma-neuver	int. class used	tp rate in %	tp rate in %	tp rate in %	tp rate in %	tp rate in %
R	yes	83.6	58.6	71.4	82.7	72.3
	no	76.2	52.1	**72.0**	77.9	57.7
S	yes	76.5	35.0	37.8	87.2	62.4
	no	**79.6**	20.2	35.2	81.3	**65.0**
L	yes	80.7	72.5	66.7	78.4	68.1
	no	**81.7**	65.2	66.7	67.5	67.9
all	y	80.0	55.3	57.7	83.3	67.3
	n	79.6	45.8	57.0	76.5	63.6

Comparing the results shows that the four prediction rates in bold in the table have slightly better prediction performance for a single maneuver while neglecting intersection classes rather than predictions considering intersection classes. The overall prediction performance of all maneuvers at $ttmi = 1$ s prior to the reference point is higher for all intersection classes after separating intersection classes in the training process. The increase in prediction performance depends on the type of intersection class. While the overall gain for intersection class 2 and 4 is below 1 %, true prediction rates of intersection classes 3, 5 and 8 are raised by 9.5 %, 6.8 % and 3.7 % using intersection classes. The average prediction rates for all three maneuver types within each intersection class are raised using the intersection classification scheme.

7.4 Exclusion Results

In the evaluation of the exclusion method utilized here, an exclusion is considered true if a maneuver that differs from the driver's executed maneuver is excluded . Exclusions are calculated for multiple prediction horizons. For means of comparing the results achieved by the exclusion approach to the results of the positive approach, the same representation is selected here. Exclusions from all predictions horizons are transferred to the same reference points used in positive approach. The exclusion of the prediction horizon that corresponds to the distance remaining to the reference point is selected and used for evaluation. Figure 7-10 shows the true exclusion rates achieved by the prototypic implementation for driving on priority roads separated by maneuvers the driver performs.

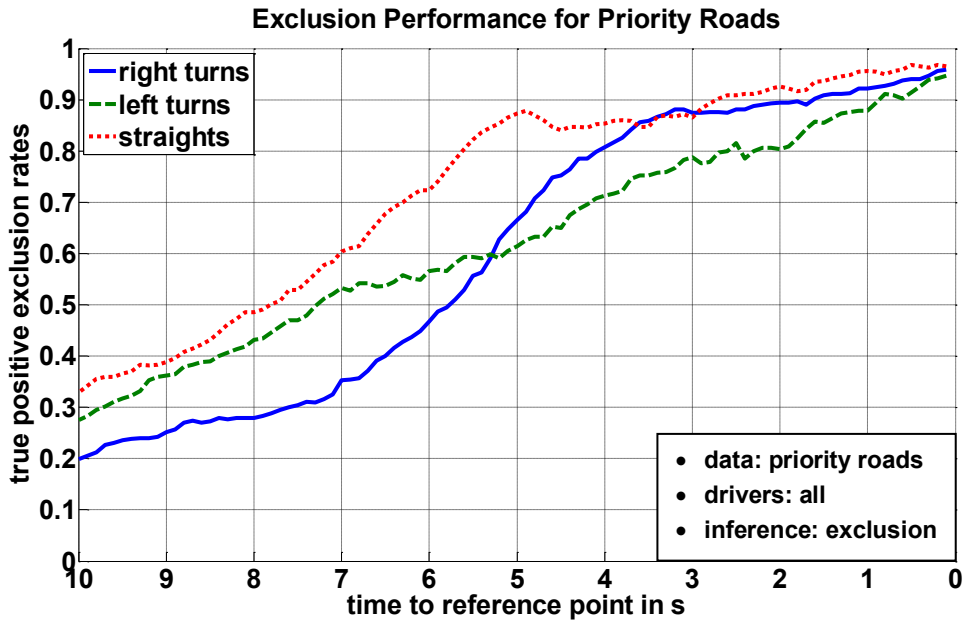

Figure 7-10: Exclusion performance

The figure shows that a true exclusion rate of 92.2 % is reached for right turns on priority roads 1 second prior to maneuver initialization (*ttmi* = 1 s). This means that in 92.2 % of all intersection approaches with right turns performed by the driver, a maneuver different from a right turn is excluded by the system. Analogously, the exclusion rates for left turns are 87.9 % and 95.6 % for straight driving maneuvers. Table 7-3 compares the true positive rates of the positive calculation method and the exclusion method, showing that the exclusion calculation clearly outperforms the positive calculations in terms of true positive rates.

Table 7-3: Prediction and exclusion rates

maneuver	R		L		S	
ttmi	tp rates in %	exclusion rates in %	tp rates in %	exclusion rates in %	tp rates in %	exclusion rates in %
1	82.7	92.2	78.4	87.9	87.2	95.6
2	71.6	89.5	67.5	80.4	75.0	92.6
3	61.6	87.4	56.7	78.7	72.2	86.5

8 Driver-specific Adaptation

Prediction results described in the previous section were generated using data from all test subjects considered in this work. Differences in the individual driving behavior among the test subjects has not been taken into account so far. This section analyzes the potential of improving the intention detection system's prediction quality by adapting the indicators' transfer functions to different driving styles. A review of the literature shows that at least two different driving styles have to be considered: careful and relaxed drivers on the one hand and sporty drivers on the other hand.[171] In general, relaxed driving is characterized by lower longitudinal and lateral accelerations when compared to sporty driving. A careful driver initiates a braking maneuver during intersection approach earlier and applies less deceleration than a sporty driver.[172] In general, two different methods can be applied to adapt a driving style and are therefore considered here. The goal of both methods is to conform to the driver's individual behavior:

- The first method classifies the driving style and combines all drivers of the test study with the same driving style into one group. Transfer functions are created using training data only from drivers within the groups.
- The second method calculates individual transfer functions for each driver. Here, the transfer functions are adapted to the driver's individual behavior.

Adapting the transfer functions to the driving style of only one driver requires copious amounts of data during the training process for each intersection class. Considering only data from one driver instead of data generated by all drivers results in a decrease to the size of the training set to 1/30 of the initial amount of data. Note that the amount of data available is reduced even further by splitting recorded data into a training and a test set. Applying this procedure to the training data generated in this project shows that the amount of data available for an individual driver is too low for reliable maneuver prediction. Thus, the second method is discarded here and the first method is applied. The procedure to analyze the adaptation potential of the intention detection system is outlined in the following:

- Drivers are categorized into a predefined number of groups using a classification measure.

[171] Donges, E.: Driver Behavior Models (2016), pp. 29–30.

[172] Meitinger, K.-H.: Diss., Aktive Sicherheitssysteme für Kreuzungen (2009), p.41.

- Group-specific (adapted) transfer functions are calculated based only on training data from drivers within one group.
- The prediction system's performance using the adapted transfer functions for drivers within one group is evaluated for all groups.
- The system's prediction performance using the adapted transfer functions is compared to the prediction performance using non-adapted transfer functions.

8.1 Driver Classification

There are several methods known in the literature for classifying driving behavior. A commonly used approach is to provide a questionnaire to test subjects and let drivers to a self-assess of their driving style. Based on Keller[173] and Porst[174], a questionnaire with labeled endpoints is developed and presented to test subjects before starting test drives. Among other things, the questionnaire asks the test subjects to assess their own driving style on a scale of 1 to10 with 10 labeled as "sporty" and 1 labeled as "relaxed/careful". Out of the 30 participants of the test study, 6 drivers classified themselves as sporty drivers (with a score from 8 to 10). 10 test subjects classified their own driving style as relaxed and careful (with a score from 1 to 3). The remaining 14 test subjects stated that their own driving style was neither sporty nor relaxed based on scores from 4 to 7 on the questionnaire. The results of the questionnaire are summarized in Table 8-1. Aside from the driver's self-assessment, a classification of whether the test subject behaved more or less sporty as compared to the average of all drivers is given in the table. Note that a variety of methods for assessing drivers' driving styles can be applied. Graichen et al.[175] found significant differences between different drivers in the ego-vehicle's speed when releasing the accelerator pedal, as well as for maximum longitudinal acceleration after turning. Cheng et al.[176] analyzes the use of the acceleration pedal, the steering wheel angle and the lateral accelerations tolerated by the driver to identify driving behavior. A survey of different methods for driving style recognition is given by Bolovinou et al.[177] For means of maneuver prediction, the driving behavior during intersection approach is of interest to this work. Here, the ego-vehicle's speed and the longitudinal acceleration applied by the driver during intersection approach is analyzed. For the analysis, inter-

[173] Keller, D.: Skala in Fragebögen (2013).

[174] Porst, R.: Fragebogen (2014).

[175] Graichen, M.; Nitsch, V.: Effects of Driver Characteristics (2017), pp. 15–29.

[176] Chen, Y.; Li, L.: Advances in Intelligent Vehicles (2014), p.151.

[177] Bolovinou, A. et al.: Driving style recognition (2014), pp. 73–78.

section approach data is used from give way sign regulated intersections, stop sign regulated intersections, and intersections with priority to right regulations. These intersection classes are selected for driving style analysis because external conditions influencing the driver's behavior are minimized: The driver has to slow down during all intersection approaches due to priority regulations and is aware of the need to slow down at an early phase of the approach.[178] Thus, the approaching behavior is not influenced by external conditions such as traffic lights. In this work, it has proven that using the longitudinal acceleration during intersection approach enables a better driver classification at different intersections with varying geometry as opposed to using the vehicle's speed for driver classification.

Thus, longitudinal accelerations applied by the driver during intersection approach are compared to the accelerations applied by all drivers in the same situations. Figure 8-1 exemplarily shows a cumulated distribution of lateral accelerations applied by test subject No. 16 while approaching give way sign regulated intersections. For means of comparison, the eCDF of longitudinal accelerations recorded for all drivers under the same conditions is given, as well.

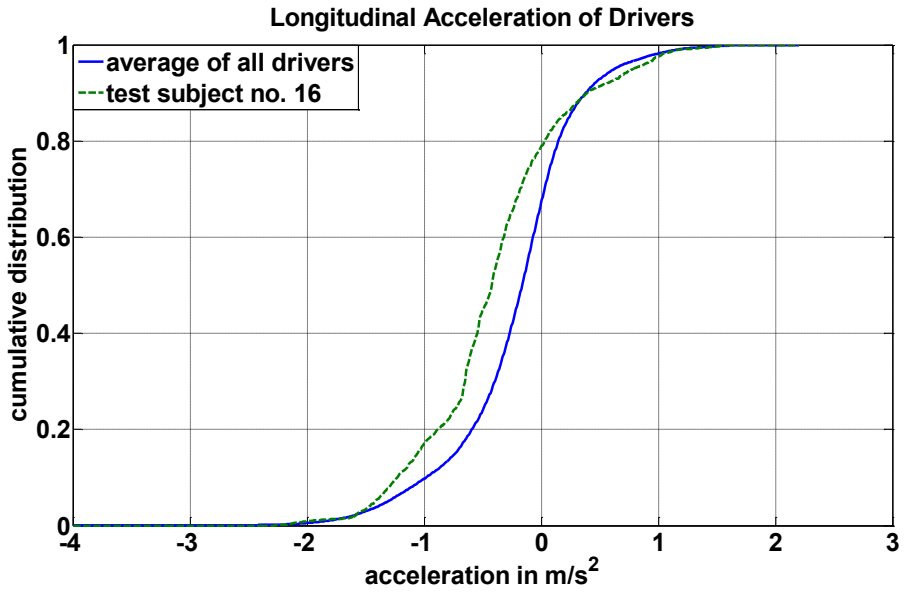

Figure 8-1: Driving style comparison

Depending on the relative position of both eCDF curves, the driver is classified as either sporty (+), medium (o) or relaxed (-) in relation to the other test subjects of the study.

[178] In contrast to situations when approaching traffic light intersections, where a light change could potentially force the driver to slow down more quickly than anticipated, the intersection classes used here have unchanging regulations, so it is clear to the driver that he has to slow down at the beginning of the intersection approach sequence.

Table 8-1 shows the results of this relative assessment, as well as whether the relative assessment correlates to the driver's self-assessment.

Table 8-1: Sporty driving assessment

driver no.	sporty driving (self-assessment)	sporty driving (test)	self assessment correct?
1	9	+	y
2	6	o	y
3	8	o	n
4	3	-	y
5	6	o	y
6	2	o	n
7	5	+	n
8	5	o	y
9	8	o	n
10	6	+	n
11	10	-	n
12	3	o	n
13	2	o	n
14	6	o	y
15	7	o	y
16	6	+	n
17	5	-	n
18	3	o	n
19	6	-	n
20	3	o	n
21	3	o	n
22	6	-	n
23	1	+	n
24	10	+	y
25	6	o	y
26	4	o	y
27	1	-	y
28	3	o	n
29	8	-	n
30	6	-	n

As shown in the table, only 11 out of 30 drivers have matching self-assessments and relative assessments. Thus, drivers are not grouped based on their self-assessment, but based on the classification done by the longitudinal accelerations measured during intersection approach.

8.2 Results of the Adaptation Process

This section shows the results of the driving style adaptation as introduced above. Three groups of drivers are considered: The first group contains drivers that drive more relaxed and carefully, with lower longitudinal accelerations during intersection approach as compared to the average of all drivers in the study. The second group consists of drivers that show only small differences to the average acceleration profile. Finally, the third group contains drivers that use higher longitudinal accelerations than the average driver. The classification of drivers into either the average or one of the other groups is done according to the amount of RMSE between the eCDFs.

At stop sign regulated intersections (class 3), no positive effect of the driving style adaptation could be found for the first group (relaxed) and the third group (sporty). In contrast, raised true prediction rates for right turns and straight driving have been found for the second group containing only the drivers that match the average acceleration profiles, as shown in Figure 8-2. The adapted prediction rates are compared to the non-adapted rates in Table 8-2.

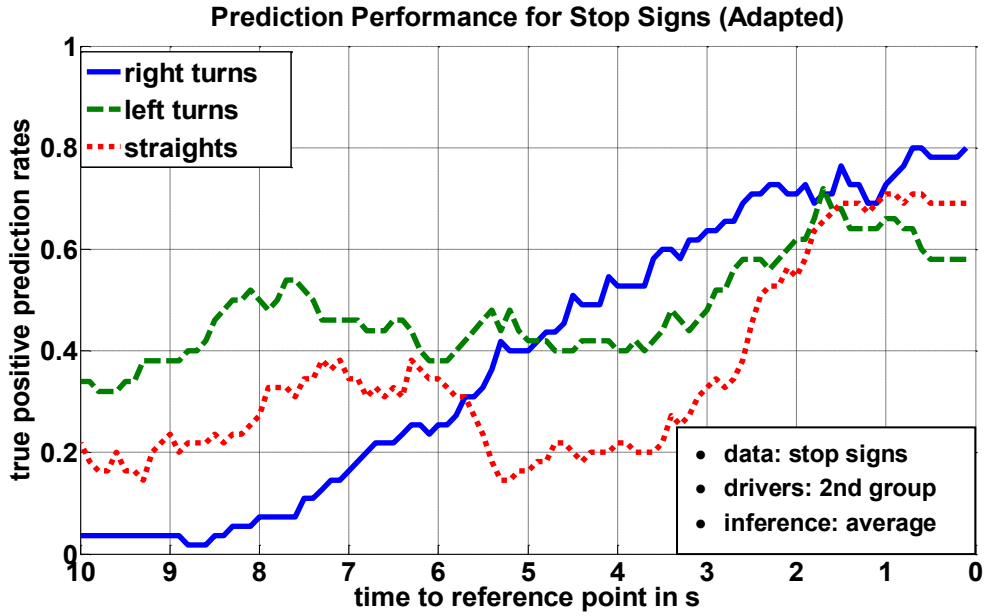

Figure 8-2: Driving style adapted prediction performance class 3

Table 8-2: Adapted prediction performance at *ttmi* = 1 s

maneuver	tp rate in % (non-adapted)	tp rate in % adapted	increase in %
R	58.6	72.3	+13.7
L	72.5	66.0	-6.5
S	35.0	70.9	+35.9
all maneuvers	55.3	69.7	+14.4

The adaptation results for give way sign regulated intersections (class 4) are similar to those of class 3 shown above. While the results for the first group and the third group are nearly the same as the non-adapted true positive rates for all maneuvers (58.9 % with an increase of +1.2 % for the first group and 60.7 % (+3 %) for 3rd group), the prediction performance of the second group is clearly increased, as shown in Figure 8-3 and Table 8-3.

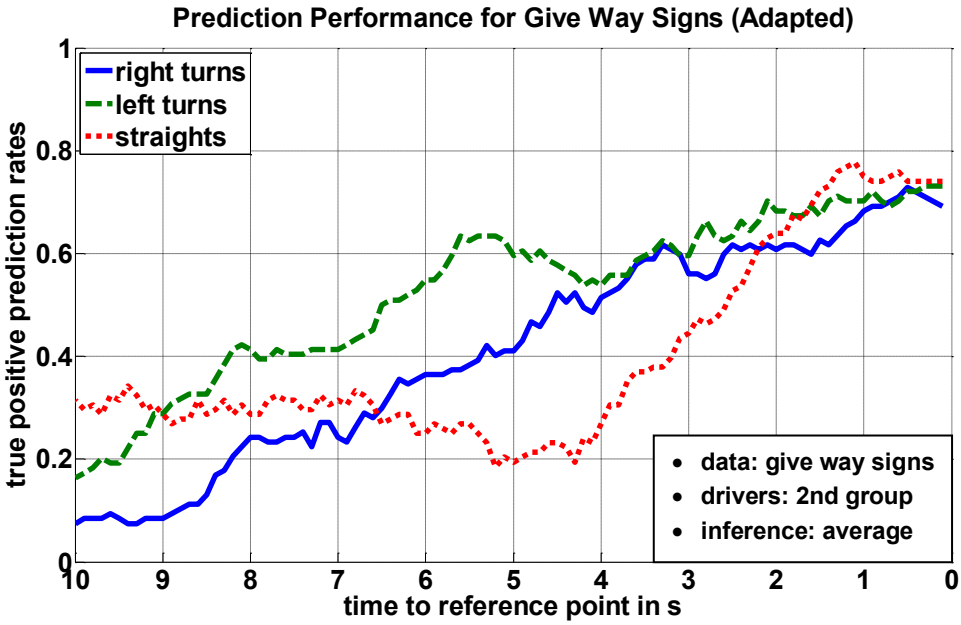

Figure 8-3: Driving style adapted prediction performance class 4

Table 8-3: Adapted prediction performance at *ttmi* = 1 s

maneuver	tp rate in % (non-adapted)	tp rate in % adapted	increase in %
R	71.4	68.2	-3.2
L	66.7	70.2	+3.5
S	37.8	75.0	+37.2
all maneuvers	57.7	71.1	+13.4

For priority to right regulated intersections (class 8), the effect of using an adapted transfer function on prediction results is minor: The first group (relaxed) results in 71.4 % overall true positive rates, the second group (average) in 66.8 % overall true positive rates, and the third group (sporty) in 69.2 % overall true positive rates. All results only show small improvements over the 67.3 % overall true positive rate for non-adapted calculations. The effect of the adaptation is further reduced in intersection class 2 (general traffic lights) and 5 (priority roads). For both intersection classes, the results of all three groups' true positive rates vary within 2 % of the non-adapted true positive rates.

In conclusion, a positive effect of the adaptation process, including increased true prediction rates, is found especially for the second group of drivers (containing drivers close to average behavior) for intersections regulated by stop signs and give way signs. For driving on priority roads and priority to right regulated intersections, no appreciable effect on the results can be found.

8.3 Adaptation Methods in Real Driving

This chapter describes the procedure of driver-individualized adaptation of transfer functions and the challenges arising in series implementation. The basic principle of the process is summarized in Figure 8-4. In the initialization phase shown in the upper half of the figure, the driver is identified. If the driver is classified as already known to the system, the driver specific data pool is selected corresponding to the driver. Otherwise, the default data pool provided by the system is used. Based on the active data pool, the indicators' transfer functions are calculated as described in section 5.1.

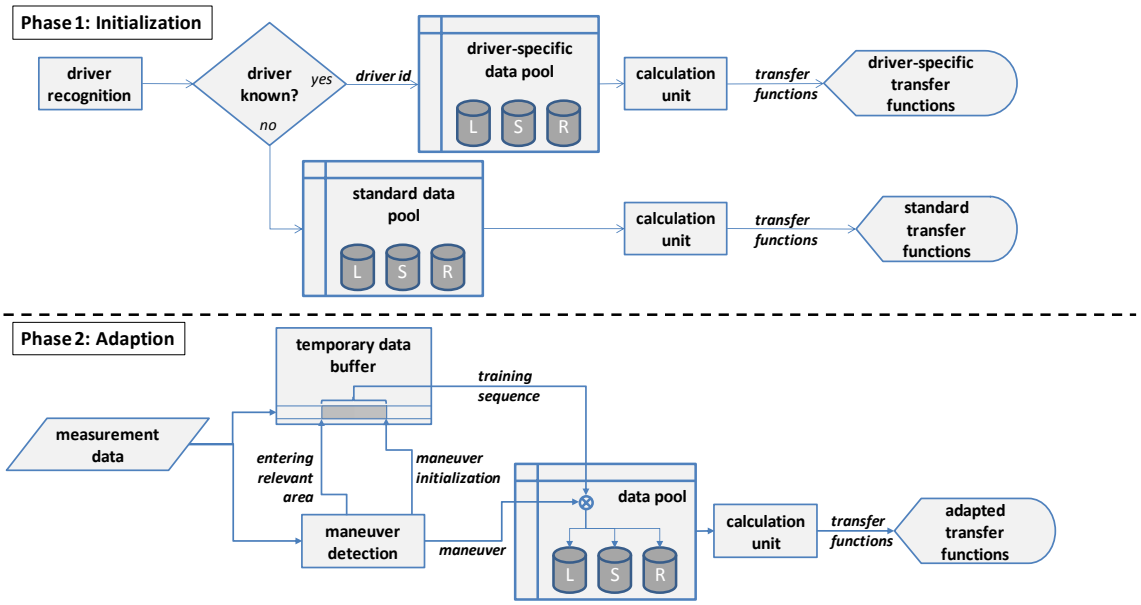

Figure 8-4: Adaptation Process

After completing the initialization phase, the adaptation process is started, as shown in the lower part of Figure 8-4. Here, new intersection approach sequences are added to the data pool. Based on the modified data pool, driver specific adapted transfer functions are generated. Modified transfer functions are stored along with the driver's identifica-

tion. Necessary elements shown in the figure for transforming measurement data into driver-individualized adapted transfer functions are:[179]

1. Temporary Data Buffer
   needed to buffer data of intersection approach until maneuver initialization (termination of approach sequence)
2. Maneuver Detector
   mandatory for classifying approach sequence; maneuver performed by driver is determined a posteriori
3. Data Pool
   containing frequency of occurrences of indicators
4. Calculation Unit
   generates transfer functions from the data pool
5. Driver Identification Unit
   needed to switch or reset adapted transfer functions for different drivers
6. Monitoring Function
   for limiting the of amount of new intersection approach data added to the data pool from reaching saturation for a single driver

8.4 Biasing

Adapting the transfer functions in real road application, as proposed in the prior section, leads to the challenge of biasing. Challenges arise from choice of typical routes (routing bias) and local overfitting, as described in the following.

8.4.1 Routing Bias

Analyzing drivers' normal routing in urban areas shows a pattern that is applied for most urban drives. When starting in residential areas, drivers usually select a direct path to a nearby main street or priority road and stay on this road as long as possible until reaching their destination. This strategy results in shorter travel times than driving solely on residential roads, due to higher average speed on main and priority streets. This is the same basic principle that is applied in navigation devices for routing calculations.[180] As a matter of fact, most urban main streets and priority roads run more or less straight through urban areas. Hence, a challenge arises for the adaptation process: Driving on main streets and adding each intersection sequence to the data pool mainly results in

[179] The functionality of these elements is described in greater detail in Annex J.

[180] Kleine-Besten, T. et al.: Navigation and Transport Telematics (2016), p.1365.

straight driving sequences being added. The longer the adaptation process is active, the more the initial data pool becomes distorted by adding many more straight driving sequences versus turning sequences. Using such a distorted data pool (containing several times more straight driving sequences than turn maneuvers), the most common maneuver (straight driving) will be predicted most of the time. Thus, a compensation method is needed. Two potential methods of compensation can be applied:

In the first method, new sequences are only added in a set of three to the data pool with every set containing a sequence for right turns, one for left turns, and one for straight driving. Applying this method ensures that the data pool is not distorted by a different amount of sequences for each maneuver. The disadvantage of this method is that the adaptation process is slower. In extreme cases, the adaptation process can even be disabled if there are not enough training sequences containing a set of three sequences for each type of intersection within one trip. The second method uses each intersection approach sequence and integrates it into the data pool. The different numbers of intersection approaches are accepted here and taken into account by weighting factors. The weighting factors are calculated by the number of sequences available for each maneuver. The calculation is done analogously to the weighting factors introduced for the exclusion method in Section 6.6.3.

8.4.2 Local Overfitting

Regularly driving the same route may lead to local overfitted transfer functions that are adapted to exactly this route (e.g. if a vehicle is used mainly for commuting to and from work). Each sequence that is added to the data pool originates from the same limited set of intersections. As long as the driver sticks exactly to this route, the prediction will perform well, but in case a different route is used than the regularly driven one, the prediction results might be worse than using non-adapted transfer functions. The problem is demonstrated by the following situation: Assuming the regularly driven route contains exactly one maneuver of the intersection class priority to right and there is a parking spot hindering the driver from driving straight towards the intersection as depicted in Figure 8-5.

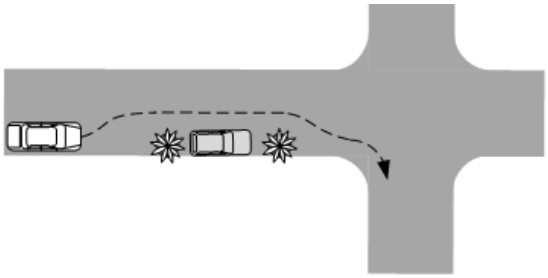

Figure 8-5: Local overfitting example

If this approach sequence is added to the data pool regularly, each time the driver passes this intersection, the initial share of data for this intersection class is influenced significantly and the pool becomes overfitted. In this case, the system is falsely adapted to the information that this driver always performs an evasive maneuver before turning at priority to right intersections. This example shows that aside from the approach sequence itself and the maneuver executed, the intersection at which the approach sequence is generated has to be considered. To avoid local overfitting, the maximum number of additional sequences generated at the same intersection and approach direction has to be limited. The limit on how many approach sequences of the same intersection are tolerated in the data pool has to be determined in real road tests and is dependent upon the routes and if they are regularly driven by the driver. Therefore, it is possible that this issue is only of theoretical nature and may not be relevant in real use of an adaptation system.

9 Conclusion and Outlook

In this work, it has been analyzed to which extent the detection of intentions (corresponding to a prediction of maneuvers) is possible before maneuvers are initialized by the driver without using the vehicle's turn indicator state at all.

The option to enable or disable indicators depending on the situation, without altering the overall design, is the key feature for the flexibility of the indicator principle. To enable the intention detection system to perform at arbitrary urban intersections, a classification system for urban intersections has been introduced based on official priority regulations.[181] Applying the prototypic implementation of the intention detection system to data recorded in the test subject study done in this work shows that more than 80 % of all maneuvers are predicted correctly one second before the maneuver is initialized on priority roads with and without existence of traffic lights.

The results show that a maneuver prediction system on guidance level at urban intersections based on the indicator concept and series or close-to-production sensor systems is able to operate at varying intersection types. Despite using only a close to series localization unit and no information from the upcoming intersection aside from the right-of-way regulation, the prediction system implemented here is able to predict maneuvers at a great variety of urban intersections. Indicators can be replaced or additional indicators can be added without altering the approach at all. Thus, the system can be easily modified in case additional sensor systems are added to the vehicle or additional driver's behavior is modeled. Within the development of the approach, different inference methods and algorithms for combining the indicators outputs were analyzed. As a result, it is concluded that either simple inference methods, such as the average or product function, can be used or more sophisticated approaches based on machine learning methods can be applied to the indicators outputs (e.g. Bayesian networks or support vector machines). Each system has individual advantages and disadvantages. A recent survey comparing the most common methods for automated decision making is given by Firl.[182]

Comparing results achieved with different inference methods shows that the quality of the inputs to the inference method is more important than the inference method itself. For that reason, a quality measure based on the indicators ability of maneuver separation is defined and applied in this work. Aside from intersection and distance dependent

[181] Bundesministeriums der Justiz und für Verbraucherschutz: StVO (2015).

[182] Firl, J.: Diss., Probabilistic Maneuver Recognition (2014), pp. 11–31.

selection of highly discerning indicators, the quality measure is used for optimizing the indicators itself.

Besides the "classic" method of inferring which maneuver the driver is about to perform, a complimentary approach is developed in this work in parallel. The novelty of the so-called "exclusion approach" is that it relies on excluding alternative maneuvers that the driver is not going to perform. The advantage of this approach is that false positive alerts of IAS are avoided effectively by excluding potential maneuver options. The exclusion approach is based on the same indicators as the positive calculation method. Comparing the results of both approaches shows that the exclusion method reaches higher true positive rates than the positive calculation, even at several seconds before maneuver initialization by the driver. Thus it offers high potential for use in series application without annoying drivers by frequent false alerts.

Note that the selection of reference points has enormous impact on the system's detection performance. The closer to the intersection center a reference point is defined, the better the prediction performance gets. In addition, the accuracy of the reference point effects the system's performance. Another key feature of this work is the definition of localization-independent reference points: As discussed in this work, the initialization of maneuvers is heavily dependent on the intersections' geometry and size. Consequently, for performance evaluation in this work, reference points have been defined based solely on the ego-vehicle's driven trajectory. Note that this procedure is only applicable for means of a posteriori performance evaluation. An a priori determination of the reference point during intersection approach before a turn maneuver is initiated is not possible as a matter of principle. Due to varying reference points used in related works, a comparison of the prediction performance reached by the prototype implementation done here to related works is not feasible.

In addition to the system's general feasibility to detect intentions at different types of intersections, the potential of adapting the indicators' transfer functions to different driving styles has been analyzed in this work. Using the longitudinal acceleration during intersection approach, drivers are categorized as either sporty, average, or relaxed. Using transfer functions adapted to one driving style, a potential enhancement of the intention detection system is given for drivers of the average group for intersection classes 3 (stop signs) and 4 (give way signs). For this group of drivers, a raised prediction performance of 14.4 % and 13.4 % respectively, has been demonstrated. The results are in line with the expectations: The highest potential for increasing the prediction performance was found for intersection classes with the predictions depending only on the driving behavior. All kinds of information that is beneficial for maneuver prediction on priority roads, such as environmental information and especially road markings, are usually not available for maneuver prediction at stop sign or give way sign regulated intersections. For drivers of the other two groups (sporty and relaxed drivers) no raised

prediction performance could be identified in the adaptation analysis. Further research has to address the question if this is caused by the size of the groups. In the test study done here, the average driver group consisted of about twice the number of drivers than the other two groups. The effect of the amount of drivers in the two smaller groups has to be addressed in further extended studies. However, a critical review of the data recorded in test drives leads to the assumption that the test subjects adapted their driving behavior to the test situation: Test subjects showed a turn indicator usage rate of approximately 95 % for turn maneuvers. This rate is 20 % higher than the rate observed in natural driving.[183] In addition, with the test conductor being present in the vehicle and test subjects being aware of data recording, most drivers showed a careful driving style. Even drivers who claimed to have a very sporty driving style in self-assessment rarely exceed lateral accelerations of $a_y = 3.5\ \frac{m}{s^2}$ in test drives (< 5 % of all turn maneuvers). Further research potential lies in analyzing the effect of drivers being aware of test conditions and data recording to their driving style. To answer the question if drivers alter their intersection approach behavior in this case, data from a long-term field operation test (FOT) [184] has to be used for analyzing the driver's natural intersection approach behavior. Aside from gathering a much larger amount of data in a FOT, the potential of the adaptation procedures has to be re-evaluated.

[183] Ponziani, R.: Turn Signal Usage Rate Results (2012), p.6.

[184] FOT-Net: Field operational tests (2010).

A Driver Inputs for Maneuver Detection

The distribution of minimum and maximum steering wheel angles recorded at all intersection approaches of the test subject study[185] with straight driving maneuvers is given in Figure A-1 as a cumulated distribution function. Regarding the range between $\delta_{low,5} = 5\,\%$ and $\delta_{high,95} = 95\,\%$ results in a range $r_\delta = [-49°, 54°]$ for steering wheel angles linked to straight driving maneuvers.

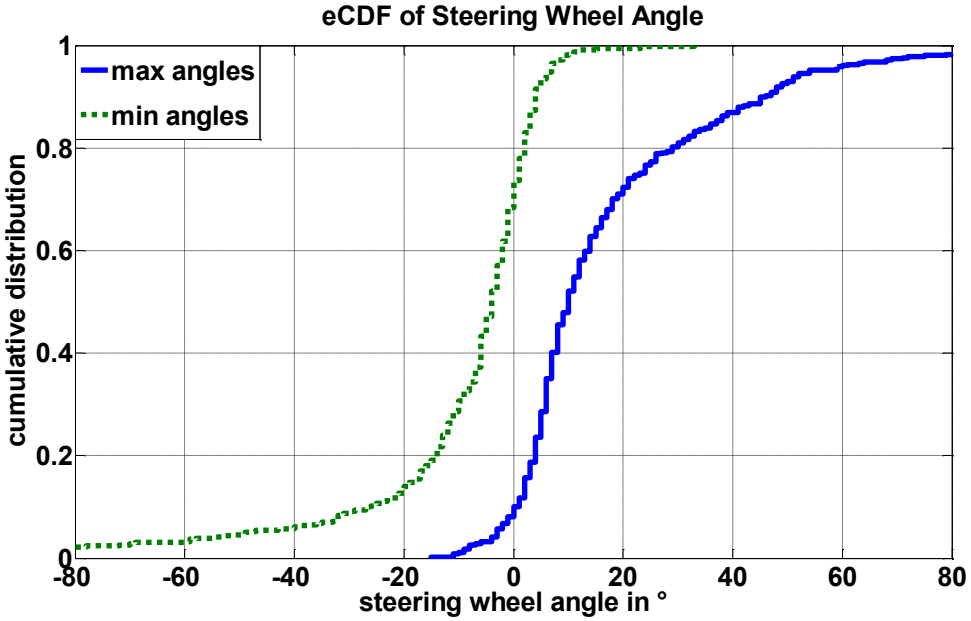

Figure A-1: Minimum and maximum steering wheel angles δ while driving straight

If a limit of $|\delta| > 50°$ is used for turn maneuver detection, the resulting time delay between initialization of a turn maneuver[186] and reaching a steering wheel angle $|\delta| > 50°$ is given in Figure A-2.

The figure shows eCDFs of $t_{del} = t_{ini} - t_{\delta,50}$ for each of the turn maneuvers recorded in the test subject study. It is found that 78 % of all left turns and 54 % of all right turns are detected with a time delay of $t \geq 1$ s after maneuver initialization.

[185] See Section 4.4 for details of the test subject study.

[186] Initialization of a turn maneuver is determined using the calculated reference point as described in section 6.3.2.

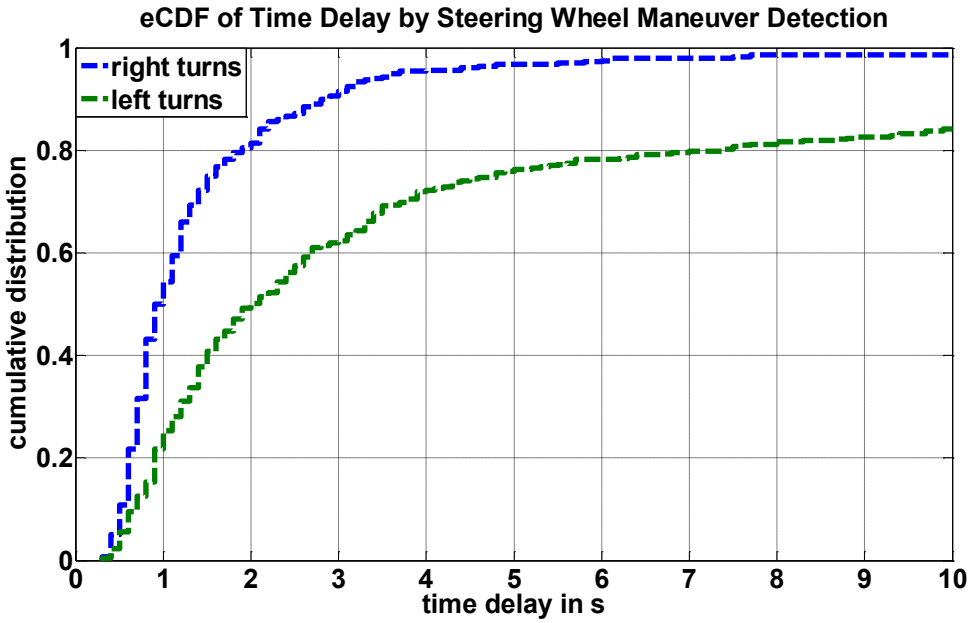

Figure A-2: Time delay between reference point and maneuver detection by steering

Applying the same procedure described above to the vehicle's lateral acceleration results in 89 % of all left turns and 71 % of all right turns being detected with a time delay of $t \geq 1$ s between maneuver initialization and exceeding the turn detection limit as shown in Figure A-3.

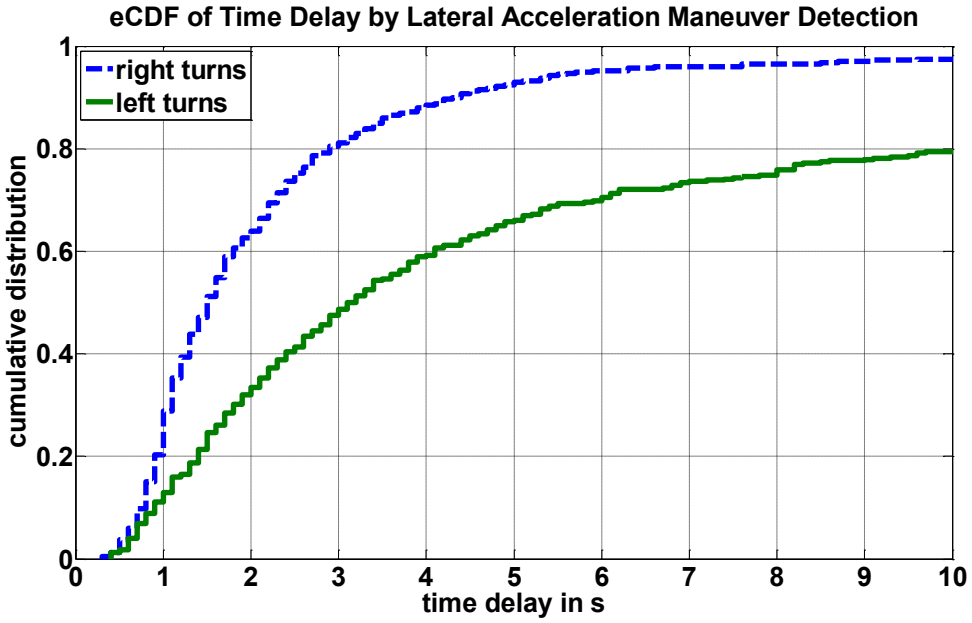

Figure A-3: Time delay reference point and maneuver detection by lateral acceleration

The same applies to using the vehicle's yaw rate $\dot{\psi}$ instead of lateral acceleration following the same procedure. As shown in Figure A-4, 81 % of all left turns and 56 % of all right turns show a delay of $t \geq 1$

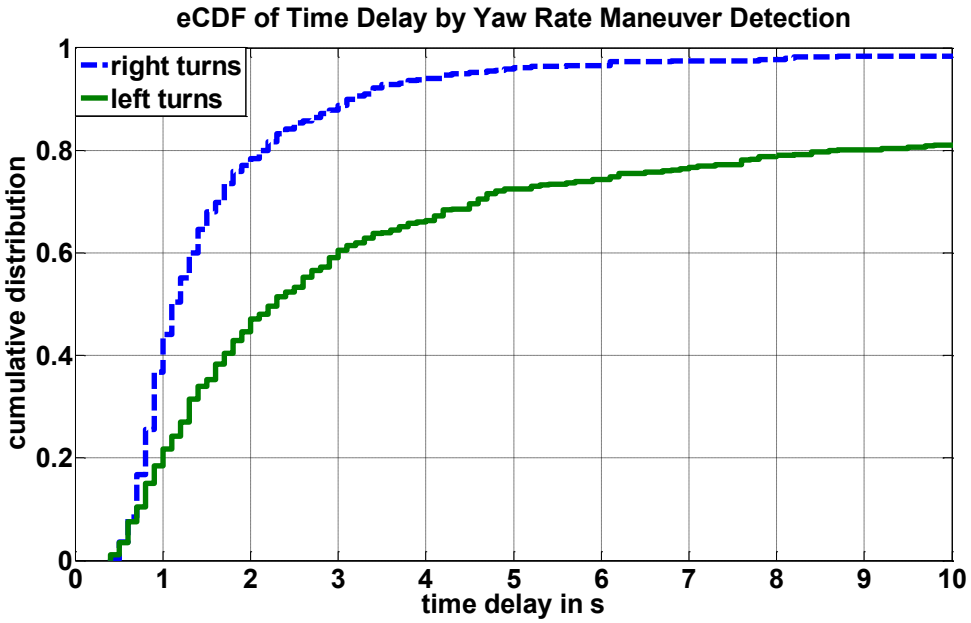

Figure A-4: Time delay between reference point and maneuver detection by yaw rate

B Radar Based Lane Detection

A brief summary of the basic working principle of the radar-based lane detection is given here.

All objects detected by radar sensors are categorized according to their positions in relation to the ego-vehicle and their motion state. Based on the ego-vehicle's speed and the measured relative speed of the radar objects, each object is classified as moving in the same direction, stationary, or oncoming, and according to its position on the left or right of the ego-vehicle. Based on the ego-vehicle's motion state, an ego-path prediction is done using a linear single track model. Objects are only taken into account if they are detected in a range of $d \leq d_{lim}$ in front of or behind the ego-vehicle and within a lateral range of $y \leq y_{lim}$ to the ego-vehicle's center along the predicted path. Each object classified as moving is assigned an existence value for an adjacent lane on the side of the vehicle the object is detected (right/left). Depending on the lateral position of the object, a weighting function w_{lat} is applied to the object's existence value, modifying it within the range between zero and one. Furthermore, a weighting function w_{lon} is applied to reduce the influence of detected objects at higher distances with respect to increasing inaccuracies of path prediction at higher distances. For lane existence calculation, all objects of each category (stationary/oncoming/moving in same direction) are summed up along with their existence values. The more moving objects are detected by the radar sensors, the higher the lane existence likelihood is. The total number of n moving objects on either the left or the right side of the ego-vehicle is used for calculating the lanes existence likelihoods:

$$p_{ex} = \sum_{i=0}^{n} p_i \tag{B-1}$$

Static objects are considered in the same way as the dynamic objects. Combining all relevant static objects leads to existence values for solid elements p_{stat} and therefore no accessible adjacent lanes next to the ego-vehicle.

Depending on the relation between static and moving objects, the existence likelihood of a lane is calculated as follows:

$$p_{lane\ exist} = \frac{p_{ex} - p_{stat} + 1}{2} \tag{B-2}$$

Formula (B-2) automatically returns an existence likelihood that is normalized to the range between 0 and 1 with 0.5 representing a state without detections.

In addition, the driving direction for the left lane is estimated, taking the relation between static and moving objects in account. This is done by subtracting the two sums of weighted likelihoods of all relevant objects: The sum of all oncoming object likelihoods is subtracted from the sum of all object likelihoods moving in the same direction as the ego-vehicle:

$$dd = \sum_{i=1}^{n} p_{\,i,same\ direction} - \sum_{i=1}^{m} p_{\,i,oncoming} \tag{B-3}$$

n = number of relevant objects in same driving direction

m = number of relevant objects in opposite driving direction

Depending on the value of dd, the model outputs the following values:

$$dd = \left\{ \begin{matrix} 0.5 \\ 0.5 \cdot dd \\ 1 \end{matrix} \middle| \begin{matrix} dd \leq 1 \\ for\ 1 < dd \leq 2 \\ 2 < dd \end{matrix} \right\} \tag{B-4}$$

A lower limit is applied for a minimum number of S sufficient objects that need to be detected for calculation of a lane existence. If less than N_{min} moving objects are detected on the left of the ego-vehicle, the first row of (B-4) is activated and the model outputs $dd = 0.5$ corresponding to no information. If sufficient moving objects ($n > N_{min}$) moving in the same direction are detected on the left of the ego-vehicle, the third row is activated and the model outputs $dd = 1$ indicating that there is an adjacent lane to the left in the same direction. If both objects driving in the same direction and oncoming objects are detected, the model outputs a linear interpolation between the two states. The more objects there are driving in the same direction in relation to detected oncoming objects, the higher dd is. For means of indicator calculation, the existence likelihood of the left lane is evaluated in combination with the lane's driving direction.

C Localization

To distinguish whether an intersection is within a relevant area in front of the ego-vehicle, the ego-vehicle's driving direction on a digital road needs to be determined. This is done by comparing the last matched positions on the same edge. Thus, a minimum of two consecutive GPS positions are needed. The resulting information from this step is whether the vehicle is moving in the same or the opposite direction of the road modeled on the digital map. Knowing the driving direction, the next node in the vehicle's driving direction in the road network is analyzed. For detection of an intersection, the number of edges from this node to further nodes needs to be larger than one. If no intersection is detected at the next node in front of the ego-vehicle, the node after the next one is analyzed. This procedure is extended to all following nodes until an intersection is found. With the known position of the next intersection and the ego-vehicle's position, the remaining distance to the next intersection along the path of the digital map is calculated by summing up the length of road segments between the vehicle's position and the intersection. Having identified the next intersection, the edge's angles α in relation to the edge leading to the intersection are calculated as shown in Figure C-5. Knowing the relative angles α enables an allocation of the edges to driving directions.

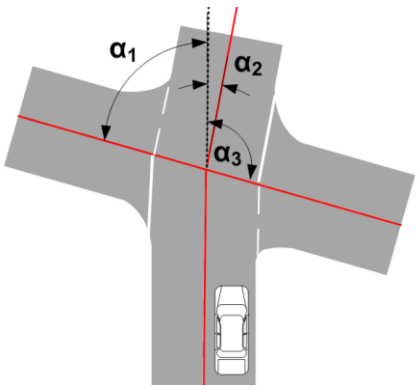

Figure C-5: Road direction allocation

In this step, information of the paths and the potential driving directions at the intersection are extracted from the map. Subsequently, information about the legality of the corresponding maneuvers is needed. If there are any restrictions stored in the map denying the execution of a maneuver by traffic regulations, a maneuver dependent legality flag is set to zero. In addition, the calculation checks if the edges are labeled as one-way roads. In that case, the legal driving direction of the road is extracted from the map, as well. If a potential maneuver at an intersection leads to entering a one-way road from the wrong direction, the legality flag is set to zero, as well.

D Image Processing

Working Principle

The front camera is operated in logarithmic mode using a pinhole model. The camera is used for detection of direction arrows and the type of lane markings (dashed or solid) on the road surface. The distance to the leading vehicle (ACC target) provided by the prototype control unit is used for limiting the detection area. Without a limit, false positive detections can occur because parts of leading cars may look similarly to parts of templates. Thus, if a leading vehicle is detected, its distance is transferred into a maximum height limiting the detection area in the video image. The following section gives a survey of the detection process. Detections are carried out by matching parts of the image with predefined templates. Before the matching is done, the amount of data that has to be evaluated is reduced due to performance reasons.

The template matching process is done using a bird's eye view of the scene. This allows for the use of the same template for matching at any point in the video image without having to adapt the templates to the relative position to the ego-vehicle. For the matching process, template arrows are reduced to the upper parts of the arrows, with the arrowhead defining the type of arrow. These templates are compared to contents of the search windows and similarity measures calculated. Numerous similarity measures can be found in the literature.[187] Here, the normalized squared Euclidean distance (SQDIFF) is selected as similarity measure:[188]

$$RM(x_{im}, y_{im}) = \frac{\sum_{x'_{im}, y'_{im}} \left(T(x'_{im}, y'_{im}) - I(x_{im} + x'_{im}, y_{im} + y'_{im})\right)^2}{\sqrt{\sum_{x'_{im}, y'_{im}} T(x'_{im}, y'_{im})^2 \cdot \sum_{x'_{im}, y'_{im}} I(x_{im} + x'_{im}, y_{im} + y'_{im})^2}} \quad \text{(D-1)}$$

In (D-1), T represents the template image, I the content of the search window and RM describes the matching metrics of T and I for each location (x_{img}, y_{img}) of the template in the source image.[189] The global maximum of RM represents the best matches of the template with the search window and is labeled as a matching score.

If at least one matching score exceeds a limit γ_{score}, the detection is considered valid. The value of γ_{score} is determined in tests, evaluating the false and true positive detec-

[187] Mitchell, H. B.: Image Fusion (2010), pp. 167–185.

[188] Möller, B.; Williams, D.: Tracking (2003), pp. 5–9.

[189] Opencv Dev Team: Template Matching (2016).

tion rates of the system. The best two template matches are selected and sent to the control unit for each lane. If both best matches result from the same template, the template with the third best matching score is transferred, as well. Thus, up to two different direction arrows are detected in the ego-vehicle's lane, the adjacent lane to the left, or the adjacent lane to the right.

Direction Arrow Indicator

When the ego-vehicle changes lanes, it is necessary to extract information from lane markings in order to detect such lane changes in urban conditions. Thus, detecting lane markings on the road surface using video sensors is a crucial factor in using direction arrows for maneuver prediction.[190]

If the ego-vehicle is driving on a road with multiple lanes leading towards an intersection and the lanes head in different directions after the intersection, they are marked with differing direction arrows. If a direction arrow is detected in one lane and the ego-vehicle changes to another lane heading in a different direction, the change has to be recognized to incorporate the new direction arrow information. Without the recognition of the lane change, the detected arrows are wrong, as given in the example in Figure D-6. Here, both direction arrows are detected during the intersection approach and assigned to the lanes correctly at position 1. Assuming the ego-vehicle changes to the turning lane at position 2 and neither the lane change is noticed nor the arrows are re-detected, the information derived from the direction arrows is wrong. Without noticing the lane change to the right, the detected arrows remain as "straight-left" in the ego-lane and "right" for the (at position 3 nonexistent) right lane leading to wrong predictions at position 3.

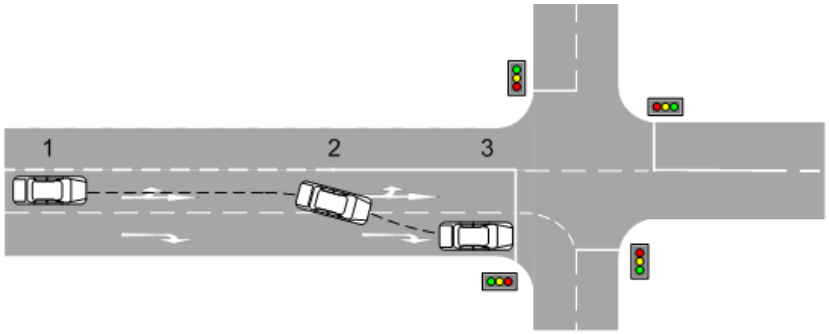

Figure D-6: Direction arrows without lane change detection

[190] Bar Hillel, A. et al.: Recent progress in road and lane detection (2014), pp. 727–745.

The calculation of likelihoods is done as follows: All intersection approaches from the training data are checked for the appearance of each direction arrow in each lane. This is done separately for each maneuver (right turns, left turns, and straight driving). Having processed all training data, a total amount for the number of appearances for each direction arrow is available.

The indicator calculation for direction arrows in adjacent lanes is done analogously to the calculation of ego-lane arrows likelihoods. Here, some boundaries arise: Arrows indicating the driving direction of an adjacent lane limit potential maneuvers for vehicles in the ego-lane: Multiple lanes heading in the same direction towards an intersection have to be collision free. This means, that no maneuver from any lane may lead to crossing an adjacent lane heading in the same direction. Thus, if a direction arrow is detected in an adjacent lane indicating a maneuver where a vehicle in that lane has to cross the path of the ego-vehicle, the ego-vehicle has to perform the same maneuver, as well. The only exception from this rule is applied in the case of hook turns.[191] However, with respect to perception errors, the statistical evaluation of detected arrows has to be applied in the same way as used for direction arrows in the ego-lane.

[191] Currie, G.; Reynolds, J.: Hook Turns (2011), pp. 10–19.

E Intersection Classification

Intersections Regulated by Traffic Lights

Intersections operated by traffic lights are divided into two classes: Intersections with separate direction specific traffic lights (class 1) and intersections with combined traffic lights regulating all lanes and their driving directions (class 2). As shown in Figure E-1 in class 1, priority traffic does not have to be considered for any maneuver. In the following figures, priority traffic is depicted as blue vehicle with the index indicating the direction the priority traffic is coming from (O=oncoming, R=right, L=left) and the ego-vehicle is shown in yellow. While class 2 is the same as class 1 for straight driving and right turns, oncoming traffic has to be considered by the driver for left turns, as shown in Figure E-2.

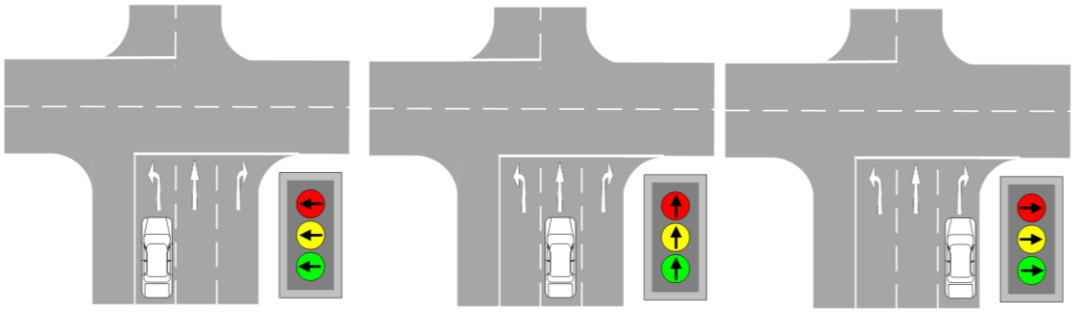

Figure E-1: Class 1: direction specific traffic lights

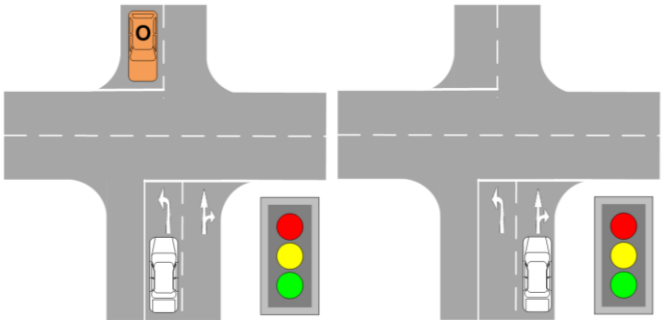

Figure E-2: Class 2: traffic lights for all directions

Intersections with green right turn arrows, as shown in Figure E-3 allowing a right turn even at red traffic lights, are a special case of class 2. For the ego-vehicle driving

straight or turning left, there is no difference to class 2, at all. Only when turning right at red lights does the ego-vehicle have to give priority to all other traffic.

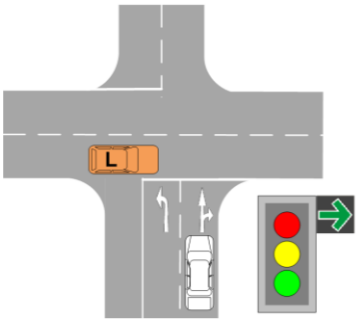

Figure E-3: Special case of class 2: green right turn arrow

Intersections Regulated by Priority Signs

In general, intersections controlled by priority signs form classes 3 to 7.

Intersections operated by stop or give way signs form classes 3 & 4 (see Figure E-4). Here, crossing traffic has priority to the ego-vehicle in all cases. Oncoming vehicles only have priority to the ego-vehicle if the ego-vehicle is turning left and the oncoming vehicle is not performing a left turn. The difference between both classes is that stopping for all maneuvers is mandatory in class 3, while it is not in class 4. Note that both classes share the common feature that drivers have to approach the intersection at low speeds due to checking for priority traffic.

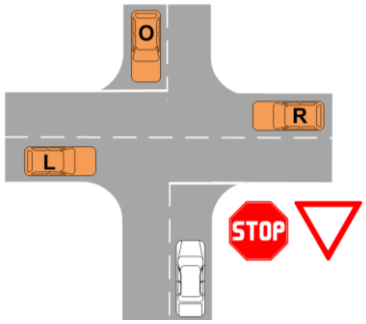

Figure E-4: Class 3: stop sign, class 4: give way sign

Class 5 includes intersections with priority signs "priority road" and "priority" according to Figure E-5. The ego-vehicle has priority for straight driving and right turns, whereas oncoming traffic has to be considered by the ego-vehicle's driver for left turns.

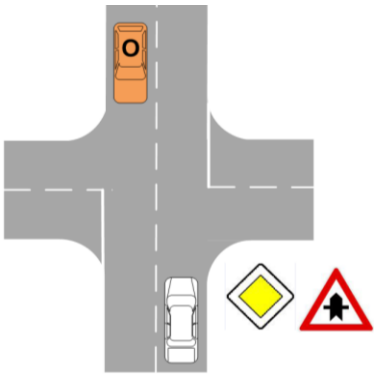

Figure E-5: Class 5: priority road and priority sign

Classes 6 and 7 contain turning priority roads that turn both directions. This class is only relevant for the ego-vehicle driving on the priority road. If the ego-vehicle is approaching a turning priority road via a minor road, class 3 or 4 is applied because of the give-way regulations for minor roads intersecting with priority roads. On right turning priority roads (class 6), the ego-vehicle has to consider oncoming traffic (from the right) on the priority road for straight driving and left turns, as shown in Figure E-6. For left turning priority roads (class 7), the ego-vehicle has priority for every maneuver.

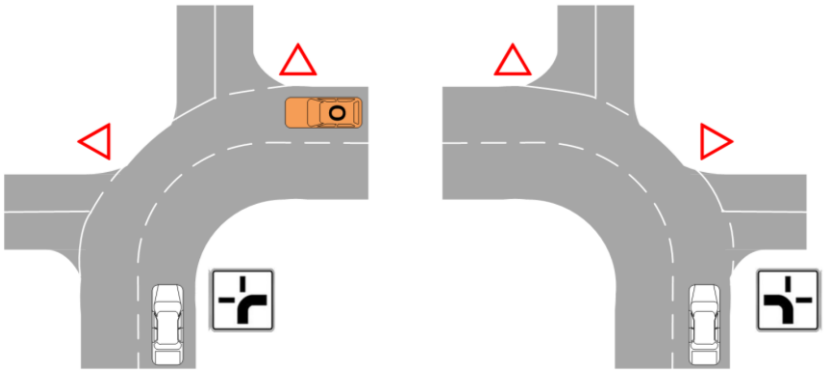

Figure E-6: Class 6 and class 7: turning priority roads

Intersections Regulated by General Regulations

Intersections operated by priority to right regulation are represented by class 8. Here, oncoming traffic has priority for ego-vehicle left turns and crossing traffic from the right is relevant for all maneuvers as shown in Figure E-7.

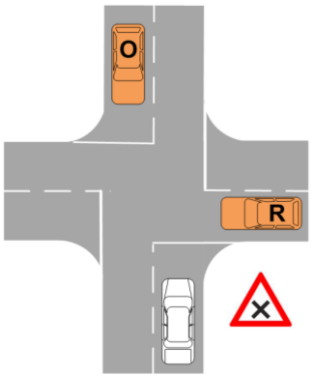

Figure E-7: Class 8: priority to right

Intersection with Bypass Roads

Intersections with bypass roads to the right (allowing right turns without having to line up at traffic lights) are represented by class 9, as shown in Figure E-8. For a straight driving or left turning ego-vehicle, the situation is the same as class 2. In cases of right turns, only crossing priority traffic from the left is relevant for the ego-vehicle's driver.

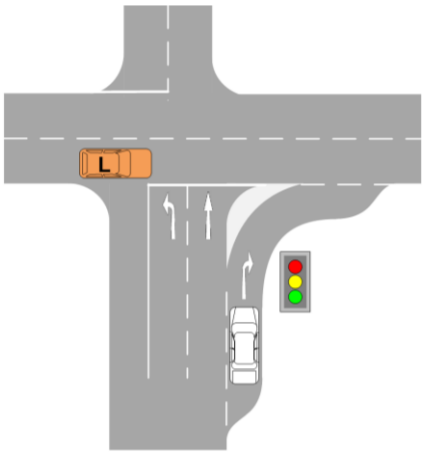

Figure E-8: Class 9: Bypass roads

F Test Drives

The following table summarizes the driving instructions provided to test subjects during driving.

Start in Heinrich-Fuhr-Straße in public parking lot
drive straight, crossing Heinrich-Fuhr-Straße
turn left on to Wilhelm-Jäger-Straße
turn right on to Gundolfstraße
turn left on to Heidenreichstraße
turn right on to Roßdörfer Straße
turn right on to Inselstraße
turn right on to Soderstraße
turn right on to Heidenreichstraße
drive straight, crossing Roßdörfer Straße
turn right on to Heinrichstraße
turn right on to Inselstraße
turn right on to Roßdörfer Straße
drive straight, crossing Heidenreichstraße
turn right on to Frankenäckerweg
turn left on to Heinrichstraße
turn left on to Erlenweg
turn left on to Roßdörfer Straße
drive straight, crossing Hicklerstraße
turn right on to Wilhelm-Jäger-Straße
turn left on to Gundolfstraße, then turn left on to Heidenreichstraße
drive straight, crossing Roßdörfer Straße
turn left on to Heinrichstraße
turn right on to Rehkopfweg
turn left on to Kohlbergweg
turn left on to Dachsbergweg
turn left on to Heinrichstraße, turn right in Frankenäckerweg
turn left on to Roßdörfer Straße
drive straight, crossing Heidenreichstraße
turn left on to Inselstraße
drive straight, crossing Kiesstraße
drive straight, crossing Heinrichstraße
drive straight, crossing Glasbergweg
turn left on to Kohlbergweg
turn left on to Heidenreichstraße

drive straight, crossing Glasbergweg
drive straight, crossing Heinrichstraße
turn left on to Roßdörfer Straße, then turn left on to Inselstraße
turn right on to Heinrichstraße
drive straight, crossing Beckstraße
turn right on to Gervinusstraße
drive straight, crossing Kiesstraße
drive straight, crossing Roßdörfer Straße
turn right on to Soderstraße
turn right on to Beckstraße
drive straight, crossing Roßdörfer Straße
turn right on to Kiesstraße
turn left on to Gervinusstraße
turn right on to Heinrichstraße
turn right on to Wienerstraße
drive straight, crossing Kiesstraße
drive straight, crossing Roßdörfer Straße
turn left on to Soderstraße
drive straight, crossing Martin-Buber-Straße
turn left on to Teichhausstraße
drive straight, crossing Nieder-Ramstädter Straße
turn left on to Heinrichstraße
turn left on to Gervinusstraße
turn left on to Kiesstraße
drive straight, crossing Wienerstraße
turn right on to Nieder-Ramstädter Straße
turn right on to Roßdörfer Straße
drive straight, crossing Martin-Buber-Straße
turn right on to Wienerstraße
turn right on to Kiesstraße, then turn right on to Nieder-Ramstädter Straße
turn left on to Nieder-Ramstädter Straße
drive straight, crossing Riedlingerstraße
turn left on to Hochstraße
turn left on to Kiesstraße
turn right in Hoffmannstraße
drive straight, crossing Heinrichstraße, then turn right on to Hochstraße
drive straight, crossing Heinrichstraße
turn left on to Kiesstraße
turn left on to Karlstraße
turn left on to Heinrichstraße
turn right on to Martinstraße
drive straight, crossing Rückertstraße

turn right on to Steinackerstraße
turn right on to Karlstraße, then turn left on to Annastraße
drive straight, crossing Wilhelminenstraße
drive straight, crossing Eichbergstraße
drive straight, crossing Stauffenbergstraße
turn right on to Heidelberger Straße
turn right on to Hügelstraße
turn left on to Saalbaustraße
turn left on to Elisabethenstraße
drive straight, crossing Neckarstraße
turn left on to Landgraf-Philipps-Anlage
turn left on to Hügelstraße
turn left on to Neckarstraße
turn right on to Elisabethenstraße
turn right on to Saalbaustraße, then turn right on to Hügelstraße
turn right on to Neckarstraße
drive straight, crossing Elisabethenstraße
drive straight, crossing Adelungstraße
drive straight, crossing Rheinstraße, then turn left on to Bleichstraße
turn left on to Steubenplatz
turn right on to Rheinstraße
turn right on to Feldbergstraße, then turn right on to Mornewegstraße and Steubenplatz
turn left on to Rheinstraße
turn right on to Neckarstraße
turn left on to Adelungstraße
turn right on to Saalbaustraße
drive straight, crossing Elisabethenstraße
turn right on to Hügelstraße
turn left on to Neckarstraße
drive straight, crossing Riedeselstraße
drive straight, crossing Heinrichstraße
drive straight, crossing Annastraße
drive straight, crossing Hermannstraße
turn right on to Ehretstraße
turn left on to Donnersbergring
turn left on to Bessunger Straße
turn right on to Heidelberger Straße
drive straight, crossing Sandbergstraße
turn left on to Weinbergstraße
drive straight, crossing Brüder-Knauß-Straße
drive straight, crossing Sturzstraße
turn left on to Ludwigshöhstraße

drive straight, crossing Sandbergstraße
turn right on to Jahnstraße, then turn into roundabout back on to Jahnstraße
turn left on to Bessunger Straße
turn right on to Sandbergstraße
turn left on to Kiesbergstraße
turn left on to Weinbergstraße, then turn left on to Ludwigshöhstraße
turn left on to Bessunger Straße
turn right on to Heidelberger Straße
drive straight, crossing Niederstraße
turn right on to Hermannstraße
drive straight, crossing Eichbergstraße
drive straight, crossing Bessunger Straße
turn right on to Klappacher Straße, then turn left in roundabout in Jahnstraße
turn right on to Clemensstraße
turn right on to Seekatzstraße
turn left on to Klappacher Straße
turn right on to Herrngartenstraße
turn left on to Prälat-Diehl-Straße
drive straight, crossing Moosbergstraße
turn left on to Landskronstraße
turn left on to Klappacher Straße
turn left on to Moosbergstraße
drive straight, crossing Mendelssohnstraße
turn right on to Prälat-Diehl-Straße
turn right on to Herrngartenstraße
turn right on to Moosbergstraße, then drive straight, crossing Mendelssohnstraße
turn left on to Prälat-Diehl-Straße, then turn left on to Landskronstraße
turn right to stay on Landskronstraße
turn left on to Nieder-Ramstädter Straße
turn left on to Heinrichwingertsweg
(destination reached)

G Accuracy of Input Signals

Data Acquired via CAN Bus

All input data used for maneuver prediction acquired from the vehicle's sensors via CAN bus are listed below. Typical values for the accuracy of state-of-the-art automotive sensor systems are given and used for the analysis of effects in the following.

Typical steering wheel angle sensors have an accuracy of $\Delta\delta = 0.1°$.[192] Inaccuracies in the steering wheel angle affect the path prediction of the linear one track model. The path prediction influences all information gathered by image processing, the detection of adjacent lanes, and detection of vehicle follow behavior. Data from test drives done in this work shows that steering wheel angles of $\delta = \pm 15°$ are used by test subjects for corrective lane keeping actions even when driving straight. Furthermore, drivers do not drive curves with constant steering wheel angles, as shown in Figure G-1. They adapt their steering wheel angle according to the yaw motion of the vehicle in relation to the desired path. Depending on the steering behavior, the inaccuracy in the path prediction is of one or two orders of magnitude higher than $\Delta\delta$.

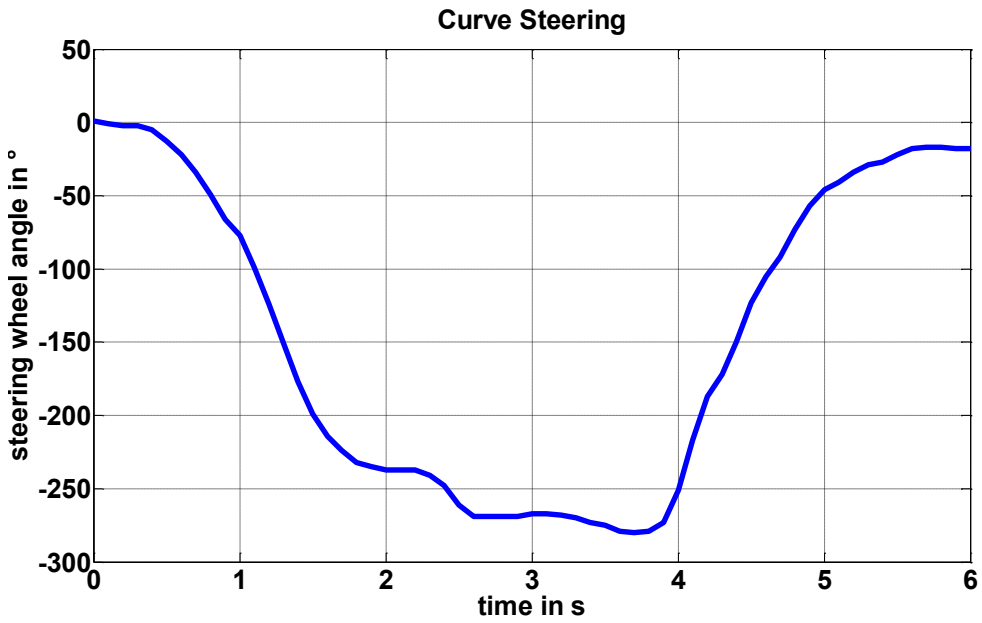

Figure G-1: Exemplary steering motion during turning

[192] Mörbe, M.: Vehicle Dynamics Sensors for DAS (2016), p.293.

Automotive ego-speed measurement is done by wheel rotation sensors. Actual speed sensors reach an accuracy of $\Delta v_{ego} = 0.1\ \frac{\text{km}}{\text{h}}$.[193] The vehicle's speed is used for the speed indicator itself, calculation of predicted stop distances, estimated lateral accelerations in cases of turns, detection of adjacent lanes, and detection of vehicle follow behavior. Even when using a total of 50 speed intervals $\left(1\ \frac{\text{km}}{\text{h}} = 1\ \text{bin}\right)$, the maximum error caused by inaccuracies in the speed signal is 10 times smaller than the interval width and is therefore neglected for the speed indicator. The predicted stop distance is calculated according to (5-12) and (5-13). Here, the error Δd_{pre} caused by a speed inaccuracy of $\Delta v_{ego} = 0.1\ \frac{\text{km}}{\text{h}}$, assuming a typical acceleration of $a_{lon} = -2\ \frac{\text{m}}{\text{s}^2}$ and an approach speed of $v_{ego} = 30\ \frac{\text{km}}{\text{h}}$, is $\Delta d_{pre} = 0.23$ m. Thus, the effect of Δv_{ego} is negligible in comparison to the distance inaccuracy caused by the localization system. Lateral accelerations based on the distance to the next intersection and road geometry, as estimated in (5-9), are affected by Δv_{ego}, as well. Assuming a minimum turn radius of $R = 10$ m and an approach speed of $\Delta v_{ego} = 30\ \frac{\text{km}}{\text{h}}$ results in an error of $\Delta a_{y,R} = 0.03\ \frac{m}{s^2}$ that is ignored, as well. Finally, the ego-vehicle's speed is used to classify radar objects detected around the ego-vehicle in oncoming traffic and driving in same direction. Here, the relative speeds of objects detected by the radar sensors are at least two orders of magnitude higher than Δv, so that Δv is without effect on the classification. The same applies to the effect of Δv on the detection of vehicle follow behavior: While driving, the ego-vehicle's speed is two orders of magnitudes higher than Δv_{ego}.

Sensors for measuring longitudinal accelerations for vehicle dynamics control show a measurement accuracy of $\Delta a_{lon} = 0.02\ \frac{\text{m}}{\text{s}^2}$.[194] The ego-vehicle's lateral acceleration is used for the acceleration indicator and the calculation of the predicted stop distance. The interval width of the acceleration indicator is one order of magnitude higher than Δa_{lon}, so the influence of Δa_{lon} is neglected. Using the same assumptions as above, an inaccuracy of $\Delta d_{pre} = 1.74$ m results from Δa_{lon}. Due to the fact that varying intersection geometries influence the driver's behavior and therefore result in varying predicted stop distances, Δd_{pre} is without effect on the detection of a predicted stop near the intersection center.

[193] Niehues, D.: Diss., Positionsbestimmung von Fahrzeugen, p.66.

[194] Mörbe, M.: Vehicle Dynamics Sensors for DAS (2016), pp. 296–297.

Automotive yaw rate sensors reach an accuracy of approx. $\Delta\dot{\psi} = 2\ \frac{^\circ}{\mathrm{s}}$.[195] The vehicle's yaw rate is used to calculate the curvature of the path driven during a turn maneuver. The curvature is used to define the reference point a posteriori, as described in section 6.3.2. Assuming typical yaw rates of $|\dot{\psi}| = 30\frac{^\circ}{\mathrm{s}}$ during turning and a turning speed of $v_{ego} = 20\ \frac{\mathrm{km}}{\mathrm{h}}$,[196] a measurement error of $\Delta\dot{\psi} = 2\ \frac{^\circ}{\mathrm{s}}$ leads to an error of $\Delta\kappa = 0.002\ \frac{1}{\mathrm{m}}$ that is two orders of magnitude smaller than κ_{max} and therefore not considered in the following.

The driver's pedal operation inputs are measured by the brake pressure sensor and the acceleration pedal sensor. Typical brake pressure sensors are within a range of $\Delta pres_{brake} = \pm 3\ \%$.[197] Typical values for the accuracy of pedal states are $\Delta acp = \pm 0.4\ \%$.[198] Inaccuracies in both signals affect only the corresponding indicator directly. The maximum error caused by the acceleration pedal inaccuracy is 10 times smaller than the interval width of the indicator. Thus, the effect of the inaccuracy of the acceleration pedal signal is neglected. Due to the higher number of intervals and the higher maximum error in the brake pressure measurement as compared to the acceleration pedal, the maximum resulting error is higher. Here, the inaccuracy of $\Delta pres_{brake} = \pm 3\ \%$ can lead to activating up to one interval higher or lower than the real value corresponds to. However, a maximum error of one interval is tolerated here.

The gear position is transferred as an absolute gear number. Thus, no measurement inaccuracy discussion is needed.

Head and Gaze Tracking Data

The inaccuracy in the measurement of the head and gaze rotation is given by $\Delta\rho_{HT} = \pm 1°$, according to the specifications of the headtracking system used.[199] The minimum width of intervals in the head and gaze indicator is five times larger than $\Delta\rho_{\mathrm{HT}}$. Thus, a maximum error of one interval can occur due to measurement inaccuracies. For the detection of a fixation on the rear view mirrors, bounding boxes that represent the mirrors are used within the head tracking software. If a fixation on a bounding box is detected by the head tracking system, the box is activated and set as the active element. To cope with inaccuracies in the gaze direction, bounding boxes are slightly

[195] Reif, K.: Automobilelektronik (2014), p.119.

[196] The typical turning speed was determined in pre-tests before starting the test subject study.

[197] N.N.: Brake pressure sensor.

[198] Mörbe, M.: Vehicle Dynamics Sensors for DAS (2016), pp. 300–301.

[199] N.N.: faceLAB5 (2009).

larger than the real mirror is. Thus, the inaccuracy in the measurement is without effect. Furthermore, the head and gaze rotation angles ρ_{HT} vary with the driver's seat adjustments, as schematically shown for a smaller and a larger driver in Figure G-2.

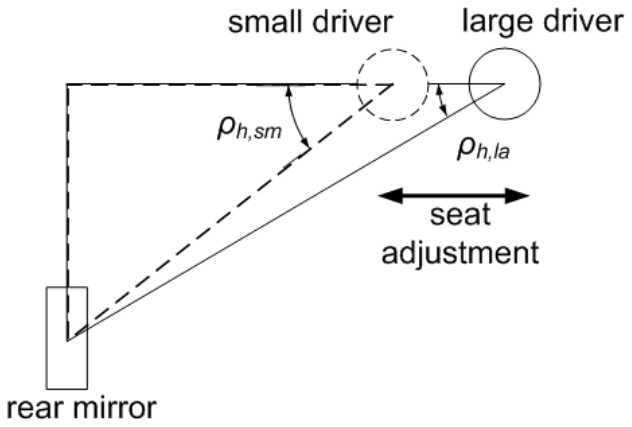

Figure G-2: Effect of seat adjustment

Assuming a longitudinal distance of $x_{lon} = 0.5$ m and a lateral distance of $x_{lat} = 0.6$ m as typical values for the distance between the driver's head and the rear mirror, a lateral seat adjustment range of $x_{seat} = 0.1$ m results in a change of $\rho_{\mathrm{HT}} = 5.2°$. Thus, the effect of $\Delta\rho_{\mathrm{HT}}$ is, however, ignored.

Radar Detections

Using the concept of radar separation capability as cell volume for the dimensions distance, relative velocity, and azimuth angle,[200] typical values for state-of-the-art automotive radar sensor are:[201]

$$\Delta d_{rad} = 0.36\ \mathrm{m}, \qquad \Delta \dot{d}_{rad} = 0.2\ \frac{\mathrm{m}}{\mathrm{s}}, \qquad \Delta\theta = 0.25° \tag{G-1}$$

The measurement inaccuracy in longitudinal distance Δd_{rad} affects the detection of vehicle follow behavior, the detection of adjacent lanes to the ego-vehicle, and the maneuver detection of a leading vehicle for multiple lanes. Due to the fact that the ttc-based and the τ-based criterion introduced in section 5.3 detect vehicle follow behavior by underruning a limit that is at least one order of magnitude higher than Δd_{rad}, the effect of Δd_{rad} is neglected. The same applies to the radar based detection of adjacent lanes and the tracking of preceding vehicles. An object detected by radar sensors is used for the calculation of adjacent lane state as soon as it is within a range defined as relevant around the ego-vehicle and being two orders of magnitude higher than Δd_{rad}.

[200] Winner, H.: Automotive RADAR (2016), p.370.

[201] Winner, H.: Automotive RADAR (2016), p.382.

Apart from the detection of follow behavior, the accuracy of objects' relative speed $\Delta\dot{d}_{rad} = 0.2\ \frac{\text{m}}{\text{s}}$ is used to classify objects detected by the radar sensors into oncoming traffic and traffic driving in the same direction. Here, the same applies as above: Relative speeds of objects are two orders of magnitude higher than $\Delta\dot{d}_{rad}$ so that $\Delta\dot{d}_{rad}$ is without effect to the classification. The same applies to the detection of follow vehicle behavior: Typical relative speeds are one order of magnitude higher than $\Delta\dot{d}_{rad}$.

The measurement accuracy of objects' azimuth angle $\Delta\theta$ affects the target selection of preceding vehicles, the assignment of objects to adjacent or ego-lanes, and the maneuver detection of a leading vehicle. Based on the regulations for designing urban roads,[202] a road with two lanes shall have a width q of $4.5\ \text{m} < q < 6.5\ \text{m}$. Considering one lane, the unknown position of the ego-vehicle in the lane, and the unknown point of reflection of a target vehicle, $q_{min} = \frac{q}{4}$ is used to calculate the maximum longitudinal distance without affecting the lane allocations caused by $\Delta\theta$:

$$d_{lon} = \frac{q_{min}}{\tan(\Delta\theta)} = \frac{1.13\ \text{m}}{\tan(0.25°)} = 257.8\ \text{m} \qquad \text{(G-2)}$$

For all objects detected at distances $\Delta d_{rad} < d_{lon}$, $\Delta\theta$ is without affect on the lane assignment. Furthermore, as mentioned above, the path prediction based on the steering wheel input by the driver creates higher inaccuracies than the inaccuracy caused by $\Delta\theta$. Therefore, the distance of objects used for detecting adjacent lanes and selecting and tracking preceding vehicles is limited to $d < d_{lon}$.

Road Markings

Detected road markings are transferred into binary into the control unit. Inaccuracies in the detection process arise due to false positive and negative detections in the image processing, nondetected lane changes of the ego-vehicle, and missed changes in the arrows during the intersection approach, as shown in Figure G-3. In this example, both direction arrows are detected at position 1. If the arrows' changed layout is not detected at position 2, both arrows are kept active for the ego-lane, even at position 3.

[202] Baier, R.: Richtlinien für die Anlage von Stadtstraßen (2007), p.69.

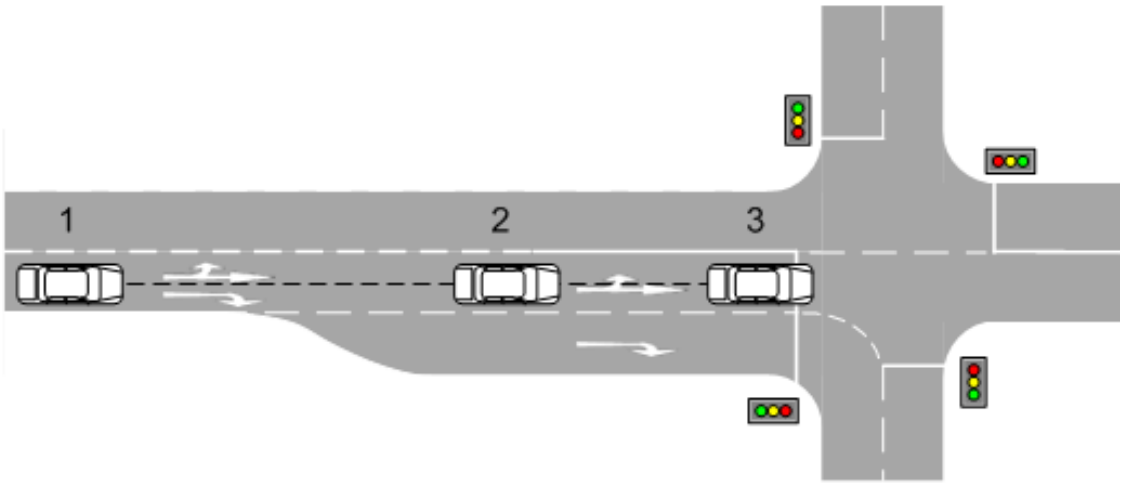

Figure G-3: Missed change detection of road markings

As discussed in section 5.4.3, imperfections in the perception of road markings are taken into account by using training data created statistically, instead of directly deriving the maneuver from the direction arrow detected.

Localization

The positioning accuracy of a conventional GNSS receiver varies with the conditions it is used in and is influenced by several sources of errors, as for example the dilution of precision (DOP), multipath scattering, atmospheric effects, and clock errors. These errors can sum up to a total inaccuracy of $\varepsilon_{GPS} > \pm 11$ m.[203]

To reduce the localization error, Inertial Navigation System (INS) that measure rotation and acceleration of the vehicle via an Inertial Measurement Unit (IMU) are combined with GNSS receivers.[204] A similar principle is applied by the dead reckoning process in the GNSS receiver used in this work. Instead of accelerations, an odometer signal provided by the vehicle is combined with a gyroscope to calculate a relative position to the starting point. This position is combined with the received GNSS position by internal models of the receiver. Thus, the localization accuracy using a GNSS receiver with dead reckoning functionality is enhanced in relation to a localization based solely on GNSS.[205] To determine the remaining positioning error, three types of errors have to be considered in this work, as shown in Figure G-4: The positioning error $\varepsilon_{GPS,DR}$ of the measured GPS position, the error ε_{map} of the digital map, and the positioning error ε_{ai} of the aerial image used as ground truth.

[203] N.N.: GNSS Error Sources (2016).

[204] N.N.: GNSS and INS (2016).

[205] N.N.: Dead Reckoning (2016).

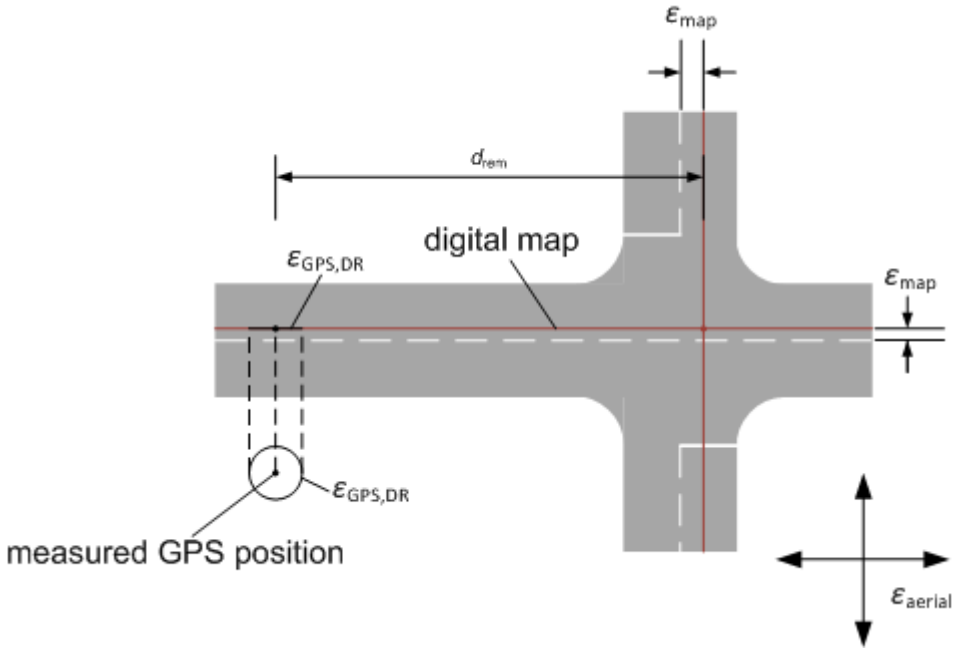

Figure G-4: Positioning errors

A recent study comparing the results of previous studies focusing on the accuracy of aerial images provided by Google Earth[206] states a root mean square error (RMSE) of 2.18 m in horizontal accuracy.[207]

Pre-tests done in this project have shown an RMSE GNSS localization error of $\varepsilon_{GNSS} = \pm 3.2$ m in relation to aerial images provided by Google Earth and an average map precision of $\varepsilon_{map} = \pm 2$ m of the road network of openstreetmap[208] in relation to the aerial image. Note that these values are only average values and that the accuracy varies depending on the location. The remaining distance to the intersection center d_{act} is extracted from the map matched position of the vehicle. According to Figure G-4, an average error of $\varepsilon_{GNSS} + \varepsilon_{map} = \pm 5$ m in relation to the aerial image occurs. Considering ε_{comb} and ε_{ai}, the maximum resulting positioning inaccuracy is $\varepsilon_{comb} = \varepsilon_{GNSS} + \varepsilon_{map} + \varepsilon_{ai} = \pm 7.2$ m. Following the approach introduced in this work relying on distance intervals, the inaccuracy ε_{comb} affects the calculation of all indicators' transfer functions due to the potentially wrong determination of the actual distance interval. In reality, the road layout of urban intersections varies heavily even within one intersection class depending upon the features of each location, available space for the intersection, type of roads connected by the intersection, and the amount of traffic using

[206] Google Earth 7.1.5.1557, access: 20.06.2015.

[207] Farah, A.; Algarni, D.: Accuracy of Googleearth (2014), p.104.

[208] N.N.: OpenStreetMap (2016).

the road.[209] Thus, a variety of geometric forms exist even within one intersection class, resulting in different trajectories. Using the intersection center is an inaccuracy itself because the layout of the intersection is not considered. However, the approach applied in this project deals with this inaccuracy by using training data acquired from a large set of intersections with varying geometry.

Furthermore, ε_{comb} affects the calculation of the predicted stop distance and the estimated lateral accelerations, as introduced in section 5.4.4. Due to varying intersection size and layout, all predicted stops near the intersection center $\left(d_{pre} \leq d_{pre,lim}\right)$ are used. Thus, a limitation for $d_{pre,lim}$ is derived:

$$d_{pre,lim} > \varepsilon_{comb} \tag{G-3}$$

[209] Baier, R.: Richtlinien für die Anlage von Stadtstraßen (2007), pp. 109–110.

H Reference Points

Especially with the ego-vehicle driving at low speeds, curvature calculation based on the vehicle's yaw rate sensor is error-prone due to signal noise. During standstill, the calculation fails completely due to the absence of a yaw rate $\dot{\psi} \neq 0$ aside from noise. A survey of different methods to derive the curvature given by Winner[210] shows that a well performing calculation of the curvature can be achieved by combining the curvature calculation based on the vehicle's yaw rate sensor $(\kappa_{\dot{\psi}})$ and the curvature calculation using the steering wheel angle (κ_{δ}). The curvature $\kappa_{\dot{\psi}}$ based on the output of the vehicle's yaw rate sensor $\dot{\psi}_{\mathrm{v}}$ and the ego-vehicle's speed is given by:

$$\kappa_{\dot{\psi}} = \frac{\dot{\psi}_{\mathrm{v}}}{v} \tag{H-1}$$

The approximation of the curvature κ_{δ} is based on a linear single track model, using the vehicle's steering wheel angle δ, the steering transmission ratio ra_{str}, the vehicle's speed v_{ego}, its characteristic speed v_{char}^2 , and the wheelbase *WB*:[210]

$$\kappa_{\delta} = \frac{\delta}{(ra_{str} \cdot WB)\left(1 + \frac{v_{ego}^2}{v_{char}^2}\right)} \tag{H-2}$$

The vehicle's characteristic speed describes the vehicle's understeering behavior based on the relation of the axles' cornering stiffness and is given by:[211]

$$v_{char} = \sqrt{\frac{c_{fr} \cdot c_{rear} \cdot WB^2}{ma_v\left(c_{fr} \cdot d_{fr} - c_{rear} \cdot d_{rear}\right)}} \tag{H-3}$$

Here, c_{fr} and c_{rear} represent the cornering stiffness of the front and rear axles, ma_v the ego-vehicle's mass, and d_{fr} and d_{rear} are the lever arms between the axles and the vehicle's center of gravity. While the curvature calculation is based solely on the yaw rate sensor when the vehicle is driving above a transition speed v_{trans}, a mixture of $\kappa_{\dot{\psi}}$ and κ_{δ} is applied below the transition speed. When the vehicle is stopped, κ_{δ} is used solely. A speed dependent factor f_{κ} is defined using the transition speed of $v_{trans} = 20\ \mathrm{km/h}$:

[210] Winner, H.; Schopper, M.: Adaptive Cruise Control (2016), pp. 1116–1117.

[211] Mitschke, M.: Dynamik von Kraftfahrzeugen (2003), p.562.

$$f_\kappa = \mathrm{MIN}\left(1, \frac{v_{ego}}{v_{trans}}\right) \tag{H-4}$$

The total curvature κ_{total} is given by

$$\kappa_{total} = \kappa_\delta \cdot (1 - f_\kappa) + \kappa_\psi \cdot f_\kappa \tag{H-5}$$

The calculation of κ_δ is simplified by neglecting the vehicle's characteristic speed v_{char}. The simplification is done based on the following assumption: Typical values of the characteristic speed for understeering vehicles are $v_{char} > 60\ \frac{\mathrm{km}}{\mathrm{h}}$.[212] Assuming $v_{char} > 60\ \frac{\mathrm{km}}{\mathrm{h}}$, the factor $\left(1 + \frac{v_{ego}^2}{v_{char}^2}\right)$ is limited to a maximum of $\left(1 + \frac{v_{ego}^2}{v_{char}^2}\right) = 1.1$, with the vehicle driving at $v_{ego} = 20\,\frac{\mathrm{km}}{\mathrm{h}}$. Using the speed dependent factor $(1 - f_\kappa)$, the total error is reduced depending on the vehicle's speed. Thus, neglecting the characteristic speed results in a maximum error in κ_{total} of 1.6 % at an ego-vehicle speed of $v_{ego} = 13\,\frac{\mathrm{km}}{\mathrm{h}}$. Thus, the simplified calculation of κ_{total} is given by:

$$\kappa_{total} = \frac{\delta}{(ra_{str} \cdot WB)} \cdot \left(1 - \mathrm{MIN}\left(1, \frac{v_{ego}}{v_{trans}}\right)\right) + \frac{\dot{\psi}_\mathrm{v}}{v_{ego}} \cdot \mathrm{MIN}\left(1, \frac{v_{ego}}{v_{trans}}\right) \tag{H-6}$$

Figure H-1 shows the curvatures of an exemplary turn maneuver. The turn maneuver is executed at a low speed resulting in a noisy signal of the ego-vehicle's yaw rate sensor and a noisy curvature κ_ψ , displayed as dashed line. The calculated curvature κ_δ is displayed as dash-dotted line and the combined curvature κ_{total} is displayed as solid line.

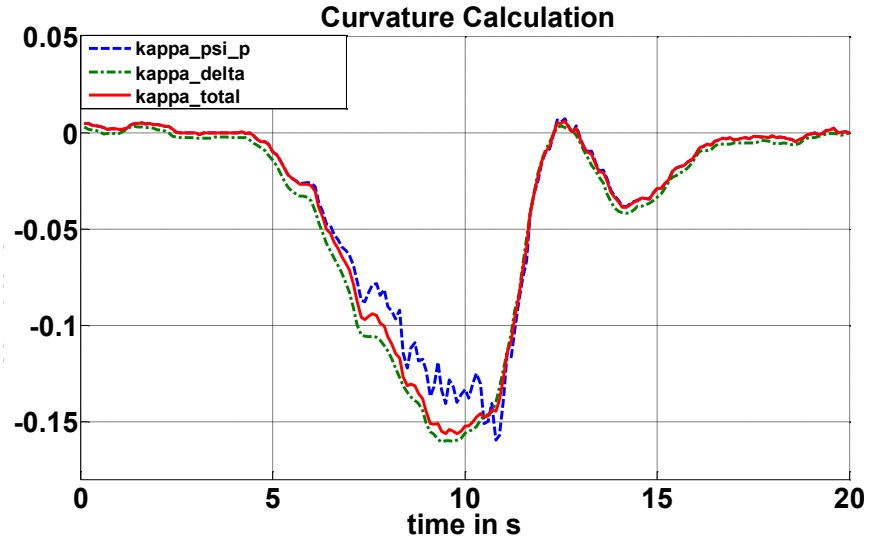

Figure H-1: Curvatures

[212] Halfmann, C.; Holzmann, H.: Kraftfahrzeugdynamik (2003), p.214.

Based on the combined curvature, the apex of the turn maneuver is determined using the area under the curvature-vs.-travelled-distance curve. The distance travelled during the turn is acquired by integrating the ego-vehicle's velocity over time:

$$apex = \frac{1}{2} \cdot \int_{\kappa_{start}}^{\kappa_{end}} \kappa_{total} \, \mathrm{d}s \tag{H-7}$$

With a known apex of the maneuver, the reference point for turn maneuver initialization is defined as a percentage of the apex's curvature.

Using a percentage of the apex results in an individualized maneuver reference point free of localization inaccuracies.

I Neglecting Intersection Classes

The figures shown in this annex present the prediction performance reached with the prediction system when intersection classes are ignored during training.

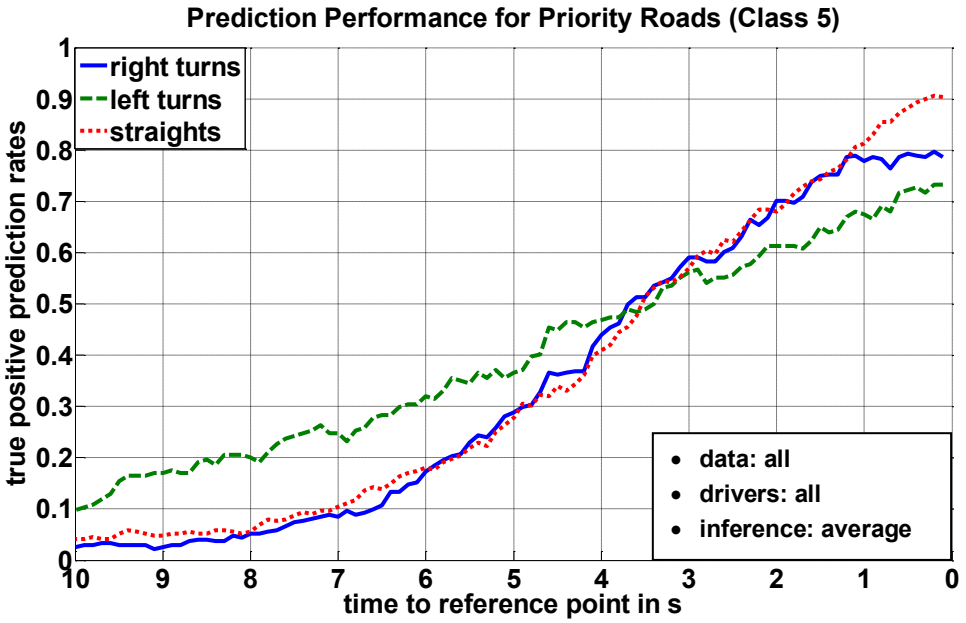

Figure I-1: Results of class 5 without separated training data (priority road and priority sign)

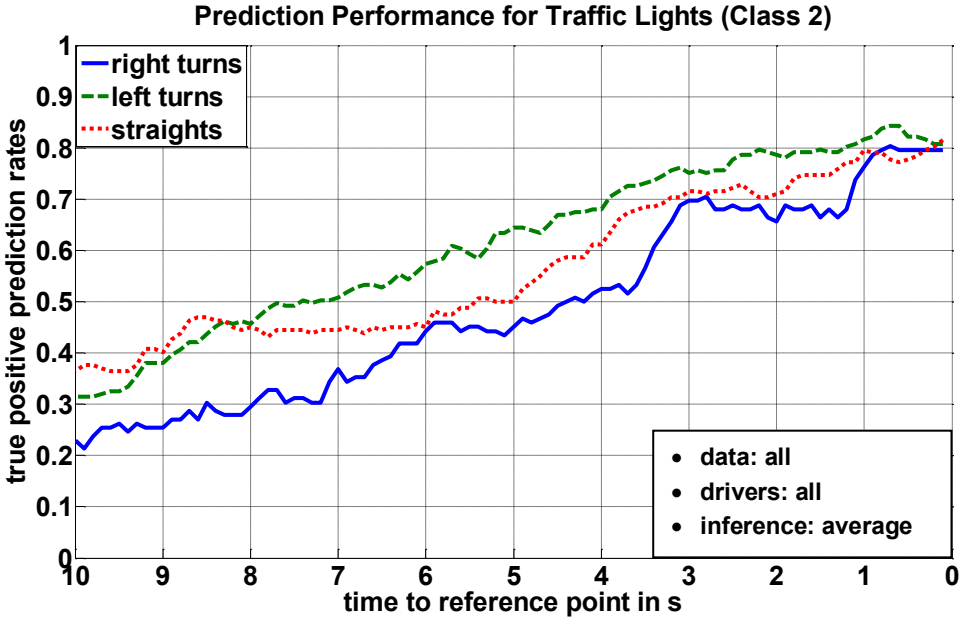

Figure I-2: Results of class 2 without separated training data (traffic lights for all directions)

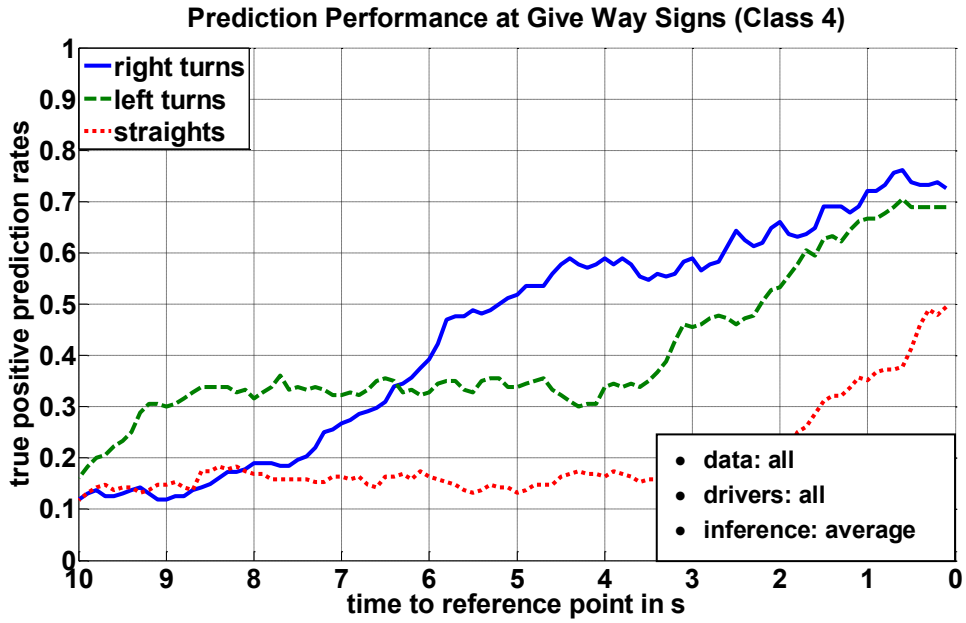

Figure I-3: Results of class 4 without separated training data (give way sign)

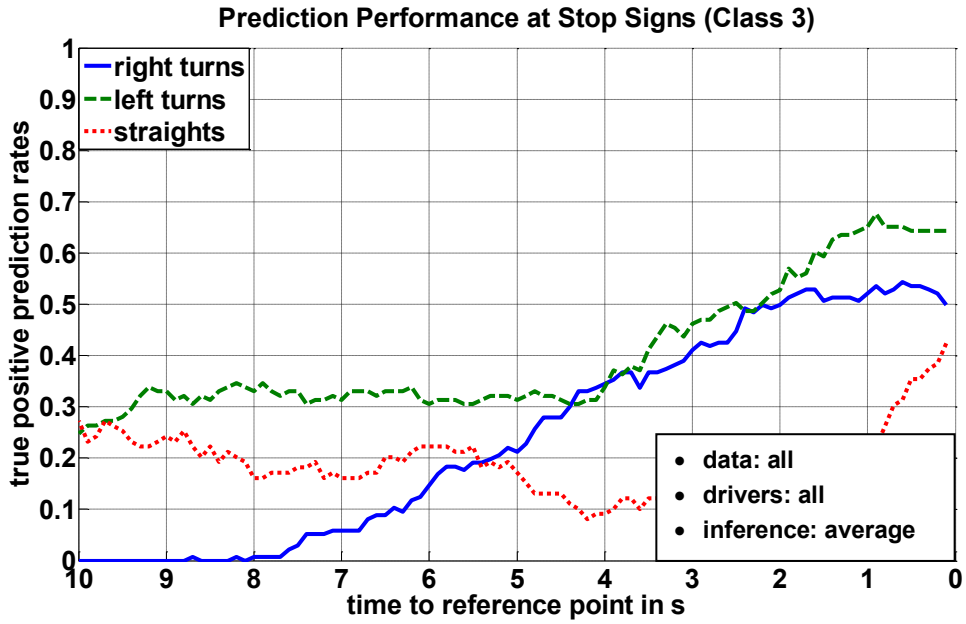

Figure I-4: Results of class 3 without separated training data (stop sign)

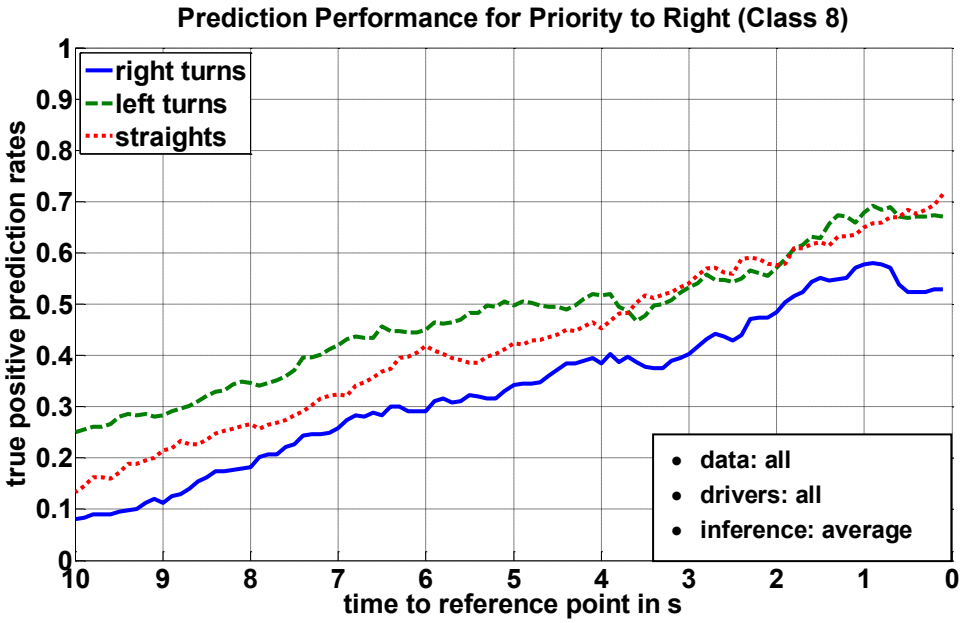

Figure I-5: Results of class 8 without separated training data (priority to right)

J Elements of the Adaptation System

Temporary Data Buffer

The adaptation process is carried out while the vehicle is in use and is driving on urban roads. Thus, a stream of measurement data and calculations are produced by the vehicle's sensors and based on sensor data. For the adaptation process, sequences of intersection approaches have to be extracted from the data stream. The beginning of these approach sequences is located at the time the ego-vehicle enters the relevant area before the intersection. The sequences terminate at the reference point of the maneuver (initialization of the maneuver). Because the termination of sequences is not known a priori, all relevant data used for maneuver prediction has to be stored in a temporary data buffer. This data is no longer needed when the ego-vehicle has left the intersection, so the sequence is transferred to the data pool and the temporary buffer is cleared.

Maneuver Detection

To classify the approach sequence, a maneuver detector is needed. The maneuver detector detects which maneuver is performed by the ego-vehicle and outputs the information to the data pool. The maneuver will be known at the very latest after the ego-vehicle has left the intersection, so the maneuver specific reference point can then be calculated.[213] Several methods can be applied for a posteriori maneuver detection. Turn maneuvers can be detected by evaluating the vehicle's steering wheel angle δ, lateral acceleration a_y or yaw rate $\dot{\psi}$. These methods all require the definition of limits that the input signal has to exceed for at least a minimum distance travelled (e.g. a turn is detected if $|\delta| \geq \delta_{lim}$ for a minimum travel distance s_{lim}). Aside from that, varying intersection size and geometry lead to false detections when applying these methods and straight driving maneuvers at intersections cannot be identified at all. To be able to detect straight driving maneuvers, information of the existence of an intersection is needed. This information is taken from a localization system and a digital map as described in section 4.2. Using a localization system and a digital map offers an alternative maneuver detection manner: With the ego-vehicle's position matched to the streets of a digital map, the maneuver is detected as follows: The way id[214] and vehicle's driving direction

[213] Note that the reference point marks the initialization of the maneuver itself and the end of the approach sequence.

[214] A way id is an unique identifier in OSM used to identify a way.

after passing an intersection is compared to the values before reaching the intersection. To detect maneuvers only by using the digital map, a lookup table is needed for every intersection connecting the way identifications and driving directions with the maneuvers. An example of the procedure is shown in Figure J-1. The excerpt used for this example from the corresponding lookup table is given in Figure J-1.

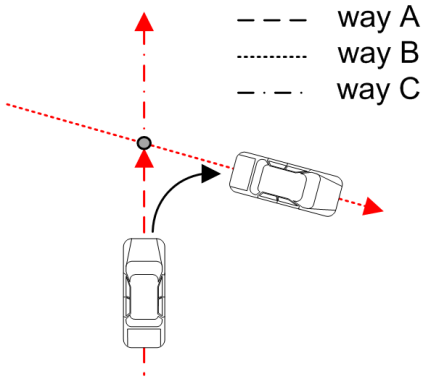

Figure J-1: Maneuver detection by digital map

Table J-1: Lookup table maneuver detection

	before intersection	after intersection	maneuver
way id	A	C	right
driving direction	same	same	

This method is only applicable if the road is modeled very simply, as in the example of Figure J-1. Furthermore, way identification and driving direction assignment to maneuvers must be done separately for each way connected to the intersection. If the map matching process temporarily fails, the resulting assignment is wrong. Thus, another method is proposed here that is able to handle even complex intersections that relies on the vehicle's relative heading: The relative heading ψ_{rel} after leaving an intersection in relation to the beginning of the approach sequence is calculated. Approximating the relative heading solely by integrating the vehicle's yaw rate $\dot{\psi}$ has to fail at low speeds due to the yaw rate signal level being similar to the sensor noise. Thus, the calculated curvature κ_{calc} as introduced in section 6.3.2 is applied. The benefit of κ_{calc} is that the calculation even generates a reliable non-zero signal at low speeds and standstill times. Based on the equations of the linear single track model, the radius a vehicle drives is given by:[215]

$$Rd_v = \frac{v_{ego}}{\dot{\psi} + \dot{\beta}} \tag{J-1}$$

[215] Schramm, D. et al.: Vehicle dynamics (2014), pp. 223–226.

Neglecting the side slip angle change rate $\dot{\beta}$ and using $\kappa = \frac{1}{Rd_v}$ leads to:

$$\kappa = \frac{\psi}{v_{ego}} \tag{J-2}$$

Integrating the product of the calculated curvature κ_{calc} and the ego-vehicle's speed results in the vehicle's relative heading ψ_{rel}. Here, $s0$ is the start of the intersection approach sequence and $s1$ the end of the maneuver after having left the intersection.

$$\psi_{rel} = \int_{s0}^{s1} \kappa_{calc} \cdot v_{ego}\, ds \tag{J-3}$$

However, information of the existence of an intersection is necessary for this calculation method, as well. The advantage of this method is that the detection is independent of the intersection's size and geometry. The only information that is needed is the intersection's existence. Figure J-2 shows the cumulative distribution functions of the ego-vehicle's relative heading after leaving the intersection. The figure is based on data from the test drives, as described above. Thus, using the calculated relative heading, right turn maneuvers are detected at relative headings $\psi_{rel} > 50°$, left turns at $\psi_{rel} < -50°$, and straight drives are detected for $-50° < r_{\psi} < 50°$.

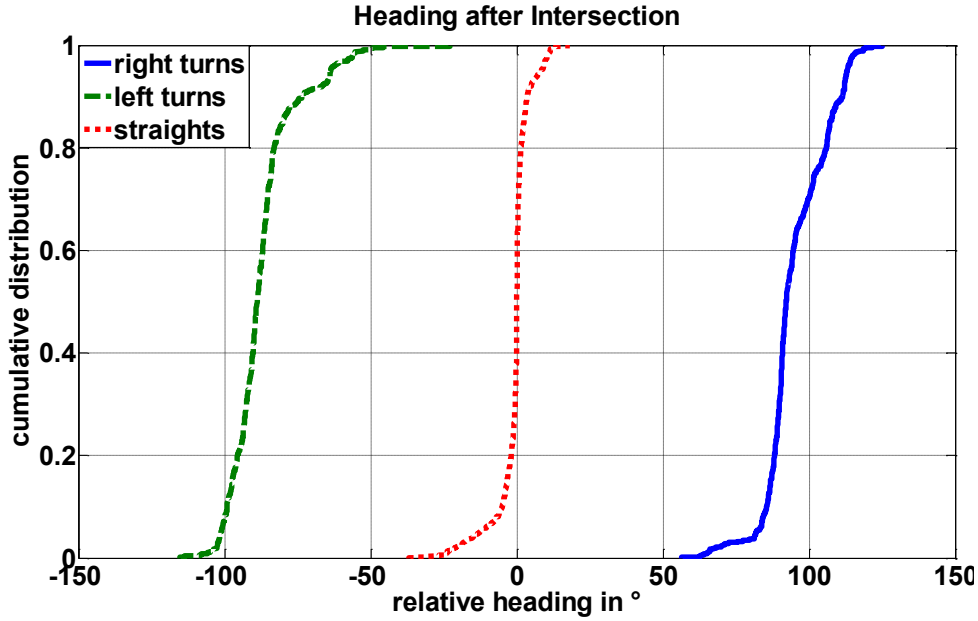

Figure J-2: Vehicle's relative heading after leaving intersection

Data Pool and Calculation Unit

With a known start and end of the approach sequence and the information from the performed maneuver (right turn, left turn, or straight driving), the approach sequence is extracted from the temporary buffer and sent to the vehicle's data pool. The data pool contains all $3xN$ approach sequences known to the prediction system (N for each poten-

tial maneuver). Thus, before the adaptation process is started, the data pool contains the initial set of training sequences from all drivers. Within the adaptation process, sequences extracted from the data stream are added to the data pool according to the maneuver detected by the maneuver detection unit.

The calculation unit performs the calculations for generating the updated transfer functions, using all $3xN + 1$ sequences of the updated data pool. The result of this calculation is adapted transfer functions.

Driver Identification

A driver identification unit is essential for the system to cope with various drivers. If a vehicle is used by more than one driver (or the ownership is transferred to another person), each driver needs for the transfer functions to be adapted to his personal driving style, or at least to be a reset to the initial version. Nevertheless, an individual data pool needs to be stored for each driver. Furthermore, the driver must be identified by the system to select the personal data pool and to calculate the corresponding transfer functions. In addition, a copy of the initial data pool must always be accessible in the vehicle that is used if the system fails to identify the driver or a driver is using the vehicle for the first time. Driver identification here means that the system has to be able to distinguish between different people and to recognize individuals already known to the system. Potential methods of identifying the driver are introduced in the following.

The easiest but most inaccurate way of driver identification is identifying different drivers by their memory seat adjustments. This method needs no additional sensors, but is error-prone for several reasons. If there are more drivers than memory positions available for seat adjustment, the driver's seat adjustment will automatically vary each time the setting is done manually. This leads to false detections. If similar settings are used among different drivers, the system cannot distinguish the drivers as well. Thus, this method is not feasible.

A more reliable method is using personalized ignition keys or personal tags for each driver. The latter is available on the market for commercial vehicles that are regularly driven by various drivers. Here, a couple of systems based on RFID tags that the driver needs to start the vehicle are available on the market.[216] This method has the advantage that drivers are identified reliably as long as they use their own tag. The disadvantage of this method is that an additional RFID reader must be placed in the dash and it is less comfortable for the driver. Especially as keyless starter systems become more and more popular, having to provide the RFID tag each time the vehicle is used is expected to have little approval from drivers.

[216] N.N.: Automatic driver identification (20161).

A third method for identifying the driver is using video. Here, a camera is used that is placed on the vehicle's dashboard facing towards the driver. The driver's face is recognized by biometric features. Assuming that the camera is mounted in the vehicle for monitoring the driver's state and fatigue anyway, no additional hardware is needed. This method offers the most reliable driver identification without loss of comfort for the driver. A prototype of such an identification system for automotive use was presented several years ago.[217]

Monitoring of Adaptation Process

With the adaptation functionality working as described above, the number of intersection approach sequences stored in the data pool increases with each intersection the vehicle crosses. Due to limitations of physical storage and computing power, a monitoring function that limits the process of adding new sequences to the data pool is needed. The increase in prediction performance of the individualized driver adaptation has to reach a saturation level if the adapted transfer functions absolutely conform to the individual driving style. Adding additional training sequences beyond the saturation only increases the data pool without altering the transfer functions. Thus, a monitoring function is applied that regularly compares the adapted transfer functions to a copy of an older state. If the correlation between the "old" state of the functions and the current one is above a predefined limit, the adaptation process is aborted.

Note that intervals between the current and the "old" set of transfer functions that are compared have to be big enough for reliable comparison results. Comparing two sets of transfer functions with insufficient training sequences to distinguish both data pools used for creating the functions will lead to the false decision that the training process is finished. Based on that wrong decision, no additional sequences are accepted for further increasing the data pool. The interval that is needed for reliable assessment of whether the training process is finished or not has to be identified by real road tests.

[217] N.N.: BMW Fahrererkennung (2008).

List of References

ADAC e.V.: Autotest Volvo XC90
ADAC e.V.: Autotest Volvo XC90 D5 Momentum AWD Geartronic

Alhayaseen, W. et al.: Variation of Left-turning Vehicle (2011)
Alhayaseen, Wael; Asano Miho; Suzuki Kazufumi; Nakamura Hideki: Analysis on the Variation of Left-turning Vehicle Spatial Trajectories Inside Intersections, in: Journal of the Eastern Asia Society for Transportation Studies , Issues 9, pp. 1543–1557, 2011

Auto.de: Als die Automatik schalten lernte (2015)
Auto.de: Als die Automatik schalten lernte; http://www.auto.de/magazin/als-die-automatik-schalten-lernte/, 2015, Access 07.09.2016

Bai, J.; Zhang, L.: Identification of Driver's Intentions (2010)
Bai, Jingwen; Zhang, Licai: Study on Identification of Driver's Intentions Based on Cloud Model, in: Institute of Electrical and Electronics Engineers (IEEE) (Ed.): 2010 International Conference on E-Product E-Service and E-Entertainment (ICEEE 2010), 2010

Baier, R.: Richtlinien für die Anlage von Stadtstraßen (2007)
Baier, Reinhold: Richtlinien für die Anlage von Stadtstraßen (RASt), FGSV , Issues 200, 2006. Edition, FGSV-Verl., Köln, 2007

Bar Hillel, A. et al.: Recent progress in road and lane detection (2014)
Bar Hillel, Aharon; Lerner, Ronen; Levi, Dan; Raz, Guy: Recent progress in road and lane detection: a survey, in: Machine Vision and Applications (3) , Issues 25, pp. 727–745, 2014

Bartels, A. et al.: Lane Change Assistance (2016)
Bartels, Arne; Meinecke, Marc-Michael; Steinmeyer, Simon: Lane Change Assistance, in: Winner, Hermann et al. (Eds.): Handbook of Driver Assistance Systems, Springer Verlag, 2016

BASt: Richtlinien für die Markierung von Straßen (1980)
Bundesanstalt für Straßenwesen: Richtlinien für die Markierung von Straßen, Bonn, 1980

Benesty, J.: Noise reduction in speech processing (2009)
Benesty, Jacob (Ed.) Noise reduction in speech processing, Springer Topics in Signal Processing , Issues 2, Springer, Berlin, London, 2009

Berndt, H. et al.: Driver Braking Behavior (2007)
Berndt, Holger; Wender, Stefan; Dietmayer, Klaus: Driver Braking Behavior during Intersection Approaches and Implications for Warning Strategies for Driver Assistant Systems, in: Institute of Electrical and Electronics Engineers (IEEE) (Ed.): 2007 IEEE Intelligent Vehicles Symposium (IV), 2007

Berndt, H.: Diss., Fahrerabsichtserkennung und Gefährlichkeitsabschätzung (2016)
Berndt, Holger: Fahrerabsichtserkennung und Gefährlichkeitsabschätzung für vorausschauende Fahrerassistenzsysteme, Dissertation Universität Ulm, Schriftenreihe des Instituts für Mess-, Regel- und Mikrotechnik Band 16, Universität Ulm, Institut für Mess-, Regel- und Mikrotechnik, Ulm, 2016

Berndt, H.; Dietmayer, K.: Driver intention inference (2009)
Berndt, Holger; Dietmayer, Klaus: Driver intention inference with vehicle onboard sensors, in: Institute of Electrical and Electronics Engineers (IEEE) (Ed.): 2009 IEEE International Conference on Vehicular Electronics and Safety (ICVES), 2009

Blobel, V.; Lohrmann, E.: Datenanalyse (1998)
Blobel, Volker; Lohrmann, Erich: Statistische und numerische Methoden der Datenanalyse, Teubner-Studienbücher : Physik, Teubner, Stuttgart, Leipzig, 1998

Bolovinou, A. et al.: Driving style recognition (2014)
Bolovinou, Anastasia; Amditis, Angelos; Bellotti, Francesco; Tarkiainen, Mikko: Driving style recognition for co-operative driving: A survey, in: IARIA (Ed.): Proceedings of 6th International Conference on Adaptive and Self-Adaptive Systems and Applications, 2014

Bonnin, S. et al.: General Behavior Prediction (2014)
Bonnin, Sarah; Weisswange, Thomas H.; Kummert, Franz; Schmuedderich, Jens: General Behavior Prediction by a Combination of Scenario-Specific Models, in: IEEE Transactions on Intelligent Transportation Systems (4) , Issues 15, pp. 1478–1488, 2014

Bubb, H.: Haptik im Kraftfahrzeug (2001)
Bubb, Heiner: Haptik im Kraftfahrzeug, in: Jürgensohn, Thomas; Timpe, Klaus-Peter (Eds.): Kraftfahrzeugführung, Springer Berlin Heidelberg, Berlin, Heidelberg, 2001

Bubb, H.: Wie viele Probanden braucht man (2003)
Bubb, Heiner: Wie viele Probanden braucht man für allgemeine Erkenntnisse aus Fahrversuchen?, in: Landau, Kurt; Winner, Hermann; Abendroth, Bettina (Eds.): Fahrversuche mit Probanden? Nutzwert und Risiko, Fortschrittberichte VDI, Verkehrstechnik / Fahrzeugtechnik Nr. 12, Düsseldorf, 2003

Bundesministeriums der Justiz und für Verbraucherschutz: StVO (2015)
Bundesministeriums der Justiz und für Verbraucherschutz Straßenverkehrs-Ordnung; Straßenverkehrs-Ordnung vom 6. März 2013 (BGBl. I S. 367), die zuletzt durch Artikel 2 der Verordnung vom 15., 2015

Chen, Y.; Li, L.: Advances in Intelligent Vehicles (2014)
Chen, Y.; Li, L.: Advances in Intelligent Vehicles, Elsevier Science, 2014

Cheng, S. Y.; Trivedi, M. M.: Turn-Intent Analysis Using Body Pose (2006)
Cheng, Shinko Y.; Trivedi, M. M.: Turn-Intent Analysis Using Body Pose for Intelligent Driver Assistance, in: IEEE Pervasive Computing (4) , Issues 5, pp. 28–37, 2006

Chiang, C.-C. et al.: Detecting and recognizing traffic lights (2011)
Chiang, Cheng-Chin; Ho, Ming-Che; Liao, Hong-Sheng; Pratama, Andi; Syu, Wei-Cheng: Detecting and recognizing traffic lights by genetic approximate ellipse detection and spatial texture layouts, in: International Journal of Innovative Computing, Information and Control (12) , Issues 7, pp. 6919–6934, 2011

Coelingh, E. et al.: Collision Warning with Full Auto Brake and Pedestrian Detection (2010)
Coelingh, Erik; Eidehall, Andreas; Bengtsson, Mattias: Collision Warning with Full Auto Brake and Pedestrian Detection, in: Institute of Electrical and Electronics Engineers (IEEE) (Ed.): 2010 IEEE Annual Conference on Intelligent Transportation Systems (ITSC), IEEE, [Piscataway, N.J.], 2010

Currie, G.; Reynolds, J.: Hook Turns (2011)
Currie, Graham; Reynolds, James: Managing Trams and Traffic at Intersections with Hook Turns, in: Transportation Research Record: Journal of the Transportation Research Board , Issues 2219, pp. 10–19, 2011

Dagli, I.; Reichardt, D.: Motivation-based approach to behavior prediction (2002)
Dagli, I.; Reichardt, D.: Motivation-based approach to behavior prediction, in: Institute of Electrical and Electronics Engineers (IEEE) (Ed.): 2002 IEEE Intelligent Vehicle Symposium, 2002

Darms, M. et al.: Classification and tracking of dynamic objects (2008)
Darms, Michael; Rybski, Paul; Urmson, Chris: Classification and tracking of dynamic objects with multiple sensors for autonomous driving in urban environments, in: Institute of Electrical and Electronics Engineers (IEEE) (Ed.): 2008 IEEE Intelligent Vehicles Symposium (IV), 2008

Dingus, T. A. et al.: Automotive Headway Maintenance (1997)
Dingus, Thomas A.; McGehee, Daniel V.; Manakkal, Natarajan; Jahns, Steven K.; Carney, Cher; Hankey, Jonathan M.: Human Factors Field Evaluation of Automotive Headway Maintenance/Collision Warning Devices, in: Human Factors: The Journal of the Human Factors and Ergonomics Society (2) , Issues 39, pp. 216–229, 1997

Donges, E.: Driver Behavior Models (2016)
Donges, Edmund: Driver Behavior Models, in: Winner, Hermann et al. (Eds.): Handbook of Driver Assistance Systems, Springer Verlag, 2016

Doshi, A.; Trivedi, M.: exploration of eye gaze and head motion (2008)
Doshi, Anup; Trivedi, Mohan: A comparative exploration of eye gaze and head motion cues for lane change intent prediction, in: Institute of Electrical and Electronics Engineers (IEEE) (Ed.): 2008 IEEE Intelligent Vehicles Symposium (IV), 2008

Doshi, A.; Trivedi, M. M.: Tactical driver behavior prediction and intent inference: A review (2011)
Doshi, Anup; Trivedi, Mohan M.: Tactical driver behavior prediction and intent inference: A review, in: Institute of Electrical and Electronics Engineers (IEEE) (Ed.): 2011 14th International IEEE Conference on Intelligent Transportation Systems - (ITSC 2011), 2011

Endsley, M. R.: Toward a theory of situation awareness in dynamic systems (1995)
Endsley, Mica R.: Toward a theory of situation awareness in dynamic systems, in: Human Factors: The Journal of the Human Factors and Ergonomics Society (1) , Issues 37, pp. 32–64, 1995

Enke, M.: Collision probability (1979)
Enke, M.: Collision probability related to the shift forward of driver reaction, in: National Highway Traffic Safety Administration (Ed.): Proceedings of 7th International Technical Conference on Experimental Safety Vehicles, 1979

Farah, A.; Algarni, D.: Accuracy of Googleearth (2014)
Farah, Ashraf; Algarni, Dafer: Positional Accuracy Assessment of Googleearth in Riyadh, in: Artificial Satellites (2) , Issues 49, 2014

Fecher, N.; Hoffmann, J.: Driver Warning Elements (2016)
Fecher, Norbert; Hoffmann, Jens: Driver Warning Elements, in: Winner, Hermann et al. (Eds.): Handbook of Driver Assistance Systems, Springer Verlag, 2016

Fenton, N. E.; Neil, M.: Risk assessment and decision analysis (2012)
Fenton, Norman E.; Neil, Martin: Risk assessment and decision analysis with Bayesian networks, Taylor & Francis, Boca Raton, 2012

Firl, J.: Diss., Probabilistic Maneuver Recognition (2014)
Firl, Jonas: Probabilistic Maneuver Recognition in Traffic Scenarios, Dissertation Karlsruher Institut für Technologie, Schriftenreihe / Institut für Mess- und Regelungstechnik, Karlsruher Institut für Technologie , Issues 031, KIT Scientific Publishing, Karlsruhe, 2014

FOT-Net: Field operational tests (2010)
FOT-Net: Field operational tests, 2010

Fuchs, H. et al.: Vehicle-2-X (2016)
Fuchs, Hendrik; Hofmann, Frank; Löhr, Hans; Schaaf, Gunther: Vehicle-2-X, in: Winner, Hermann et al. (Eds.): Handbook of Driver Assistance Systems, Springer Verlag, 2016

Gipps, P. G.: Car-following model (1981)
Gipps, Peter G.: A behavioural car-following model for computer simulation, in: Transportation Research Part B: Methodological (2) , Issues 15, pp. 105–111, 1981

Graichen, M.; Nitsch, V.: Effects of Driver Characteristics (2017)
Graichen, Matthias; Nitsch, Verena: Effects of Driver Characteristics and Driver State on Predicting Turning Maneuvers in Urban Areas: Is There a Need for Individualized Parametrization?, in: Stanton, Neville A. et al. (Eds.): Advances in Human Aspects of Transportation, Advances in intelligent systems and computing Nr. 484, Springer International Publishing, Cham, 2017

Grundhoff, S.: Autos ohne Fahrer (2013)
Grundhoff, Stefan: In fünf Jahren fahren unsere Autos ohne Fahrer; http://www.focus.de/auto/ratgeber/autonomesfahren/tid-29647/autonomes-fahren-in-fuenf-jahren-fahren-unsere-autos-ohne-fahrer_aid_924084.html, 2013, Access 2016-04-01

Halfmann, C.; Holzmann, H.: Kraftfahrzeugdynamik (2003)
Halfmann, Christoph; Holzmann, Henning: Adaptive Modelle für die Kraftfahrzeugdynamik, VDI-Buch, Springer Berlin Heidelberg, Berlin, Heidelberg, 2003

Haunert, J.-H.; Budig, B.: Map Matching Given Incomplete Road Data (2012)
Haunert, Jan-Henrik; Budig, Benedikt: An Algorithm for Map Matching Given Incomplete Road Data, in: Cruz, Isabel (Ed.): 20th International Conference on Advances in Geographic Information Systems, ACM Digital Library, ACM, New York, NY, 2012

Hayashi, K. et al.: Prediction of stopping maneuver considering driver's state (2006)
Hayashi, K.; Kojima, Y.; Abe, K.; Oguri, K.: Prediction of stopping maneuver considering driver's state, in: Institute of Electrical and Electronics Engineers (IEEE) (Ed.): 2006 IEEE Intelligent Transportation Systems Conference, 2006

Hebenstreit, B.: Fahrstiltypen (1999)
Hebenstreit, Benedikt: Fahrstiltypen beim Autofahren, in: Flade, Antje; Limbourg, Maria (Eds.): Frauen und Männer in der mobilen Gesellschaft, VS Verlag für Sozialwissenschaften, Wiesbaden, 1999

Heckhausen, J.: Motivation und Handeln (2010)
Heckhausen, Jutta: Motivation und Handeln, Springer-Lehrbuch, 4. Edition, Springer, Berlin [u.a.], 2010

Henning, M.: Diss., Preparation for lane change (2010)
Henning, Matthias: Preparation for lane change manoeuvres: Behavioural indicators and underlying cognitive processes, Dissertation TU Chemnitz, 2010

Hermes, C. et al.: Long-term vehicle motion prediction (2009)
Hermes, Christoph; Wohler, Christian; Schenk, Konrad; Kummert, Franz: Long-term vehicle motion prediction, in: Institute of Electrical and Electronics Engineers (IEEE) (Ed.): 2009 IEEE Intelligent Vehicles Symposium (IV), 2009

Hoffmann, J.: Diss., Das Darmstädter Verfahren (EVITA)
Hoffmann, Jens: Das Darmstädter Verfahren (EVITA) zum Testen und Bewerten von Frontalkollisions-gegenmaßnahmen, Dissertation TU Darmstadt, Darmstadt

Hofmann, M. et al.: Prädiktion potentieller Zielorte (2001)
Hofmann, M.; Bengler, K.; Lang, M.: Ein Assistenzsystem zur fahrer- und situationsadaptiven Prädiktion potentieller Zielorte für eine robuste Interaktion mit sprachgesteuerten Navigationssystemen, in: VDI Verlag (Ed.): Tagungsband "Elektronik im Fahrzeug", Baden-Baden, VDI-Verlag, 2001

Hohm, A.: Diss., Überholassistenzsystem (2010)
Hohm, Andree: Umfeldklassifikation und Identifikation von Überholzielen für ein Überholassistenzsystem, Dissertation TU Darmstadt, Fortschritt-Berichte VDI : Reihe 12, Verkehrstechnik, Fahrzeugtechnik , Issues 727, VDI-Verl., Darmstadt, 2010

Hulshof, W. et al.: Autonomous Emergency Braking Test Results (2013)
Hulshof, Wesley; Knight, Ian; Edwards, Alix; Avery, Matthew; Grover, Colin: Autonomous Emergency Braking Test Results, 2013

IEEE: 2008 IEEE Intelligent Vehicles Symposium (IV) (2008)
Institute of Electrical and Electronics Engineers (Ed.) 2008 IEEE Intelligent Vehicles Symposium (IV), 2008

IEEE: ITSC 2010 (2010)
Institute of Electrical and Electronics Engineers (Ed.) 2010 IEEE Annual Conference on Intelligent Transportation Systems (ITSC), IEEE, [Piscataway, N.J.], 2010

IEEE: ITSC 2011 (2011)
Institute of Electrical and Electronics Engineers (Ed.) 2011 14th International IEEE Conference on Intelligent Transportation Systems - (ITSC 2011), 2011

Ikenishi, T. et al.: Steering Intention Based on Brain-Computer Interface (2007)
Ikenishi, Toshihito; Kamada, Takayoshi; Nagai, Masao: Classification of Driver Steering Intention Based on Brain-Computer Interface Using Electroencephalogram, in: SAE International (Ed.): Asia Pacific Automotive Engineering Conference, SAE Technical Paper Series, SAE International, Warrendale, Pennsylvania, USA, 2007

Ikenishi, T. et al.: Steering Intentions Using EEG (2008)
Ikenishi, Toshihito; Kamada, Takayoshi; Nagai, Masao: Classification of Driver Steering Intentions Using an Electroencephalogram, in: Journal of System Design and Dynamics (6) , Issues 2, pp. 1274–1283, 2008

IPG Automotive GmbH: CarMaker (2016)
IPG Automotive GmbH: CarMaker; http://ipg.de/de/simulation-software/carmaker/, 2016, Access 27.09.2016

Jensen, F. V.: An introduction to Bayesian networks (1996)
Jensen, Finn V.: An introduction to Bayesian networks, Springer, New York, 1996

Jentsch, M.: Diss., Eignung von Daten im Fahrsimulator (2014)
Jentsch, Martin: Eignung von objektiven und subjektiven Daten im Fahrsimulator am Beispiel der Aktiven Gefahrenbremsung - eine vergleichende Untersuchung, Dissertation TU Chemnitz, 1. Edition, Universitätsverlag der TU Chemnitz, Chemnitz, 2014

Johnson, D. A.; Trivedi, M. M.: Driving style recognition (2011)
Johnson, Derick A.; Trivedi, Mohan M.: Driving style recognition using a smartphone as a sensor platform, in: Institute of Electrical and Electronics Engineers (IEEE) (Ed.): 2011 14th International IEEE Conference on Intelligent Transportation Systems - (ITSC 2011), 2011

Keller, D.: Skala in Fragebögen (2013)
Keller, Daniela: Wahl der Skala in Fragebögen; http://www.statistik-und-beratung.de/2013/02/wahl-der-skala-in-fragebogen/, 2013, Access 10.09.2016

Kessler, C.: Aktive Sicherheit (2006)
Kessler, Christoph: Aktive Sicherheit durch erweiterte Bremsassistenz und die erforderliche Aktuatorik, in: TÜV Akademie (Ed.): brake.tech 2006, 2006

Klanner, F.: Diss., Entwicklung eines Querverkehrsassistenten
Klanner, Felix: Entwicklung eines kommunikationsbasierten Querverkehrsassistenten im Fahrzeug, Dissertation TU Darmstadt, Darmstadt

Kleine-Besten, T. et al.: Navigation and Transport Telematics (2016)
Kleine-Besten, Thomas; Kersken, Ulrich; Pöchmüller, Werner; Schepers, Heiner; Mlasko, Thorsten; Behrens, Ralph; Engelsberg, Andreas: Navigation and Transport Telematics, in: Winner, Hermann et al. (Eds.): Handbook of Driver Assistance Systems, Springer Verlag, 2016

Knecht, J.: Probleme des Autonomen Fahrens (2016)
Knecht, Jochen: Autonomes Fahren: Die größten Probleme; http://www.auto-motor-und-sport.de/news/autonomes-fahren-probleme-2016-11523070.html, 2016, Access 27.08.2016

Köhlker, L. et al.: Beanspruchung des Fahrers bei einer Kreuzungsüberquerung (2013)
Köhlker, L.; Mergl, C.; Blaese, D.; Bengler, K.: Fahrerbeanspruchung im urbanen Raum, in: VDI Verlag (Ed.): 7. VDI-Tagung Der Fahrer im 21. Jahrhundert Nr. 2205, VDI-Verlag, Düsseldorf, 2013

Kosch, T.; Ehmanns, D.: Entwicklung von Kreuzungsassistenzsystemen (2006)
Kosch, T.; Ehmanns, D.: Entwicklung von Kreuzungsassistenzsystemen und Funktionalitätserweiterungen durch den Einsatz von Kommunikationstechnologien, in: TÜV Akademie (Ed.): 2. Tagung Aktive Sicherheit durch Fahrerassistenz, 2006

Koter, R.: Advanced Indication of Braking (1998)
Koter, Reuven: Advanced Indication of Braking: A Practical Safety Measure for Improvement of Decision-Reaction Time for Avoidance of Rear-End Collisions, 1998

Kühn, M. et al.: Fahrerassistenzsysteme für schwere Lkw (2012)
Kühn, Matthias; Hummel, Thomas; Bende, Jenö: Ermittlung des Nutzenpotentials von Fahrerassistenzsystemen für schwere Lkw auf Basis des Schadengeschehens der Deutschen Versicherer, in: DEKRA Automobil GmbH (Ed.): DEKRA Symposium 2012 Sicherheit von Nutzfahrzeugen, 2012

Kurt, A. et al.: Hybrid-state driver/vehicle modelling (2010)
Kurt, Arda; Yester, John L.; Mochizuki, Yutaka; Ozguner, Umit: Hybrid-state driver/vehicle modelling, estimation and prediction, in: Institute of Electrical and Electronics Engineers (IEEE) (Ed.): 2010 IEEE Annual Conference on Intelligent Transportation Systems (ITSC), IEEE, [Piscataway, N.J.], 2010

Land, M. F.: Predictable eye-head coordination (1992)
Land, Michael F.: Predictable eye-head coordination during driving, in: Nature (6393) , Issues 359, pp. 318–320, 1992

Lefevre, S. et al.: Context-based estimation of driver intent at road intersections (2011)
Lefevre, Stephanie; Ibanez-Guzman, Javier; Laugier, Christian: Context-based estimation of driver intent at road intersections, in: Institute of Electrical and Electronics Engineers (IEEE) (Ed.): 2011 IEEE Symposium On Computational Intelligence In Vehicles And Transportation Systems, 2011

Liebner, M. et al.: Der Fahrer im Mittelpunkt (2012)
Liebner, Martin; Klanner, Felix; Stiller, Christoph: Der Fahrer im Mittelpunkt–Eye-Tracking als Schlüssel zum mitdenkenden Fahrzeug?, in: Uni-DAS e.V. (Ed.): 8. Workshop Fahrerassistenzsysteme, 2012

Liebner, M. et al.: Driver intent inference at urban intersections (2012)
Liebner, Martin; Baumann, Michael; Klanner, Felix; Stiller, Christoph: Driver intent inference at urban intersections using the intelligent driver model, in: Institute of Electrical and Electronics Engineers (IEEE) (Ed.): 2012 IEEE Intelligent Vehicles Symposium (IV), 2012

Liebner, M. et al.: Velocity-Based Driver Intent Inference (2013)
Liebner, M.; Klanner, F.; Baumann, M.; Ruhhammer, C.; Stiller, C.: Velocity-Based Driver Intent Inference at Urban Intersections in the Presence of Preceding Vehicles, in: IEEE Intelligent Transportation Systems Magazine (2) , Issues 5, pp. 10–21, 2013

Liebner, M.; Klanner, F.: Driver Intent Inference and Risk Assessment (2016)
Liebner, Martin; Klanner, Felix: Driver Intent Inference and Risk Assessment, in: Winner, Hermann et al. (Eds.): Handbook of Driver Assistance Systems, Springer Verlag, 2016

Lindkvist, A. e.: DRIVE II project V2054 (1995)
Lindkvist, A. e. a.: DRIVE II project V2054, 1995

Lou, Y. et al.: Map-matching for low-sampling-rate GPS trajectories (2009)
Lou, Yin; Zhang, Chengyang; Zheng, Yu; Xie, Xing; Wang, Wei; Huang, Yan: Map-matching for low-sampling-rate GPS trajectories, in: Wolfson, Ouri; Agrawal, Divyakant; Lu, Chang-Tien (Eds.): 17th ACM SIGSPATIAL International Conference, 2009

Mages, M.: Diss., Einbiege- und Kreuzenassistenten (2009)
Mages, Mark: Top-Down-Funktionsentwicklung eines Einbiege- und Kreuzenassistenten, Dissertation TU Darmstadt, Fortschrittberichte VDI / 12 Nr. 694, VDI-Verl., Düsseldorf, 2009

Mages, M. et al.: Intersection Assistance (2016)
Mages, Mark; Klanner, Felix; Stoff, Alexander: Intersection Assistance, in: Winner, Hermann et al. (Eds.): Handbook of Driver Assistance Systems, Springer Verlag, 2016

Mangel, T.: Diss., Inter-Vehicle Communication at Intersections (2012)
Mangel, Thomas: Inter-Vehicle Communication at Intersections, Dissertation Karlsruher Institut für Technologie, KIT Scientific Publishing, Karlsruhe, 2012

Markatou, M. et al.: Variance of Cross-Validation Estimators (2005)
Markatou, Marianthi; Tian, Hong; Biswas, Shameek; Hripcsak, George: Analysis of Variance of Cross-Validation Estimators of the Generalization Error, in: Journal of Machine Learning Research (6), pp. 1127–1168, 2005

Meitinger, K.-H.: Diss., Aktive Sicherheitssysteme für Kreuzungen (2009)
Meitinger, Karl-Heinz: Top-Down-Entwicklung von aktiven Sicherheitssystemen für Kreuzungen, Dissertation TU München, Fortschritt-Berichte VDI : Reihe 12, Verkehrstechnik, Fahrzeugtechnik , Issues 701, VDI-Verl., München, 2009

Merriam-Webster, I.: Dictionary (2015)
Merriam-Webster, Incorporated: Dictionary; http://www.merriam-webster.com/dictionary/prediction, 2015, Access 29.07.2016

Mitchell, H. B.: Image Fusion (2010)
Mitchell, H. B.: Image Fusion, Springer Berlin Heidelberg, 2010

Mitrovic, D.: Driving Events Recognition (2005)
Mitrovic, D.: Reliable Method for Driving Events Recognition, in: IEEE Trans. Intell. Transport. Syst. (IEEE Transactions on Intelligent Transportatitron Systems) (2) , Issues 6, pp. 198–205, 2005

Mitschke, M.: Dynamik von Kraftfahrzeugen (2003)
Mitschke, M.: Dynamik von Kraftfahrzeugen, 4. Edition, Springer, Berlin, 2003

Modsching, M. et al.: GPS Accuracy in a medium size city (2006)
Modsching, Marko; Kramer, Ronny; Hagen, Klaus ten: Field trial on GPS Accuracy in a medium size city: The influence of built-up, in: Niccimon, Niedersächsisches Kompetenzzentrum Informationssysteme für die Mobile Nutzung Oldenburg (Ed.): 3rd Workshop on Positioning, Navigation and Communication 2006 (WPNC' 06), Hannoversche Beiträge zur Nachrichtentechnik, Shaker, 2006

Möller, B.; Williams, D.: Tracking (2003)
Möller, Birgit; Williams, Denis: Tracking
Martin-Luther-Universität Halle-Wittenberg, Halle (Saale), Germany, 2003

Mörbe, M.: Vehicle Dynamics Sensors for DAS (2016)
Mörbe, Matthias: Vehicle Dynamics Sensors for DAS, in: Winner, Hermann et al. (Eds.): Handbook of Driver Assistance Systems, Springer Verlag, 2016

Morris, B. et al.: Lane change intent prediction (2011)
Morris, Brendan; Doshi, Anup; Trivedi, Mohan: Lane change intent prediction for driver assistance: On-road design and evaluation, in: Institute of Electrical and Electronics Engineers (IEEE) (Ed.): 2011 IEEE Intelligent Vehicles Symposium (IV), 2011

Mücke, S.; Breuer, J.: Bewertung von Sicherheitssystemen in Fahrversuchen (2007)
Mücke, S.; Breuer, J.: Bewertung von Sicherheitssystemen in Fahrversuchen, in: Bruder, Ralph (Ed.): Wie objektiv sind Fahrversuche?, Ergonomia-Verl., Stuttgart, 2007

Müller, C.: Fahrerbeobachtung als wichtiger Baustein für autonomes Fahren (2016)
Müller, Christian: Die Fahrerbeobachtung als wichtiger Baustein für autonomes Fahren-Fahrerzustandsanalyse zur Steigerung der Sicherheit und Erweiterung des HMI, in: GMM-Fachbericht-AmE 2016-Automotive meets Electronics, 2016

N.N.: Brake pressure sensor
N.N.: Brake pressure sensor

N.N.: BMW Fahrererkennung (2008)
N.N.: BMW-Innovationstag: Von der Fahrererkennung bis zur Teleprogrammierung; http://www.heise.de/autos/artikel/Vernetzte-Autowelten-BMW-zeigt-IT-Innovationen-im-Automobil-444886.html, 2008, Access 10.09.2016

N.N.: faceLAB5 (2009)
N.N.: faceLAB5, 2009

N.N.: Adaptive Transmission Management (2011)
N.N.: BMW Technology Guide : Adaptive Transmission Management (ATM); http://www.bmw.com/com/en/insights/technology/technology_guide/articles/adaptive_trans_management.html?, 2011, Access 07.09.2016

N.N.: GNSS Error Sources (2016)
N.N.: An Introduction to GNSS; http://www.novatel.com/an-introduction-to-gnss/chapter-4-gnss-error-sources/, 2016, Access 19.05.2016

N.N.: GNSS and INS (2016)
N.N.: An Introduction to GNSS; http://www.novatel.com/an-introduction-to-gnss/chapter-6-gnss-ins/gnss-ins-systems/, 2016, Access 19.05.2016

N.N.: BAS Plus (2016)
N.N.: BAS Plus; https://www.mbusa.com/mercedes/technology/videos/detail/title-safety/videoId-20f758b451127410VgnVCM100000ccec1e35RCRD, 2016, Access 03.09.2016

N.N.: Dictionary (2016)
N.N.: Dictionary - Intention; http://www.dictionary.com/browse/intention, 2016, Access 31.07.2016

N.N.: Durchschnittsalter (2016)
N.N.: Durchschnittsalter der Bevölkerung in Industrie- und Schwellenländern 2015 | Statistik; http://de.statista.com/statistik/daten/studie/37220/umfrage/altersmedian-der-bevoelkerung-in-ausgewaehlten-laendern/, 2016, Access 10.09.2016

N.N.: Jährliche Fahrleistung in Deutschland (2016)
N.N.: Jährliche Fahrleistung des PKW in Deutschland 2015; http://de.statista.com/statistik/daten/studie/183003/umfrage/pkw---gefahrene-kilometer-pro-jahr/, 2016, Access 09.09.2016

N.N.: Correlation coefficients (2016)
N.N.: MATLAB Documentation: correlation coefficients; http://de.mathworks.com/help/matlab/ref/corrcoef.html#bunkanr, 2016, Access 19.09.2016

N.N.: OpenStreetMap (2016)
N.N.: OpenStreetMap; http://www.openstreetmap.org, 2016, Access 09.09.2016

N.N.: Dead Reckoning (2016)
N.N.: u-blox 3D Automotive Dead Reckoning technology; https://www.u-blox.com/en/u-blox-3d-automotive-dead-reckoning-technology, 2016, Access 19.05.2016

N.N.: Automatic driver identification (20161)
N.N.: Frotcom - Automatic driver identification; http://www.frotcom.com/features/automatic-driver-identification, 20161, Access 10.09.2016

Newell, G. F.: A simplified car-following theory (2002)
Newell, G. F.: A simplified car-following theory: a lower order model, in: Transportation Research Part B: Methodological (3) , Issues 36, pp. 195–205, 2002

Niehues, D.: Diss., Positionsbestimmung von Fahrzeugen
Niehues, Daniel: Hochgenaue Positionsbestimmung von Fahrzeugen als Grundlage autonomer Fahrregime im Hochgeschwindigkeitsbereich, Dissertation TU Dresden, Dresden

Nordman, A.: Data Mining - Evaluation (2011)
Nordman, Aida: Data Mining, Linköping, 2011

Opencv Dev Team: Template Matching (2016)
Opencv Dev Team: Template Matching; http://docs.opencv.org/2.4/doc/tutorials/imgproc/histograms/template_matching/template_matching.html#which-are-the-matching-methods-available-in-opencv.%20access:%202016-03-29, 2016, Access 10.09.2016

Pedregosa, F. et al.: Scikit-learn: Machine Learning in Python (2011)
Pedregosa, F.; Varoquaux, G.; Gramfort, A.; Michel, V.; Thirion, B.; Grisel, O.; Blondel, M.; Prettenhofer, P.; Weiss, R.; Dubourg, V.; Vanderplas, J.; Passos, A.; Cournapeau, D.; Brucher, M.; Perrot, M.; Duchesnay, E.: Scikit-learn: Machine Learning in Python, in: Journal of Machine Learning Research , Issues 12, pp. 2825–2830, 2011

Plötz, M.; Vockenroth, N.: Navigationssysteme (2011)
Plötz, Martin; Vockenroth, Niklas: Thema des Monats: Navigationssysteme, 2011

Ponziani, R.: Turn Signal Usage Rate Results (2012)
Ponziani, Richard: Turn Signal Usage Rate Results: A Comprehensive Field Study of 12,000 Observed Turning Vehicles, SAE International, Warrendale, PA, 2012

Porst, R.: Fragebogen (2014)
Porst, Rolf: Fragebogen, Studienskripten zur Soziologie, 4. Edition, Imprint: Springer VS, Wiesbaden, 2014

Pudenz, K.: Schrittweise Automatisierung bis 2025 (2012)
Pudenz, Katrin: Schrittweise Automatisierung bis 2025: Teilautomatisierung bereits in 2016 möglich; https://www.springerprofessional.de/fahrzeugtechnik/schrittweise-automatisierung-bis-2025-teilautomatisierung-bereit/6561454, 2012, Access 04.06.2016

Reif, K.: Automobilelektronik (2014)
Reif, Konrad: Automobilelektronik, Morgan Kaufmann, [Place of publication not identified], 2014

Rieken, J. et al.: Development Process of Forward Collision Prevention Systems (2016)
Rieken, Jens; Reschka, Andreas; Maurer, Markus: Development Process of Forward Collision Prevention Systems, in: Winner, Hermann et al. (Eds.): Handbook of Driver Assistance Systems, Springer Verlag, 2016

Rodemerk, C. et al.: Exklusion alternativer Manöveroptionen (2015)
Rodemerk, C.; Kastner, R.; Winner, H.: Manöverprädiktion an innerstädtischen Knotenpunkten durch Exklusion alternativer Manöveroptionen, in: Stiller, C. (Ed.): 10. Workshop Fahrerassistenzsysteme, Uni-DAS e.V, Germany, 2015

Rodemerk, C. et al.: Predicting Driver's Turn Intentions (2015)
Rodemerk, Claas; Winner, Hermann; Kastner, Robert: Predicting the Driver's Turn Intentions at Urban Intersections Using Context-based Indicators, in: Institute of Electrical and Electronics Engineers (IEEE) (Ed.): 2015 IEEE Intelligent Vehicles Symposium (IV), 2015

Rüdenauer, J.: Diplomarbeit, Probabilistische Verfahren zur Entscheidungsfindung (2003)
Rüdenauer, Jörg: Einsatz probabilistischer Verfahren zur Entscheidungsfindung im RoboCup, Diplomarbeit
Universität Stuttgart, Stuttgart, 2003

Ruhhammer, C. et al.: Crowdsourcing zum Erlernen von Kreuzungsparametern (2014)
Ruhhammer, Christian; Atanasov, Atanasko; Klanner, Felix; Stiller, Christoph: Crowdsourcing als Enabler für verbesserte Assistenzsysteme: Ein generischer Ansatz zum Erlernen von Kreuzungsparametern, in: Färber, Berthold (Ed.): 9. Workshop Fahrerassistenzsysteme FAS 2014, Uni-DAS, Darmstadt, 2014

Schendzielorz, T. et al.: Vehicle maneuver estimation at urban intersections (2013)
Schendzielorz, T.; Mathias, P.; Busch, F.: Infrastructure-based vehicle maneuver estimation at urban intersections, in: Institute of Electrical and Electronics Engineers (IEEE) (Ed.): 2013 16th International IEEE Conference on Intelligent Transportation Systems - (ITSC 2013), 2013

Schnabel, W. et al.: Straßenverkehrstechnik (2011)
Schnabel, Werner; Lohse, Dieter; Knote, Thoralf: Straßenverkehrstechnik, Studium / Schnabel; Lohse ; Bd. 1, 3. Edition, Beuth; Kirschbaum, Berlin [u.a.], Bonn, 2011

Scholz, T.; Ortlepp, J.: Auswirkungen der Sonderphase für Linksabbieger (2010)
Scholz, Thomas; Ortlepp, Jörg: Verkehrstechnische Auswirkungen der Sonderphase für Linksabbieger an Knotenpunkten mit Lichtsignalanlage, Forschungsbericht / Gesamtverband der Deutschen Versicherungswirtschaft e.V , Issues1, GDV; Unfallforschung der Versicherer, Berlin, Berlin, 2010

Schramm, D. et al.: Vehicle dynamics (2014)
Schramm, Dieter; Hiller, Manfred; Bardini, Roberto: Vehicle dynamics, 2014

Schroven, F.; Giebel, T.: Fahrerintentionserkennung für Fahrerassistenzsysteme (2008)
Schroven, F.; Giebel, T.: Fahrerintentionserkennung für Fahrerassistenzsysteme, in: VDI Verlag (Ed.): 24. VDI-VW-Gemeinschaftstagung Integrierte Sicherheit und Fahrerassistenzsysteme, VDI-Berichte Nr. 2048, VDI-Verlag, Düsseldorf, 2008

scikit-learn developers: Choosing the right estimator (2014)
scikit-learn developers: Choosing the right estimator; http://scikit-learn.org/stable/tutorial/machine_learning_map/, 2014

Shashua, A. et al.: Pedestrian detection for driving assistance systems (2004)
Shashua, A.; Gdalyahu, Y.; Hayun, G.: Pedestrian detection for driving assistance systems: single-frame classification and system level performance, in: Institute of Electrical and Electronics Engineers (IEEE) (Ed.): 2004 IEEE Intelligent Vehicles Symposium, 2004

Statistisches Bundesamt: Unfallentwicklung auf deutschen Straßen 2012 (2013)
Statistisches Bundesamt: Unfallentwicklung auf deutschen Straßen 2012, Wiesbaden, 2013

Statistisches Bundesamt: Zeitreihen 2014 (2015)
Statistisches Bundesamt: Verkehrsunfälle, Wiesbaden, 2015

Steinlein, U.: Data Mining (2004)
Steinlein, Uwe: Data Mining als Instrument der Responseoptimierung im Direktmarketing, 1. Edition, Cuvillier, Göttingen, 2004

Stoff, A.: Diss., Automatisierter Kreuzungsassistent
Stoff, Alexander: Potential und Machbarkeit eines automatisierten Kreuzungsassistenten für den vorfahrtberechtigten Verkehrsteilnehmer, Dissertation TU Darmstadt, Fortschritt-Berichte VDI : Reihe 12, Verkehrstechnik, Fahrzeugtechnik , Issues 789, VDI-Verl., Darmstadt

Svahn, F.: In-Car Navigation Usage: An End-User Survey on Existing Systems (2004)
Svahn, Frederik: In-Car Navigation Usage: An End-User Survey on Existing Systems, in: IRIS (Ed.): Proceedings of Information Systems Research Conference in Scandinavia, 2004

Takahashi, H.; Kuroda, K.: Mental model for inferring driver's intention (1996)
Takahashi, H.; Kuroda, K.: A study on mental model for inferring driver's intention, in: Institute of Electrical and Electronics Engineers (IEEE) (Ed.): 35th IEEE Conference on Decision and Control, 1996

Treiber, M.; Kesting, A.: Elementary Car-Following Models (2013)
Treiber, Martin; Kesting, Arne: Elementary Car-Following Models, in: Treiber, Martin; Kesting, Arne (Eds.): Traffic Flow Dynamics, Springer Berlin Heidelberg, Berlin, Heidelberg, 2013

Tsogas, M. et al.: Detection of maneuvers using evidence theory (2008)
Tsogas, Manolis; Dai, Xun; Thomaidis, George; Lytrivis, Panagiotis; Amditis, Angelos: Detection of maneuvers using evidence theory, in: Institute of Electrical and Electronics Engineers (IEEE) (Ed.): 2008 IEEE Intelligent Vehicles Symposium (IV), 2008

Unselt, T.; Schöneburg, R. Bakker J.: Einführung autonomer Fahrzeugsysteme (2013)
Unselt, T.; Schöneburg, R. Bakker J.: Insassen- und Partnerschutz unter den Rahmenbedingungen der Einfuehrung autonomer Fahrzeugsysteme, in: VDI Verlag (Ed.): 9. VDI-Tagung Fahrzeugsicherheit, Sicherheit 2.0, VDI-Berichte Nr. 2204, VDI-Verl., Düsseldorf, 2013

Weisstein; W, E.: Likelihood (2016)
Weisstein; W, Eric: Likelihood; http://mathworld.wolfram.com/Likelihood.html, 2016, Access 24.08.2016

Welke, S.: Diss., Lenkmanöverprädiktion
Welke, Sebastian: Lenkmanöverprädiktion basierend auf einer Analyse der hirnelektrischen Aktivität des Fahrers, Dissertation TU Berlin, Berlin

Winner, H.: Automotive RADAR (2016)
Winner, Hermann: Automotive RADAR, in: Winner, Hermann et al. (Eds.): Handbook of Driver Assistance Systems, Springer Verlag, 2016

Winner, H. et al.: Handbook of Driver Assistance Systems (2016)
Winner, Hermann; Hakuli, Stephan; Lotz, Felix; Singer, Christina (Eds.) Handbook of Driver Assistance Systems, Springer Verlag, 2016

Winner, H.; Schopper, M.: Adaptive Cruise Control (2016)
Winner, Hermann; Schopper, Michael: Adaptive Cruise Control, in: Winner, Hermann et al. (Eds.): Handbook of Driver Assistance Systems, Springer Verlag, 2016

Wissmann, M.: VwV-StVO (2015)
Wissmann, M.: Allgemeine Verwaltungsvorschrift zur Straßenverkehrs-Ordnung (VwV-StVO); http://www.verwaltungsvorschriften-im-internet.de/bsvwvbund_26012001_S3236420014.htm, 2015, Access 10.09.2016

Witten, I. H.; Frank, E.: Data Mining (2001)
Witten, Ian H.; Frank, Eibe: Data mining, Hanser, München, Wien, 2001

Zöller, I. et al.: Wissenssammlung für valide Fahrsimulation (2015)
Zöller, Ilka; Mautes, Nicole; Ren, Wen; Abendroth, Bettina: Wissenssammlung für valide Fahrsimulation, in: ATZ - Automobiltechnische Zeitschrift Dezember, 2015

Own Publications

Rodemerk, C.; Winner, H.; Kastner, R.: Fahrmanövervorhersage an innerstädtischen Kreuzungen basierend auf Kontextinformationen, in: 7. Tagung Fahrerassistenz, Munich, Germany, 2015.

Rodemerk, C.; Kastner, R.; Winner, H.: Manöverprädiktion an innerstädtischen Knotenpunkten durch Exklusion alternativer Manöveroptionen, in: 10. Workshop Fahrerassistenzsysteme, Walting im Altmühltal, Walting, Germany, 2015.

Rodemerk, C.; Kastner, R.; Winner, H.: Fahrmanövervorhersage an innerstädtischen Kreuzungen basierend auf Kontextinformationen, in: WKM Symposium 2015, Munich, Germany, 2015..

Rodemerk, C.; Winner, H.; Kastner, R.: Predicting the Driver's Turn Intentions at Urban Intersections Using Context-based Indicators, in: Proc. IEEE Intelligent Vehicles Symposium (IV), Seoul, South Korea, 2015.

Rodemerk, C., Habenicht; S., Weitzel, A., Winner, H., Schmitt, T.: Development of a general criticality criterion for the risk estimation of driving situations and its application to a maneuver-based lane change assistance system, in: Proc. IEEE Intelligent Vehicles Symposium (IV), Alcalá de Henares, Spain, 2012.

Rodemerk, C.; Kastner, R.; Winner, H.: Driver's intention prediction apparatus and method and vehicle including such an apparatus, Patent Application, Application Number: DE 10 2015 200 059.1, Filing Date: 2015-07-01

Rodemerk, C.; Kastner, R.; Winner, H.: Driving Style Evaluating Device, Patent Application, Application Number: DE 10 2015 222 963.7; Filing Date: 2015-11-20.

Rodemerk, C.; Kastner, R.; Winner, H.: Driver's intention prediction apparatus and method and vehicle including such an apparatus, Patent Application, Application Number: DE 10 2015 222 964.5; Filing Date: 2015-11-20.

Rodemerk, C.; Kastner, R.; Winner, H.: Method for maneuver prediction on priority roads during intersection approach, Patent Application.

Supervised Thesis

Ackermann, Stefan: Entwicklung eines Systems zur Eigenlokalisierung und Nutzung von Informationen aus digitalen Karten. Bachelorthesis Nr. 1153/13, 2013

Alles, Jonas; Brötz, Nicolas; Mrosek, Markus; Rösner, Arnfinn; Schneider, Jan; Seyfried, Stefan: Weiterentwicklung eines automatisierten und Smartphone-basierten Aufzeichnungssystem von Fahrdaten. Advanced Design Project Nr. 66/15, 2015

Behrendt, Maria: Entwicklung eines Algorithmus zur Fahrerabsichtsdetektion unter Verwendung Bayesscher Netze. Bachelorthesis Nr. 1164/13, 2013

Bensch, Valerie: Potentialanalyse zur Fahrerabsichtsdetektion in innerstädtischen Fahrsituationen. Masterthesis Nr. 498/12, 2012

Bobev, Galin; Louiset, Pierre; Picard, Simon; Tretter, Michael: Entwicklung einer portablen Radarmesseinrichtung zur universellen Verwendung an verschiedenen Fahrzeugen. Advanced Design Project Nr. 45/12, 2012

Fiebig, Christian: Planung, Durchführung und Auswertung von Fahrversuchen für ein Stauassistenzsystem. Studienarbeit Nr. 1122/12, 2012

Gebauer, Oliver: Entwicklung eines Systems zur videobasierten Detektion von Fahrbahnmarkierungen. Bachelorthesis Nr. 1157/13, 2013

Jow, Yun-Chen: Analyse der Kopfbewegungen und des Blickverhaltens von Fahrern bei der Annäherung an innerstädtischen Kreuzungen. Masterthesis Nr. 529/13, 2013

Knabe, Jonas: Literaturrecherche zu Konzepten und Umsetzungen von Stauassistenzsystemen. Bachelorthesis Nr. 1103/12, 2012

Röhrs, Michael: Entwicklung und Validierung einer Methodik zur Durchführung einer Probandenstudie zur Fahrerabsichtsdetektion im realen Straßenverkehr. Bachelorthesis Nr. 1198/14, 2014

Schad, Julian: Entwicklung eines Algorithmus zur Fahrerabsichtsdetektion unter Verwendung von Hidden-Markov-Modellen. Bachelorthesis Nr. 1165/13, 2013

Schäfer, Uwe: Entwicklung und Analyse eines Frameworks zur Einbindung aufgezeichneter Messfahrten in IPG CarMaker. Bachelorthesis Nr. 1189/14, 2014

Spalthoff, Stephan: Ermittlung des Stands der Forschung und Technik auf dem Gebiet der Nutzenbetrachtungen und Kosten-Nutzen-Analysen aktiver Sicherheitssysteme. Bachelorthesis Nr. 1126/12, 2012

Spalthoff, Stephan: Konzepte von Kreuzungsassistenzfunktionen. Forschungsseminar Nr. 90/13, 2013

Spohr, Thorben: Analyse der Qualität einer Umfeldwahrnehmung durch Radarsensoren. Bachelorthesis Nr. 1156/13, 2013

Weber, Moritz: Entwicklung eines Kreuzungsassistenzsystems in IPG CarMaker unter Berücksichtigung bekannter Fahrerabsichten. Masterthesis Nr. 547/14, 2014

Weible, Michael: Erstellung eines radarbasierten Modells zur Detektion benachbarter Fahrstreifen. Bachelorthesis Nr. 1181/14, 2014

Weißenseel, Stefan: Entwicklung eines Fuzzy-Logic-basierten Algorithmus zur Fahrerabsichtsdetektion. Bachelorthesis Nr. 1158/13, 2013